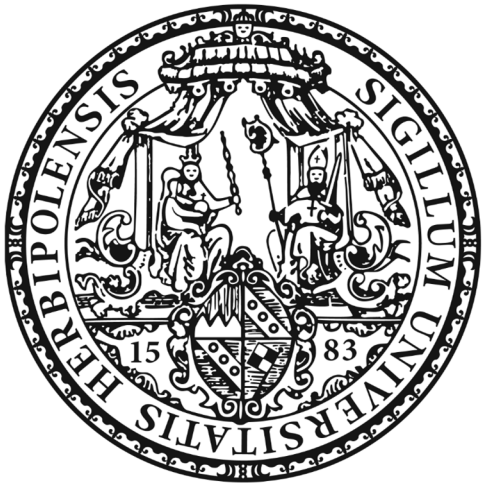


# NF-κB/NFAT Reporter Cell Platform for Chimeric Antigen Receptor (CAR)-Library Screening

# NF-κB/NFAT-Reporterzellplattform für das Screening von Chimären Antigenrezeptor (CAR)-Bibliotheken

DOCTORAL THESIS FOR A DOCTORAL DEGREE

AT THE GRADUATE SCHOOL OF LIFE SCIENCES,

JULIUS-MAXIMILIANS-UNIVERSITÄT WÜRZBURG,

SECTION INFECTION AND IMMUNITY

SUBMITTED BY

JULIAN RYDZEK

FROM

DACHAU, GERMANY

WÜRZBURG, 2018

Submitted on: ……

Office stamp

**Members of the Promotionskomitee:**

Chairperson: Prof. Dr. Thomas Rudel

Primary Supervisor: Dr. Michael Hudecek

Supervisor (Second): Prof. Dr. Thomas Herrmann

Supervisor (Third): Prof. Dr. Hermann Einsele

Supervisor (Fourth): Prof. Dr. Peter Steinberger

Date of Public Defence: ……

Date of Receipt of Certificates: ……

# Table of contents

# Summary

Immunotherapy with engineered T cells expressing a tumor-specific chimeric antigen receptor (CAR) is under intense preclinical and clinical investigation. This involves a rapidly increasing portfolio of novel target antigens and CAR designs that need to be tested in time- and work-intensive screening campaigns in primary T cells. Therefore, we anticipated that a standardized screening platform, similar as in pharmaceutical small molecule and antibody discovery, would facilitate the analysis of CARs by pre-selecting lead candidates from a large pool of constructs that differ in their extracellular and intracellular modules. Because CARs integrate structural elements of the T cell receptor (TCR) complex and engage TCR-associated signaling molecules upon stimulation, we reasoned that the transcription factors nuclear factor-κB (NF-κB) and nuclear factor of activated T cells (NFAT) could serve as surrogate markers for primary T cell function. The nuclear translocation of both transcription factors in primary T cells, which we observed following CAR stimulation, supported our rationale to use NF-κB and NFAT as indicators of CAR-mediated activation in a screening platform.

To enable standardized and convenient analyses, we have established a CAR-screening platform based on the human T cell lymphoma line Jurkat that has been modified to provide rapid detection of NF-κB and NFAT activation. For this purpose, Jurkat cells contained NF-κB- and NFAT-inducible reporter genes that generate a duplex output of cyan fluorescent protein (CFP) and green fluorescent protein (GFP), respectively. Upon stimulation of NF-κB/NFAT reporter cells, the expression of both fluorophores could be readily quantified in high-throughput screening campaigns by flow cytometry.

We modified the reporter cells with CD19-specific and ROR1-specific CARs, and we co-cultured them with antigen-positive stimulator cells to analyze NF-κB and NFAT activation. CAR-induced reporter signals could already be detected after 6 hours. The optimal readout window with high-level reporter activation was set to 24 hours, allowing the CAR-screening platform to deliver results in a rapid turnaround time. A reporter cell-screening campaign of a spacer library with CARs comprising a short, intermediate or long IgG4-Fc domain allowed distinguishing functional from non-functional constructs. Similarly, reporter cell-based analyses identified a ROR1-CAR with 4-1BB domain from a library with different intracellular signal modules due to its ability to confer high NF-κB activation, consistent with data from *in vitro* and *in vivo* studies with primary T cells. The results of both CAR-screening campaigns were highly reproducible, and the time required for completing each testing campaign was substantially shorter with reporter cells (6 days) compared to primary T cells (21 days). We further challenged the reporter cells in a large-scale screening campaign with a ROR1-CAR library comprising mutations in the $V_H$ CDR3 sequence of the R11 scFv. This region is crucial for binding the R11 epitope of ROR1, and we anticipated that mutations here would cause a loss of specificity and

affinity for most of the CAR variants. This provided the opportunity to determine whether the CAR-screening platform was able to retrieve functional constructs from a large pool of CAR variants. Indeed, using a customized pre-enrichment and screening strategy, the reporter cells identified a functional CAR variant that was present with a frequency of only 6 in $1.05x10^6$.

As our CAR-screening platform enabled the analysis of activating signal modules, it encouraged us to also evaluate inhibitory signal modules that change the CAR mode of action. Such an inhibitory CAR (iCAR) can be used in logic gates with an activating CAR to interfere with T cell stimulation. By selecting appropriate target antigens for iCAR and CAR, this novel application aims to improve the selectivity towards tumor cells, and it could readily be studied using our screening platform. Accordingly, we tested CD19-specific iCARs with inhibitory PD-1 signal module for their suppressive effect on reporter gene activation. In logic gates with CAR or TCR stimulation, a decrease of NF-κB and NFAT signals was only observed when activating and inhibitory receptors were forced into spatial proximity. These results were further verified by experiments with primary T cells.

In conclusion, our reporter cell system is attractive as a platform technology because it is independent of testing in primary T cells, exportable between laboratories, and scalable to enable small- to large-scale screening campaigns of CAR libraries. The pre-selection of appropriate lead candidates with optimal extracellular and intracellular modules can reduce the number of CAR constructs to be investigated in further *in vitro* and *in vivo* studies with primary T cells. We are therefore confident that our CAR-screening platform based on NF-κB/NFAT reporter cells will be useful to accelerate translational research by facilitating the evaluation of CARs with novel design parameters.

# Zusammenfassung

Die Immuntherapie mit modifizierten T-Zellen, die einen tumorspezifischen chimären Antigenrezeptor (CAR) exprimieren, wird präklinisch und klinisch intensiv erforscht. Dies beinhaltet ein rasant anwachsendes Portfolio an neuartigen Zielantigenen und CAR-Designs, die in zeit- und arbeitsintensiven Screenings in primären T-Zellen untersucht werden müssen. Daher haben wir angenommen, dass eine standardisierte Screening-Plattform, ähnlich wie in der pharmazeutischen Kleinmolekül- und Antikörperforschung, die Analyse von CARs erleichtern würde. Die Plattform könnte funktionelle Kandidaten aus einer großen Anzahl von CAR Konstrukten, die sich durch ihre extrazellulären und intrazellulären Module unterscheiden, herausfiltern. Da CARs strukturelle Elemente des T-Zell-Rezeptor Komplexes enthalten und T-Zell-Rezeptor-assoziierte Signalmoleküle nach Stimulation aktivieren, sind wir zu der Annahme gelangt, dass die Transkriptionsfaktoren Nukleärer Faktor κB (NF-κB) und Nukleärer Faktor aktivierter T-Zellen (NFAT) als Surrogatmarker für primäre T-Zellfunktionen dienen könnten. Die nukleäre Translokation beider Transkriptionsfaktoren in primären T-Zellen, die wir nach der CAR-Stimulation beobachten konnten, unterstützte unsere Überlegung NF-κB und NFAT als Indikatoren für die CAR-vermittelte Aktivierung in einer Screening-Plattform zu verwenden.

Um standardisierte und benutzerfreundliche Analysen zu ermöglichen, haben wir eine CAR-Screening-Plattform basierend auf der humanen T-Zell-Lymphomlinie Jurkat etabliert, die modifiziert wurde, um einen schnellen Nachweis der Aktivierung von NF-κB und NFAT zu gewährleisten. Hierfür enthielten die Jurkat-Zellen NF-κB- und NFAT-induzierbare Reportergene, die mittels dem blauen Fluorophor CFP und dem grünen Fluorophor GFP eine Doppeldetektion erlauben. Bei Stimulation der NF-κB/NFAT-Reporterzellen konnte die Expression beider Fluorophore in Hochdurchsatz-Screenings mithilfe der Durchflusszytometrie schnell quantifiziert werden.

Die Reporterzellen wurden mit CD19-spezifischen und ROR1-spezifischen CARs modifiziert und anschließend mit antigenpositiven Stimulatorzellen kokultiviert, um die Aktivierung von NF-κB und NFAT zu analysieren. CAR-induzierte Reportersignale konnten bereits nach 6 Stunden detektiert werden. Das optimale Zeitfenster zur Auslesung hoher Reporteraktivierung wurde auf 24 Stunden festgelegt, so dass die CAR-Screening-Plattform in kurzer Zeit Ergebnisse liefern kann. Ein Reporterzell-Screening mit einer Spacer-Bibliothek aus CARs, die eine kurze, mittlere oder lange IgG4-Fc-Domäne enthielten, ermöglichte die Unterscheidung zwischen funktionellen und nicht-funktionellen Konstrukten. Ebenso konnten reporterzellgestützte Analysen einen ROR1-CAR mit 4-1BB Domäne aus einer Bibliothek mit verschiedenen intrazellulären Signalmodulen aufgrund seiner hohen NF-κB Aktivierung identifizieren, was im Einklang mit Daten aus *in vitro*- und *in vivo*-Studien mit primären

T-Zellen steht. Die Ergebnisse beider CAR-Screenings waren höchst reproduzierbar und die Zeit, welche für die Durchführung jeder Testung benötigt wurde, war mit Reporterzellen (6 Tage) wesentlich kürzer als mit primären T-Zellen (21 Tage). Des Weiteren haben wir die Reporterzellen für ein groß angelegtes Screening mit einer Bibliothek aus ROR1-CARs verwendet, welche Mutationen in der $V_H$ CDR3-Sequenz des R11 scFv enthielten. Diese Region ist entscheidend für die Bindung des R11-Epitops von ROR1 und wir haben erwartetet, dass Mutationen hier zu einem Verlust der Spezifität und Affinität für die Mehrzahl der CAR-Varianten führen würden. Somit wollten wir feststellen, ob die CAR-Screening-Plattform in der Lage war funktionelle Konstrukte aus einer großen Anzahl von CAR-Varianten wiederzufinden. Tatsächlich identifizierten die Reporterzellen mittels einer angepassten Anreicherungs- und Screeningstrategie eine funktionelle CAR-Variante, die mit einer Häufigkeit von nur 6 in $1{,}05 \times 10^6$ vorkam.

Da unsere CAR-Screening-Plattform die Analyse aktivierender Signalmodule ermöglicht hat, veranlasste uns dies auch inhibitorische Signalmodule zu untersuchen, welche die Funktionsweise des CAR verändern. Ein solcher inhibitorischer CAR (iCAR) kann in Kombination mit einem aktivierenden CAR verwendet werden, um die T-Zellstimulation zu stören. Durch die Auswahl geeigneter Zielantigene für iCAR und CAR soll diese neuartige Anwendung die Selektivität gegenüber Tumorzellen verbessern und sie könnte mit unserer Screening-Plattform einfach untersucht werden. Dementsprechend haben wir CD19-spezifische iCARs mit inhibitorischem PD-1-Signalmodul hinsichtlich ihrer hemmenden Wirkung auf die Reportergenaktivierung getestet. In Kombination mit CAR- oder TCR-Stimulation wurde eine Abnahme der NF-κB- und NFAT-Signale nur dann beobachtet, wenn aktivierende und inhibitorische Rezeptoren in räumliche Nähe gebracht wurden. Diese Ergebnisse wurden durch Experimente mit primären T-Zellen weiter verifiziert.

Zusammenfassend ist festzuhalten, dass unser Reporterzellsystem als Plattformtechnologie von großem Wert ist, da es die Analyse unabhängig von primären T-Zellen erlaubt, zwischen Laboren exportierbar ist und angepasst werden kann, um klein bis groß angelegte Screenings mit CAR-Bibliotheken zu ermöglichen. Die Auswahl geeigneter Kandidaten mit optimalen extrazellulären und intrazellulären Modulen kann die Anzahl der zu untersuchenden CAR-Konstrukte in anschließenden *in vitro*- und *in vivo*-Studien mit primären T-Zellen reduzieren. Wir sind daher überzeugt, dass unsere CAR-Screening-Plattform basierend auf NF-κB/NFAT-Reporterzellen hilfreich sein wird, um die translationale Forschung zu beschleunigen, indem sie die Untersuchung von neuen Designparametern in CARs erleichtert.

# 1 Introduction

## 1.1 Cancer immunotherapy with CAR-modified T cells

Cancer immunotherapy focuses on reactivating or redirecting the immune system to recognize and eliminate tumor cells. T cells represent a preferred cell type for cancer immunotherapy because of their antigen specificity and the ability to migrate into malignant tissues and develop an immunological memory to control tumor relapse. In cancer patients, T cells can be reactivated by vaccination with tumor-specific antigenic peptides, but this requires the presence of a pre-existing T cell population that reacts against the introduced peptides.[1] Alternatively, autologous tumor-reactive or tumor-infiltrating T cells can be isolated from tumor biopsies, expanded outside of the body, and reinfused into the patient.[2] It is important to note that both therapeutic strategies require the presence of high-affinity T cell receptors (TCR) on endogenous tumor-reactive T cells to be clinically effective. To overcome this requirement, T cells can instead be genetically modified to express a tumor-specific, recombinant TCR or a chimeric antigen receptor (CAR). Both, TCR and CAR, can recognize tumor-specific or tumor-associated antigens and thereby redirect T cell specificity to cancer cells.[3] The main advantage of the CAR over the TCR is that the CAR usually detects surface antigens independently of antigen presentation by the major histocompatibility complex (MHC). Thus, tumor cells cannot escape CAR-T cell detection by downregulating MHC molecules. Moreover, in contrast to the TCR, which relies on co-receptors to initiate full T cell activation, the CAR combines stimulatory and co-stimulatory signaling domains to fully activate the T cell when the CAR binds its antigen.[4]

The manufacturing of CAR-T cells generally begins with the isolation of peripheral blood mononuclear cells (PBMCs). From the PBMCs, specific T cell subsets can be isolated and modified with a CAR by genetic engineering, for example by transduction with retro- or lentiviral vectors, or by transfection with RNA or DNA transposon systems.[5] Depending on the manufacturing protocols, CAR-positive T cells can then be enriched and/or expanded and subsequently analyzed for their *in vitro* and *in vivo* functions. For use in humans, cancer patients usually receive a lymphodepleting regimen prior to administration of autologous or allogeneic CAR-T cells.[6]

Until 2016, about 220 clinical trials with CAR-T cells, including 188 ongoing studies, were documented for hematologic and solid malignancies, conducted mainly in the USA and China. Importantly, greatest success so far has been achieved with CD19-specific CARs for B cell malignancies. Clinical studies with patients suffering from B cell acute lymphoblastic leukemia (B-ALL) or Non-Hodgkin lymphoma (NHL) achieved complete remission rates of more than 85% after treatment with CD19-CAR-T cells, and long-term follow-up demonstrated durable remissions and event-free

survival.[6] A milestone for CAR-T cell immunotherapy was reached in 2017 when Novartis and Gilead received FDA approval for the first CAR-T cell products, tisagenlecleucel for use in pediatric and young adult patients with CD19-positive relapsed or refractory B-ALL,[7] and axicabtagene ciloleucel for use in adult patients with relapsed or refractory diffuse large B cell lymphoma.[8] However, it took more than 20 years from the development of the first chimeric receptors in the early 1990s to the clinical implementation of CD19-CAR-T cell therapy.[9,10] In early 2000, the first CARs specifically targeting CD19 on B cell tumors were generated and preclinically evaluated,[11,12] but it was not until the beginning of 2010 that publications of clinical studies revealed the impressive breakthroughs of CD19-CAR-T cell therapy.[13,14] In particular, the time required for testing different CAR constructs and the optimization of individual CAR elements in preclinical research have slowed down clinical translation of CD19-CAR-T cells. To ensure that future CAR-T cell therapies enter the clinical phase earlier, it would be beneficial to extend preclinical research with novel screening platforms that facilitate and accelerate the development of CARs.

## 1.2 Structure of CAR and TCR complex

Although the structure of the CAR is largely based on components derived from the TCR complex, CAR and TCR differ regarding the mode of antigen recognition and T cell activation. Therefore, structural aspects of the CAR and their functional consequences are explained in more detail in this Chapter.

In αβ T cells, the TCR is a heterodimer that consists of one α- and one β-chain, each comprising a variable and a constant domain (Figure 1.1). The variable domains of the TCR mediate the recognition of MHC-presented small peptides through complementarity determining regions (CDR). Especially CDR3 is important in determining the binding specificity of the TCR due to its high variability that results from combinatorial and junctional diversity.[15,16] In contrast, antigen recognition of the CAR is determined by an extracellular binding module containing a single-chain fragment variable (scFv), which incorporates the variable heavy ($V_H$) and variable light ($V_L$) domains of a monoclonal antibody (mAb) connected via a linker sequence.[17] Because the scFv is derived from an antibody, CAR-antigen binding is not only MHC independent but also enables recognition of almost any cell surface antigen (e.g. proteins, carbohydrates, glycolipids) against which a monoclonal antibody can be generated.[4] If no antibody is available for a specific antigen, or targeting of an MHC-presented peptide is necessary, the scFv can be replaced in the CAR framework, e.g. by a single-chain TCR, Adnectin or DARPin.[18–20] Affinity and specificity of the scFv are decisive factors that influence the functionality of CARs and are discussed in more detail in Chapter 1.3.1

Since the TCR α and β chain lack intracellular signaling domains, an interaction with additional cell surface molecules is required, forming a TCR complex (Figure 1.1). The first signal is generated by associated CD3 molecules (CD3ζ, CD3εγ and CD3εδ), which harbor immunoreceptor tyrosine-based activation motifs (ITAM) to attract Src family kinases for the phosphorylation of downstream molecules.[21] These kinases are associated with the co-receptors CD4 or CD8, which determine binding of the TCR complex to either MHC I or II molecules.[22] To entirely activate the T cell, a second signal is required, which is induced by co-stimulatory receptors such as CD28 or 4-1BB. The regulation and termination of T cell activation is achieved through inhibitory co-receptors like CTLA-4 or PD-1.[23] In contrast, the intracellular signal module of a CAR generates both the first and the second signal by combining domains from CD3 and co-stimulatory receptors that include phosphorylation sites for the recruitment of kinases and adaptor proteins.[24] Thereby, the CD3ζ chain domain is the central component of the signal module and can be extended by co-stimulatory domains, with the presence and number of co-stimulatory domains classifying the CARs in first, second and third generation.[25,26] As the CAR signal module transmits the external stimulus into the cell and induces distinct signaling pathways, it determines CAR-T cell activation and functions, which is explained in detail in Chapter 1.4.

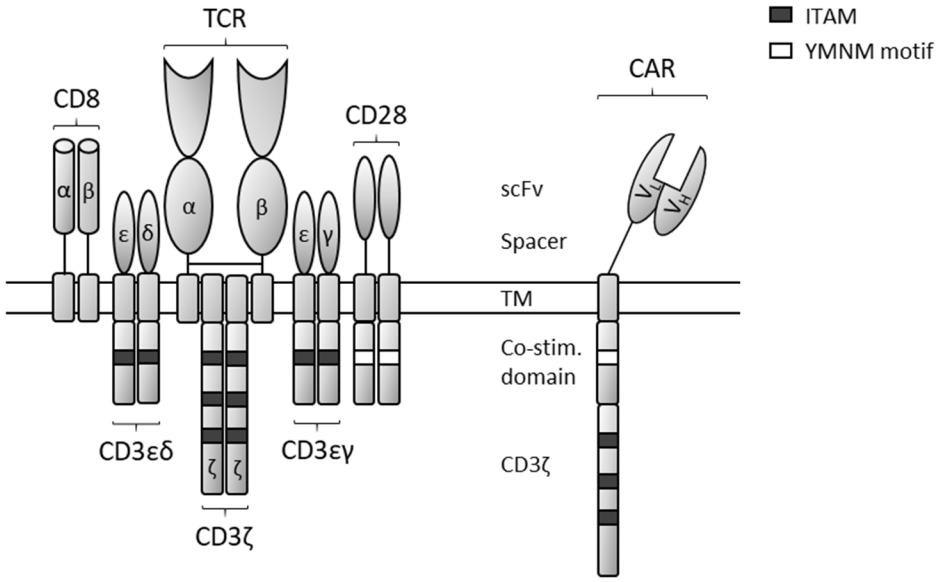


**Figure 1.1: Comparison of TCR and CAR.**

The TCR, which determines specificity to an MHC-presented peptide, forms a complex with several co-receptors that are involved in MHC recognition and signal transduction. For instance, the αβ TCR of cytotoxic T cells is associated with the CD8 co-receptor that binds MHC I. CD3 molecules (CD3ζ, CD3εγ and CD3εδ) containing ITAMs for phosphorylation and signal transduction are also associated with the TCR. Co-stimulatory receptors such as CD28 with YMNM phosphorylation sequence are recruited after TCR stimulation to amplify the signal. In contrast, CAR is a one-chain receptor combining antigen-binding and signal modules. Here, an antibody-derived scFv with variable heavy ($V_H$) and variable light ($V_L$) domains determines antigen specificity and is linked via a spacer and transmembrane (TM) domain to intracellular signaling moieties that provide motifs for phosphorylation and recruitment of kinases and adaptor proteins. The second generation CAR illustrated here contains a co-stimulatory domain in addition to a CD3ζ signal domain.

To enable the formation of a heterodimer between the α- and β-chain of the TCR, the constant domains of both chains are attached to a hinge region that comprises several cysteine residues. These cysteines form a disulfide bond and link the two chains.[15] The extracellular binding module of the CAR includes a so-called spacer domain connected to the scFv, whose primary purpose is to provide flexibility and antigen accessibility of the scFv.[27] This domain can be derived from the CD8 α-chain or from immunoglobulin-like domains of the Fc region of IgG antibodies, which may also contain cysteines leading to dimerization of CARs.[28,29] The role of the spacer domain as a steric determinant of CAR-antigen binding is described in detail in Chapter 1.3.2.

The transmembrane domain anchors the TCR to the cell surface. Basic residues within the transmembrane domain closely interact with acidic residues of the transmembrane domain of CD3 molecules, enabling association of the TCR with CD3.[30] Likewise, the transmembrane domain of the CAR serves to connect the receptor to the cell surface but is usually derived from type I membrane proteins such as CD3, CD8, CD28 or OX40. It is not primarily required for interaction with other proteins, but instead some studies suggest that it may play a role in CAR dimerization and expression.[26,31]

The TCR-encoding gene loci are located on chromosomes 7 and 14 in humans, and TCR diversity results from combinatorial recombination of gene segments and junctional diversity, forming unique segment combinations in each T cell.[15] In contrast, the CAR is an artificial protein generated *in vitro* by cloning techniques and then integrated into the genome of a T cell. Similarly to the TCR, the cell surface expression of the CAR requires a signal peptide at its N-terminus, resulting in translocation to the endoplasmic reticulum and the secretory pathway.[32] In principle, the signal peptide can originate from any transmembrane protein, but commonly GM-CSF or CD8α signal peptides are used for CARs. In addition, the CAR gene cassette often contains a transduction marker separated from the CAR through a viral 2A self-cleaving peptide sequence (Figure 1.2).[33] Truncated, non-functional versions of EGFR or LNGFR can serve as transduction markers and for enriching CAR-positive T cells.[34,35]

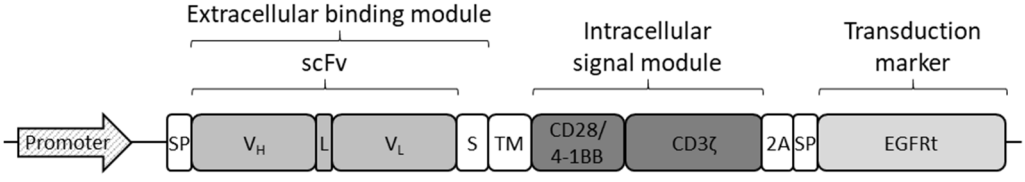


**Figure 1.2: Example of a bicistronic gene encoding a second generation CAR.**

A prototypic second generation CAR construct starts with a signal peptide (SP) and the scFv, composed of a variable heavy ($V_H$) and light ($V_L$) domain connected via a linker (L) sequence. A spacer (S) and transmembrane (TM) domain connect the signal module, which consists of a co-stimulatory domain (e. g. from CD28 or 4-1BB) and the CD3ζ signal domain. The depicted CAR gene is separated by a 2A cleaving sequence from the truncated epidermal growth factor receptor (EGFRt) transduction marker, and a promoter is located upstream of the bicistronic gene.

It remains difficult to predict the functionality of a CAR due to its modular structure. Individual CAR modules must be empirically tested, which makes preclinical research time-consuming and laborious. It is therefore desirable to develop screening platforms that facilitate the identification of optimal CAR design parameters and accelerate CAR development.

## 1.3 The extracellular binding module of CARs

### 1.3.1 Binding and affinity of the scFv

The CAR recognizes its target antigen through the antibody-derived scFv in the extracellular binding module. Here, specificity and affinity of the scFv play a crucial role, and both factors are influenced by CDR diversity. Both $V_H$ and $V_L$ domains of the scFv possess three CDR regions that form the antigen-binding pocket. CDR3 has the largest contact area with the antigen and substantially affects the binding properties of the whole scFv.[17] While TCR affinity ranges between a $K_d$ of $10^{-4}$ and $10^{-6}$ M, leading to a high off-rate to the MHC-peptide complex,[36] antibodies used to engineer scFv molecules show much higher affinity in the $K_d$ range of $10^{-6}$ to $10^{-11}$ M.[37]

A number of studies suggest that scFv affinity influences the activity of CAR-T cells. The comparison of two ROR1-specific CARs with different affinities showed that the CAR with the higher affinity conferred maximum T cell activation regarding cytokine release and proliferation.[38] Another study correlated T cell activation with the affinity of HER2-CARs, demonstrating that medium- and high-affinity CARs ($K_d < 10^{-8}$ M) activated T cells in a similar fashion, whereas low-affinity CARs ($K_d > 10^{-8}$ M) activated T cells with substantially lower efficiency.[39] However, one study also suggests that under specific conditions high scFv affinity can cause fatal side effects. Although an affinity-enhancing mutation in an anti-GD2 scFv increased the antitumor function of CAR-T cells in a human neuroblastoma xenograft model, it was associated with lethal toxicity because CAR-T cells increasingly infiltrated the brain and eliminated healthy neuronal cells with low GD2 expression.[40] In certain situations, affinity can even influence specificity, for example for a high-affinity CAR that recognizes an MHC-presented NY-ESO-1 peptide. This CAR also lysed target cells that expressed just MHC without NY-ESO-1 peptide. Lowering the scFv affinity in this CAR improved the specificity for exclusively NY-ESO-1 peptide-presenting MHC.[41]

Apparently, scFv affinity also controls the selectivity of CAR-T cells against target cells with different antigen expression levels, as an FRα-specific CAR eliminated tumor xenografts with high FRα expression more effectively than with low or moderate expression.[42] Therefore, the concept of CAR

affinity tuning is intended to increase the selectivity of CAR-T cells towards target cells. Because CARs comprising a low-affinity scFv only efficiently eliminate tumor cells with high antigen expression, healthy cells that express physiologic antigen levels are excluded, which reduces systemic off-tumor toxicity.[43,44]

While the above studies have compared only a few CAR constructs with known scFv affinities, it is also conceivable analyze a large number of CAR constructs with unknown affinities, e.g. generated through rational modifications of the $V_L$ and $V_H$ CDR regions.[45,46] To enable the processing of multiple CARs with minimal effort, a platform would be required that facilitates scalable screening campaigns and provides a quantitative readout to compare the activity of individual CARs with altered affinity.

### 1.3.2 Spacer design and length

Another component of the extracellular binding module of the CAR is the spacer domain, which affects extracellular flexibility, CAR-antigen binding and dimerization. A study compared spacer domains derived from CD8α and CD28 and showed less activation-induced cell death (AICD) and production of inflammatory cytokines for CD19-CAR-T cells with CD8α spacer. This was probably due to reduced CAR homodimer formation by the CD8a spacer, leading to less aggregation of CD3ζ molecules and consequently less T cell activation.[47] Other studies revealed that certain spacer domains can be recognized by cells of the innate immune system resulting in the elimination of CAR-T cells. For instance, the Fc-binding site of the CH2 domain of IgG4-based spacers was targeted by myeloid cells expressing Fcγ-receptors, which triggered AICD and prevented CAR-T cell engraftment in mice. However, this was averted either by removing the CH2 domain or by specific mutations of the Fc-binding site in the CH2 domain.[48,49] Similarly, the CH2 domain of an IgG1 spacer was highly recognized by monocytes, macrophages and NK cells, resulting in reduced *in vivo* CAR-T cell survival, while an IgG2 spacer abrogated this interaction and thus led to less tonic signaling and T cell senescence.[50]

Several studies have focused on the spacer length, which influences the ability of the CAR to bind its target epitope on target cells. This was generally exemplified by the comparison of CARs with and without spacer domain, showing superior *in vivo* antitumor function only by CARs with spacer domain when targeting antigens like CD19, mesothelin, PSCA, Mucin-1 or HER2.[51] Another study showed that a CEA-specific CAR with long spacer domain significantly increased T cell activation after its target epitope was transferred from a membrane-distal to a membrane-proximal position within the CEA protein.[52] The impact of spacer length and epitope position was further confirmed by ROR1-CARs that recognize epitopes at different locations in the protein. Here, a CAR with long IgG4-Fc-based spacer

caused high T cell activation when targeting the membrane-proximal R11 epitope, whereas a CAR with short IgG4-Fc-based spacer resulted in enhanced antitumor function when targeting the membrane-distal epitopes R12 or 2A2.[38,48]

Accordingly, the spacer length represents a critical factor in CAR design and needs to be considered to target membrane-distal or membrane-proximal epitopes. However, this requires careful screening campaigns for identifying the optimal spacer domain. Particularly when using primary T cells, this involves time-consuming and laborious experiments. Therefore, a cell line-based platform would facilitate these screening campaigns by accelerating the identification of CAR lead candidates with optimal spacer domain.

## 1.4 The intracellular signal module of CARs

The intracellular signal module of CARs converts the stimulus from antigen binding of the extracellular module into a signal that initiates intracellular activation pathways. Initially, CARs were developed to mimic the TCR complex in mediating antigen specificity and the first activation signal. Based on experimental results obtained from fusion proteins comprising the extracellular domain of CD8 and the cytoplasmic domain of CD3,[53] only the CD3ζ-chain was attached to scFvs, generating receptors that are known as first generation CARs.[9,10] Thus, a PSMA-specific first generation CAR could redirect a T cell to a PSMA-positive target cell, resulting in tumor lysis.[54] However, T cells expressing first generation CARs generally produced relatively low amounts of cytokines, rapidly became anergic and only caused moderately delayed tumor progression *in vivo*.[55,56]

To prevent anergy and exhaustion, and instead modulate and amplify the activation of T cells, a second signal is generated by co-receptors in addition to the first signal generated by the TCR complex.[57] Accordingly, first generation CAR-T cells, which additionally expressed ligands that stimulate T cell co-stimulatory receptors, showed improved antitumor function and persistence.[58] Based on this observation, second generation CARs include, in addition to the CD3ζ chain, the intracellular domain from co-stimulatory receptors like CD28, 4-1BB, ICOS or OX40, resulting in increased cytokine secretion, cytotoxicity and proliferation of CAR-T cells.[25] Moreover, studies in mice with B cell leukemia demonstrated prolonged survival and enhanced antitumor function with CD19-CAR-T cells containing the CD28 domain in the intracellular signal module.[11,59] In clinical studies, the CD28 co-stimulatory domain significantly improved expansion and persistence of CD19-CAR-T cells in patients with relapsed or refractory NHL,[60] and the 4-1BB co-stimulatory domain enhanced the antitumor function in patients with B cell leukemia.[61]

Interestingly, modification of second generation CAR-T cells with an additional co-stimulatory ligand further enhanced persistence and reduced exhaustion.[62] Accordingly, third generation CARs with two co-stimulatory domains in addition to the CD3ζ domain are supposed to improve CAR-T cell functionality. The combination of CD28 and 4-1BB in CARs targeting e.g. PSMA, CD171 or mesothelin amplified cytokine production and suppressed AICD of CAR-T cells, thus significantly reducing the tumor burden in mice.[63–65] Other co-stimulatory domains like ICOS, OX40 or TLR2 can be used in combination with CD28 to enhance the efficacy of CAR-T cells *in vitro* and in patients with B-ALL.[26,66,67]

At present, most studies have focused on second generation CARs with CD28 or 4-1BB co-stimulatory domain and their influence on T cell activation and effector functions. Both domains induce $T_H1$ cytokine secretion, including IL-2, IFNγ, TNFα and GM-CSF, although faster with CD28 and slower with 4-1BB.[25,63,65] $T_H2$ cytokines like IL-4 and IL-10 were produced at markedly lower concentrations by CARs with 4-1BB domain.[25,68] Further, CARs with CD28 or 4-1BB co-stimulation demonstrated similar levels of total tyrosine phosphorylation, but a CAR with CD28 domain induced the PI3K/Akt pathway in a more consistent manner.[25,65] Interestingly, in a bone-metastatic prostate cancer xenograft model, less exhaustion and improved persistence of CAR-T cells with 4-1BB domain was observed in comparison to CAR-T cells with CD28 domain.[69] The 4-1BB domain also promoted growth of $CD8^+$ central memory CAR-T cells with enhanced respiratory capacity, whereas the CD28 domain resulted in effector memory CAR-T cells with a genetic signature consistent with enhanced glycolysis.[70] In addition, one CAR study showed reduction of tonic signaling and exhaustion via 4-1BB,[71] however, this is contradictory to another CAR study where CD28 caused less tonic signaling.[72]

Although the intracellular signal module of CARs is designed for signal transduction and initiation of signaling pathways, most studies have mainly assessed the effector T cell functions that follow CAR stimulation. An alternative approach could directly focus on induced signaling pathways and transcription factors to measure and compare the differences between CAR signal modules more precisely. Thereby, high-throughput CAR-screening campaigns could identify signal modules with optimal activation profile, e.g. to induce certain T cell functions, activate specific T cell subsets or control T cell differentiation.

## 1.5 Selectivity of CAR-T cells

A major obstacle in CAR-T cell therapy is the selectivity of the CAR-modified T cells, i.e., the distinction of tumor cells from healthy cells, which can result in on-target off-tumor toxicities. This is due to the fact that a broad spectrum of tumor-associated antigens, which are targeted by CARs, are also frequently expressed by healthy cells and thus also attacked by CAR-T cells.[73] The lack of CAR-T cell

selectivity and ensuing on-target off-tumor toxicity is more predictable for hematologic than solid malignancies due to known lineage-restricted antigen expression in the hematopoietic system. Studies with CD19-CARs in mice and humans demonstrated B cell aplasia following CAR-T cell transfer, which is not life-threatening as it can be compensated by immunoglobulin infusions.[74,75] In contrast, CAR-T cell selectivity is rather challenging for solid tumors since overexpressed tumor-associated antigens are often found on healthy tissues at lower levels. Two studies in cancer patients have shown lethal complications from pulmonary or liver toxicities after treatment with HER2- or CAIX-CARs, respectively.[76,77]

Strategies have evolved that do not improve the selectivity of CAR-T cells but aim to mitigate the on-target off-tumor toxicity during CAR-T cell therapy in patients. One strategy relies on the elimination of CAR-T cells after toxicity onset, e.g. by antibody-mediated depletion, e.g. facilitated by a transduction marker like EGFRt co-expressed with the CAR,[78] or with inducible caspases that are activated by dimerization.[35] Although these approaches can be controlled in a dose-dependent manner to prevent complete CAR-T cell eradication, the therapeutic effect might be attenuated or even terminated. Therefore, other strategies based on transient CAR activation have been developed to protect healthy cells, with the negative effect that tumor cells are temporarily spared from elimination as well. For instance, an FKBP12 domain can be included in the CAR spacer to release the scFv from the cell membrane after binding a small molecule,[79] or soluble targeting modules can be used that transiently bind to the extracellular portion of the CAR to enable antigen recognition.[80]

There are also strategies that attempt to improve the selectivity of CAR-T cells by enabling distinction between malignant and healthy cells, thus preventing the onset of on-target off-tumor toxicities. For instance, CAR affinity tuning enables T cells to distinguish between different antigen expression levels, but this also excludes tumor cells with low surface antigen density from eradication.[43,44] Another strategy aims at building logic gates, e.g. consisting of two CARs targeting two separate antigens on one tumor cell. One CAR contains only the CD3ζ-chain (first signal) and the other CAR contains only the co-stimulatory domain (second signal). In this example, full CAR-T cell activation is only triggered if both CARs simultaneously bind a malignant cell that expresses both target antigens.[81,82] A logic gate can also comprise activating and inhibitory CARs, whereby the activating CAR recognizes a tumor-associated antigen on both malignant and healthy cells, but is impaired by an inhibitory CAR (iCAR) that recognizes an antigen expressed only on healthy cells.[83] However, the logic gate strategy presumably requires identification of appropriate antigen combinations and co-stimulatory or inhibitory signaling domains. Instead of analyzing these critical parameters with primary T cells and assessment of ensuing effector functions, it would be advantageous to initially employ a screening platform that allows rapid implementation and pre-selection of functional logic gates.

## 1.6 Overview of T cell signaling pathways

### 1.6.1 TCR-mediated signaling in T cells

Binding of the TCR to a specific peptide that is presented by an MHC molecule initiates T cell activation and the recruitment of CD4 or CD8 co-receptors providing the Src family kinases Lck and Fyn.[22] These kinases phosphorylate the ITAMs of TCR-associated CD3 molecules, enabling the binding of ZAP-70 to the TCR complex (Figure 1.3).[84] This results in the induction of a downstream signaling cascade via phosphorylation of the adaptor protein LAT and formation of the TCR signalosome.[85] The complex includes PLCγ1, PI3K, GRB2 and SLP-76 as well as proteins involved in actin cytoskeleton reorganization. PLCγ1 is particularly important, because it catalyzes the hydrolysis of $PIP_2$ to the second messengers DAG and $IP_3$, both essential for further signal transfer.[86]

DAG mediates the initiation of the MAPK/ERK pathway that activates the transcription factor activator protein-1 (AP-1). It also regulates PKCθ signaling, which results in the activation of the transcription factor family of nuclear factor-κB (NF-κB).[86] This family consists of the proteins RelA (p65), RelB, c-Rel, NF-κB1 (p50) and NF-κB2 (p52) that form homo- or heterodimers. In unstimulated cells, NF-κB is associated with inhibitor of NF-κB (IκB) family members that retain the protein in the cytosol. Upon activation, IκB is degraded, which allows NF-κB to translocate into the nucleus where it binds to its target genes.[87] These genes determine T cell survival, proliferation and homeostasis, e.g. through regulation of chemokines (IFNγ), growth factors (GM-CSF), immune receptors (ICOS), adhesion molecules (CCR7) and cell cycle regulators (cyclin D1).[88]

The other second messenger, $IP_3$, stimulates calcium-permeable ion channel receptors in the endoplasmic reticulum, which results in the release of $Ca^{2+}$ into the cytosol. This activates the calcium-calmodulin-dependent phosphatase calcineurin, which dephosphorylates members of the nuclear factor of activated T cells (NFAT) family, leading to their translocation to the nucleus. Four calcium-regulated members (NFATc1 to NFATc4) are known, which remain inactive in the cytosol until the nuclear localization signal is unmasked by dephosphorylation.[89] In the nucleus, NFAT can form co-operative complexes with other transcription factors such as AP-1 or STAT family members. NFAT activation also integrates additional signaling pathways associated with transcription factors like T-bet and GATA3, which results in differential gene expression patterns.[89,90] Thereby, NFAT controls T cell development, differentiation and effector functions by expression of cytokines (IL-2, IFNγ, TNFα) and immune receptor ligands (CD40L, CD95L), as well as downregulation of cell cycle regulators (CDK4).[89]

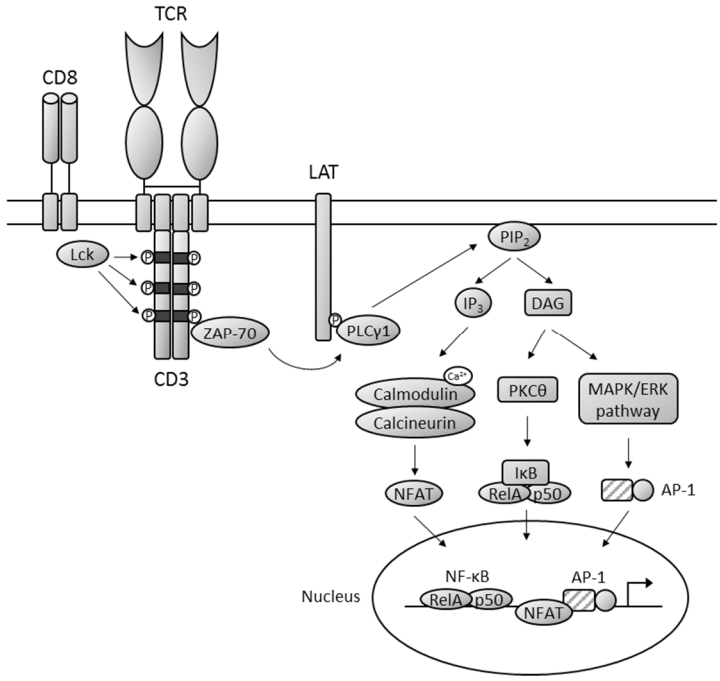


**Figure 1.3: Simplified illustration of TCR-induced signaling pathways.**

Upon TCR engagement, CD8 supplies the kinase Lck that phosphorylates ITAMs of CD3 molecules. ZAP-70 is recruited and phosphorylates the adaptor protein LAT, leading to the binding of PLCγ1. This protein catalyzes the hydrolysis of $PIP_2$ into the second messengers DAG and $IP_3$. DAG induces the MAPK/ERK signaling pathway to activate transcription factor AP-1 and causes the inhibitor IκB to detach from the NF-κB heterodimer via PKCθ. $IP_3$ results in an increase of intracellular $Ca^{2+}$ that bind to calmodulin, forming a complex with calcineurin to dephosphorylate NFAT. All three transcription factors then migrate into the nucleus and bind to response elements located in the proximity of genes to activate their expression.

TCR-induced signaling is amplified by co-stimulatory receptors, which are recruited to the TCR complex. For instance, CD28 affects cytokine production, cell cycle progression, apoptosis and metabolism via recruitment of Ras, Lck and PKCθ, thereby activating NFAT.[91] Additionally, CD28 regulates the kinase mTOR as well as the transcription factors c-Myc and NF-κB via the PI3K/Akt pathway.[92,93] The co-stimulatory receptor 4-1BB enhances proliferation and cytotoxicity, and prevents AICD.[94] These positive effects are presumably related to 4-1BB-induced TNF receptor-associated factors that affect NF-κB, MAPK/ERK or PI3K/Akt pathways.[95–97]

Several studies have shown that transcription factors, in particular NF-κB and NFAT, are indicators of the strength and duration of TCR-mediated T cell activation. For instance, NFAT induction correlates positively with TCR stimulation and is a regulator of the resulting T cell response.[98–100] Similarly, NF-κB induction depends on the magnitude of the TCR signal, thus affecting cytokine production, T cell proliferation and survival.[101–103] Accordingly, screening campaigns were conducted based on transcription factors,[104] suggesting that platforms that detect both NF-κB and NFAT could be employed to analyze the functionality of stimulatory receptors.

### 1.6.2 CAR-mediated signaling in T cells

Recent studies suggest that CAR-antigen binding activates proteins of signaling pathways that are also activated by TCR stimulation in human T cells. For instance, early events like phosphorylation of the CD3ζ signaling domain or the Src family kinase Lck also occur after CAR stimulation. Further, depending on the type of co-stimulatory CAR domain, phosphorylation of receptor proximal signaling proteins like ZAP-70 and LAT is detectable besides activation of downstream signaling proteins like Ras, ERK, CREB and calmodulin.[105,106] These proteins, typically required for efficient TCR signaling, are partially involved in the MAPK/ERK pathway and affect activation of transcription factors like NF-κB or NFAT. In addition, the members of the PI3K/Akt pathway are controlled by CARs depending on the included co-stimulatory signaling domains.[65,107] Direct comparison between TCR and CAR stimulation by reverse phase protein lysate microarray showed that the same signaling proteins (e.g. PKCδ, ERK or c-Met) are expressed at comparable levels. After a short time, however, this changed for 43 of the 308 assessed proteins involved in protein trafficking, proliferation and cell survival, suggesting that typical TCR signaling pathways are temporary altered upon CAR stimulation.[108]

Release of intracellular calcium as part of the calcium-mediated signaling pathway that activates NFAT and represents a characteristic event in T cell activation, was also observed following CAR stimulation.[109] Moreover, studies reported NFAT activation via inducible reporter gene systems or inducible cytokine secretion in T cells and Jurkat cells,[110–113] and similarly, NF-κB signaling after CAR stimulation has been described.[26,114] Transcription factors of the STAT family, which are often associated with NFAT, were also found activated and phosphorylated after CAR stimulation.[115] Further, triggering of the CAR results in the expression of proteins that typically appear upon TCR stimulation, including cytokines like IL-2 and IFNγ, and surface proteins like CD25.[66,106]

These observations collectively lead to the conclusion that CAR and TCR engage similar signaling pathways but presumably at different intensities and influenced by the type of co-stimulatory domain in the CAR framework. Moreover, CAR stimulation apparently causes activation of NF-κB and NFAT, suggesting that these factors could be used as surrogate markers of CAR-T cell functions and provide a quantitative readout when an adequate detection method is applied. Consequently, the analysis of both NF-κB and NFAT, implemented in a cellular platform, could facilitate screening campaigns for the evaluation of different CAR modules and the selection of CAR lead candidates for further investigation.

## 1.7 Functional analysis of CAR-T cells

In preclinical studies, the functionality of extracellular and intracellular CAR modules is evaluated by testing and comparing individual CAR constructs in primary T cells using distinct

methods (Figure 1.4). Typically, CAR-T cells are graded by the level of target cell lysis. Thereby, CAR-mediated target cell lysis is often quantified by radioactive chromium-51 release or luciferase activity.[64,116] Cytokines like IL-2 or IFNγ, which are secreted by $CD4^+$ T helper cells and $CD8^+$ cytotoxic T cells at different amounts following stimulation, are frequently measured with ELISA or bead-based multiplex assay.[38,117] Proliferation of CAR-T cells is studied to conclude whether the cells will persist *in vivo*. The labeling of CAR-T cells with fluorescent cell staining dyes like CFSE is frequently used to estimate the number of cell divisions upon activation but takes several days.[25] In addition, markers of T cell activation and differentiation that are expressed on the cell surface, such as the receptors CD25 and CD69 or the co-stimulatory ligands CD40L and CD137L, are stained with fluorophore-labeled antibodies and detected by flow cytometry.[118]

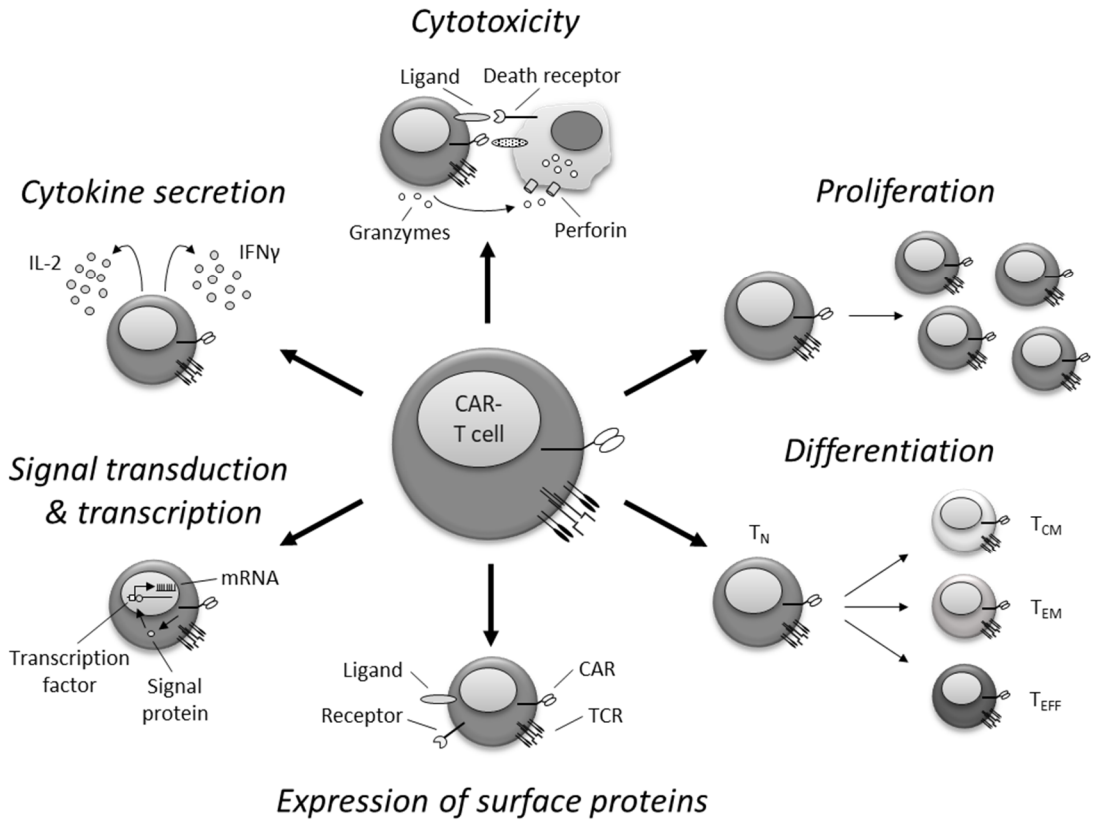


**Figure 1.4: Induced T cell functions and events upon CAR stimulation.**

CAR functionality is frequently evaluated by measuring T cell functions and events that are induced upon antigen-specific stimulation. For example, cytotoxicity of CAR-T cells can be assessed, resulting from the elimination of target cells by granzymes and perforin or by death receptor engagement. CAR-T cell activation can also trigger the release of cytokines (e.g. IL-2, IFNγ) detectable in the supernatant, or induce proliferation reflected by increased number of cell divisions. In addition, CAR stimulation leads to the activation of signaling pathways and a quantifiable increase in transcriptional activity, which is accompanied by differentiation, e.g. in central memory ($T_{CM}$), effector memory ($T_{EM}$) or effector ($T_{EFF}$) T cells, and expression of phenotypic proteins that can be detected on the cell surface.

Cytokine production, proliferation and expression of surface proteins are events resulting from the induction of intracellular signaling pathways. Thus, CAR functionality can also be assessed by the analysis of signaling proteins and second messengers. For instance, intracellular calcium flux can be measured by fluorescence microscopy,[109] or phosphorylated signaling proteins can be analyzed by western blot or microarrays upon CAR stimulation.[66,105] Alternatively, CAR activity can be evaluated by the detection of transcription factors such as NF-κB or NFAT. Inducible reporter genes can be used for example, which are integrated into primary T cells and indicate transcription factor activation via fluorescence or luminescence.[26,112] Likewise, transcriptional analysis, e.g. of genes involved in differentiation and exhaustion, by quantitative PCR or microarrays allows conclusions regarding CAR functionality.[62,71]

Since these analyses are commonly performed in primary T cells, CAR-screening campaigns are often laborious, time-intensive and confounded by donor-to-donor variability in T cell subset composition, variable genomic insertion of the CAR gene, and ensuing differences in CAR surface expression.[72,119,120] This can result in a high degree of variability and poor reproducibility between individual testing campaigns performed in the same or in different laboratories. In contrast, pharmaceutical small molecule and antibody discovery identifies lead compounds from library-screening campaigns using standardized platforms, which are often based on cell lines.[121,122] A standardized platform that is able to identify functional CAR lead candidates with high accuracy would therefore be desirable but requires a rapid and robust readout without using primary T cells. However, most of the methods described above can only be performed in primary T cells or are too time-consuming, cost-intensive or complex to be employed in platform-based screening campaigns. Instead, detection of activated signaling proteins, e.g. by reporter genes stably integrated into a cell line, would provide a robust platform technology to rapidly analyze CAR functionality and to enable large-scale CAR-screening campaigns.

## 1.8 Hypotheses and aims of this study

Immunotherapy with CAR-T cells represents a transformative, novel treatment in hematology and oncology.[6] CARs are synthetic designer molecules whose functionality is influenced by the choice of the extracellular binding module, including the antigen-binding domain and its affinity as well as the length and composition of the spacer domain, and the intracellular signal module, which comprises stimulatory and co-stimulatory moieties.[5] It is important to note that the use of CARs with non-optimized modules in T cells can lead to significantly impaired or even absent tumor cell recognition and antitumor function.[38,48] The current state-of-the-art for identifying the optimal CAR

composition is to perform screening campaigns in primary T cells which, however, have limited capacity and are unable to interrogate the number of variations in CAR design that are conceivable by combining available variants of the extracellular binding and intracellular signal modules.

We reasoned that these challenges could be addressed with a standardized CAR-screening platform that is independent of primary T cells but provides an easy-to-measure, quantitative readout as a surrogate for primary T cell function. Because Jurkat cells comprise the entire signaling machinery of primary T cells that turns them into an intuitive tool for the analysis of T cell immunoreceptors, we have chosen these cells as the basis for developing the CAR-screening platform. We hypothesized that the transcription factors NF-κB and NFAT could be used as indicators of CAR stimulation and signaling output of the platform. We approached this by introducing NF-κB and NFAT-inducible reporter genes that encode fluorescent proteins to readily quantify CAR activation and enable scalable screening campaigns of CAR libraries for identifying lead candidates with optimal design parameters.

To test our hypotheses, we designed a work program with the following specific aims:

I. Evaluation of the transcription factors NF-κB and NFAT as indicators for CAR activation in primary T cells.

II. Generation of a Jurkat-based CAR-screening platform with a quantitative readout of NF-κB and NFAT activation.

III. Validation of the platform in small-scale screening campaigns with CAR modules that provide optimal function in primary T cells.

IV. Implementation of a large-scale screening campaign with a complex library comprising a high number of CAR variants.

V. Investigation of CARs with inhibitory signal modules in logic gate applications.

To address these specific aims, we planned to pursue several experimental approaches. First, $CD4^+$ or $CD8^+$ primary T cells from healthy donors should be prepared and modified with a ROR1-specific CAR to analyze by western blot whether antigen-dependent stimulation would lead to NF-κB and NFAT activation. According to these findings, a CAR-screening platform based on Jurkat cells should be established that allows quantitative analysis of NF-κB and NFAT activation by inducible reporter genes. To determine whether NF-κB/NFAT reporter cells could measure CAR-mediated activation, ROR1- and CD19-specific CARs should be integrated into reporter cells, and the NF-κB- and NFAT signals should be analyzed upon stimulation by flow cytometry. Moreover, since we expected CAR-mediated

activation of NF-κB and NFAT to follow kinetics with signal increase, plateau and decrease, we aimed to analyze activation at different times to define the optimal time window for signal detection.

Next, to validate the CAR-screening platform and verify its accuracy and significance, we intended to perform small-scale screening campaigns with CAR libraries that have recently demonstrated functionality in primary T cells. One library should consist of ROR1-CARs that differ in the extracellular spacer domain. After transduction of reporter cells with these CARs, the CAR reporter cells should be stimulated by ROR1-positive target cells to assess if they could identify the construct with optimal spacer length for targeting the R11 epitope. A second library should consist of ROR1-CARs that differ in the intracellular signal module regarding the co-stimulatory domains. Again, we sought to transduce reporter cells with these CARs and stimulate them antigen-dependently to investigate whether NF-κB and NFAT signals reflect the outcome of recent studies with primary T cells.

A large-scale screening campaign should provide the opportunity to determine whether the platform was able to retrieve functional constructs from a large pool of CAR variants. The library should consist of many variants of a ROR1-CAR due to mutations in its scFv, which were supposed to modulate specificity and affinity to ROR1. The library should be integrated into reporter cells by nucleofection, and individual cells should be separated based on high NF-κB and NFAT activation using fluorescence-activated cell sorting (FACS). We speculated that cell clones with high reporter gene signals would contain functional CAR variants, and therefore, we sought to isolate their genomic DNA to analyze the scFv-encoding sequences of the integrated CAR variants.

To assess whether the platform allows the analysis of novel applications such as logic gates with CARs comprising inhibitory signal modules, a library of CD19-specific CARs with inhibitory PD-1 domain should be challenged by CAR or TCR stimulation. To verify the observations from the reporter cell screening campaign, the results should then be reproduced with primary human T cells to eventually demonstrate that the CAR-screening platform enables the accurate analysis of iCARs.

# 2 Materials

## 2.1 Human subjects

Peripheral blood from healthy donors was obtained after written informed consent to participate in research protocols that were approved by the Institutional Review Board of the University of Würzburg.

## 2.2 Cell lines

**Table 2.1: Cell lines.**

| Name | Supplier | Description |
|---|---|---|
| BTLA (NF-κB/NFAT) reporter | Dr. P. Steinberger | NF-κB/NFAT reporter cells transduced with human BTLA |
| BW5147 | Dr. P. Steinberger | Murine lymphoma T cell line |
| BW/CD19 | In-house production | BW5147 cells transduced with human CD19 |
| BW/OKT3 | Dr. P. Steinberger | BW5147 cells transduced with membrane-bound OKT3 scFv |
| BW/OKT3+CD19 | Dr. P. Steinberger | BW5147 cells transduced with membrane-bound OKT3 scFv and human CD19 |
| BW/OKT3+HVEM | Dr. P. Steinberger | BW5147 cells transduced with membrane-bound OKT3 scFv and human HVEM |
| BW/OKT3+PD-L1 | Dr. P. Steinberger | BW5147 cells transduced with membrane-bound OKT3 scFv and human PD-L1 |
| BW/ROR1 | In-house production | BW5147 cells transduced with human ROR1 |
| BW/ROR1+CD19 | In-house production | BW5147 cells transduced with human ROR1 and human CD19 |
| (NF-κB/NFAT) reporter | Dr. P. Steinberger | Jurkat clone E6.1 transduced with NF-κB- and NFAT-inducible reporter genes |
| JeKo-1 | ATCC: CRL-3006 and in-house production | Human mantle cell lymphoma transduced with firefly luciferase |
| Jurkat clone E6.1 | ATCC: TIB-152 | Human T cell lymphoma line |
| K562 | ATCC: CCL-243 and in-house production | Human chronic myelogenous leukemia cell line transduced with firefly luciferase |

| Name | Supplier | Description |
|---|---|---|
| K562/HLA-A*0201 | In-house production | K562 cells transduced with firefly luciferase and HLA-A*0201 |
| K562/HLA-A*0201+CD19 | In-house production | K562 cells transduced with firefly luciferase, HLA-A*0201 and human CD19 |
| K562/ROR1 | In-house production | K562 cells transduced with firefly luciferase and human ROR1 |
| K562/CD19 | In-house production | K562 cells transduced with firefly luciferase and human CD19 |
| K562/ROR1+CD19 | In-house production | K562 cells transduced with firefly luciferase, human ROR1 and human CD19 |
| Lenti-X™ 293T | Takara: 632180 | HEK 293T cell clone for lentivirus production |
| PD-1 (NF-κB/NFAT) reporter | Dr. P. Steinberger | NF-κB/NFAT reporter cells transduced with human PD-1 |
| Platinum A | Cell Biolabs: RV-102 | HEK 293T cell clone for retrovirus production |
| TM-LCL | Dr. S. Riddell | Lymphoblastoid EBV-transformed B cell line, donor initials TM |

## 2.3 Media

**Table 2.2: Adherent cell line medium.**

| Ingredient | Volume (f.c.) |
|---|---|
| DMEM medium with 4.5 g/L glucose and 25 mM HEPES | 500 mL |
| Fetal Calf Serum (heat inactivated) | 50 mL (9% v/v) |
| Penicillin/Streptomycin (10000 U/mL) | 5 mL (90 U/mL) |
| GlutaMAX™ Supplement (100x) | 5 mL (0.9x) |
| All ingredients were mixed and sterilized with 0.22 µm PES-membrane filter | |

**Table 2.3: Reporter medium.**

| Ingredient | Volume (f.c.) |
|---|---|
| IMDM medium with 25 mM HEPES and L-glutamine | 500 mL |
| Fetal Calf Serum (heat inactivated) | 50 mL (9% v/v) |
| Penicillin/Streptomycin (10000 U/mL) | 5 mL (90 U/mL) |
| GlutaMAX™ Supplement (100x) | 5 mL (0.9x) |
| All ingredients were mixed and sterilized with 0.22 µm PES-membrane filter | |

**Table 2.4: Freezing medium.**

| Ingredient | Volume (f.c.) |
|---|---|
| Fetal Calf Serum (heat inactivated) | 45 mL (90% v/v) |
| DMSO | 5 mL (10% v/v) |

**Table 2.5: T cell medium.**

| Ingredient | Volume (f.c.) |
|---|---|
| RPMI 1640 medium with 25 mM HEPES and L-glutamine | 500 mL |
| Human Serum (heat inactivated at 56 °C for 30 min) | 50 mL (9% v/v) |
| Penicillin/Streptomycin (10000 U/mL) | 5 mL (90 U/mL) |
| GlutaMAX™ Supplement (100x) | 5 mL (0.9x) |
| 2-Mercaptoethanol (50 mM) | 0.5 mL (45 µM) |
| All ingredients were mixed and sterilized with 0.22 µm PES-membrane filter | |

**Table 2.6: Tumor cell medium.**

| Ingredient | Volume (f.c.) |
|---|---|
| RPMI 1640 medium with 25 mM HEPES and L-glutamine | 500 mL |
| Fetal Calf Serum (heat inactivated) | 50 mL (9% v/v) |
| Penicillin/Streptomycin (10000 U/mL) | 5 mL (90 U/mL) |
| GlutaMAX™ Supplement (100x) | 5 mL (0.9x) |
| All ingredients were mixed and sterilized with 0.22 µm PES-membrane filter | |

## 2.4 Vectors

**Table 2.7: Vectors.**

| Name (of transgene) | Vector # | Description |
|---|---|---|
| CD19 | pMH0174 | epHIV7 vector, full-length human CD19 protein |
| CD19-CAR-zBB | pJ02459 | epHIV7 vector, GM-CSF signal peptide, c-Myc tag, FMC63 scFv, IgG4-Fc hinge, CD28 transmembrane, 4-1BB + CD3ζ signaling, T2A sequence, EGFRt transduction marker |
| CD19-iCAR 101 | pJR0101 | epHIV7 vector, GM-CSF signal peptide, c-Myc tag, FMC63 scFv, PD-1 hinge, PD-1 transmembrane, PD-1 signaling, T2A sequence, EGFRt transduction marker |

| Name (of transgene) | Vector # | Description |
|---|---|---|
| CD19-iCAR 102 | pJR0102 | epHIV7 vector, GM-CSF signal peptide, c-Myc tag, FMC63 scFv, IgG4-Fc hinge, CD28 transmembrane, PD-1 signaling, T2A sequence, EGFRt transduction marker |
| CD19-iCAR 103 | pJR0103 | epHIV7 vector, GM-CSF signal peptide, c-Myc tag, FMC63 scFv, CD8α hinge, CD8α transmembrane, PD-1 signaling, T2A sequence, EGFRt transduction marker |
| CD19-tCAR | pJR0306 | epHIV7 vector, GM-CSF signal peptide, FMC63 scFv, IgG4-Fc hinge, CD28 transmembrane, T2A sequence, HER2t transduction marker |
| ffluc | pJ01668 | epHIV7 vector, firefly luciferase, T2A sequence, GFP |
| Gag and Pol | pCHGP-2 | Packaging vector 1 for lentivirus production |
| HLA-A*0201 | pJR0803 | LZRS-pBMN-Z vector, full-length HLA-A*0201 protein |
| Rev | pCMV-Rev2 | Packaging vector 2 for lentivirus production |
| ROR1 | pMH0172 | epHIV7 vector, full-length human ROR1 protein |
| ROR1-CAR intermediate spacer (R11) | pMH0127 | epHIV7 vector, GM-CSF signal peptide, R11 scFv, IgG4-Fc hinge + CH3, CD28 transmembrane, 4-1BB + CD3ζ signaling domain, T2A sequence, EGFRt transduction marker |
| ROR1-CAR long spacer (R11) | pMH0128 | epHIV7 vector, GM-CSF signal peptide, R11 scFv, IgG4-Fc hinge + CH2 + CH3, CD28 transmembrane, 4-1BB + CD3ζ signaling, T2A sequence, EGFRt transduction marker |
| ROR1-CAR scFv library (R11) | pJR0906 | pT2/HB vector, GM-CSF signal peptide, R11 CDR3 mutated scFv, IgG1 hinge-CH2-CH3, CD28 transmembrane, 4-1BB + CD3ζ signaling, T2A sequence, EGFRt transduction marker |
| ROR1-CAR short spacer (R11) | pMH0122 | epHIV7 vector, GM-CSF signal peptide, R11 scFv, IgG4-Fc hinge, CD28 transmembrane, 4-1BB + CD3ζ signaling, T2A sequence, EGFRt transduction marker |
| ROR1-CAR WT (R11) | pJR0905 | pT2/HB vector, GM-CSF signal peptide, R11 scFv, IgG1-Fc hinge + CH2 + CH3, CD28 transmembrane, 4-1BB + CD3ζ signaling, T2A sequence, EGFRt transduction marker |
| ROR1-CAR-z (R12) | pH0109 | epHIV7 vector, GM-CSF signal peptide, R12 scFv, IgG4-Fc hinge, CD28 transmembrane, CD3ζ signaling, T2A sequence, EGFRt transduction marker |

| Name (of transgene) | Vector # | Description |
|---|---|---|
| ROR1-CAR-z28 (R12) | R12HL_LIBspeEI_sh28 | epHIV7 vector, GM-CSF signal peptide, R12 scFv, IgG4-Fc hinge, CD28 transmembrane, CD28 + CD3ζ signaling, T2A sequence, EGFRt transduction marker |
| ROR1-CAR-z28BB (R12) | R12HL_LIBEI_sh28BB | epHIV7 vector, GM-CSF signal peptide, R12 scFv, IgG4-Fc hinge, CD28 transmembrane, CD28 + 4-1BB + CD3ζ signaling, T2A sequence, EGFRt transduction marker |
| ROR1-CAR-zBB (R12) | pMH0123 | epHIV7 vector, GM-CSF signal peptide, R12 scFv, IgG4-Fc hinge, CD28 transmembrane, 4-1BB + CD3ζ signaling, T2A sequence, EGFRt transduction marker |
| Sleeping Beauty transposon MC | SB100X MC | Minicircle vector encoding Sleeping Beauty transposon |
| VSV-G | pCMV-G | Envelope vector for lentivirus production |

## 2.5 Primers

**Table 2.8: Primers.**

| Name | NT sequence 5’ -> 3’ | Description |
|---|---|---|
| CAR28tm fwd | ATGTTCTGGGTGCTGGTG | Sequencing in epHIV7 and pT2/HB |
| CAR28tm library rev | ACCACCAGCACCCAGAAC | Sequencing in epHIV7 and pT2/HB, PCR of ROR1-CAR scFv library |
| CAR28tm rev | GATGAAGGCCACGGTGA | Sequencing in epHIV7 and pT2/HB |
| CAR panel epHIV7 fwd | CAGATCCAAGCTGTGACCG | Sequencing in epHIV7 and pT2/HB, PCR of ROR1-CAR scFv library |
| M13 rev | CAGGAAACAGCTATGACC | Sequencing in pCR4-TOPO-TA and pT2/HB |
| NotI-tEGFR rev1 | GAATTCCTGCAGCCCGGGTCTAGA | Sequencing in epHIV7 and pT2/HB |
| pBMN-5’ fwd | GCTTGGATACACGCCGC | Sequencing in LZRS-pBMN-Z |
| R11 scFv primer 1 fwd | GCGACGTATTTCTGTGCGAGGGGGTATNNKNNNKNNNKGGTGATTTCAACATCTGGGGT | Generation of ROR1-CAR scFv library |

| Name | NT sequence 5’ -> 3’ | Description |
|---|---|---|
| R11 scFv primer 2 rev | CCCGTTAAGGTCCTGATG | Generation of ROR1-CAR scFv library |
| R11 scFv primer 3 fwd | CCTACTCTAGAAGCTGGGTACCG | Generation of ROR1-CAR scFv library |
| R11 scFv primer 4 rev | ATACCCCCTCGCACAGAAATACGTCGC | Generation of ROR1-CAR scFv library |

## 2.6 Antibodies and flow cytometry staining reagents

**Table 2.9: Antibodies for flow cytometry.**

| Specificity | Clone | Conjugate | Reactivity | Isotype | Supplier |
|---|---|---|---|---|---|
| CD3 | BW264/56 | APC | Human | mouse IgG2a, κ | Miltenyi |
| CD4 | M-T466 | VioBlue | Human | mouse IgG1, κ | Miltenyi |
| CD8 | BW135/80 | FITC | Human | mouse IgG2a, κ | Miltenyi |
| CD8 | BW135/80 | VioBlue | Human | mouse IgG2a, κ | Miltenyi |
| CD14 | M5E2 | FITC | Human | mouse IgG2a, κ | BioLegend |
| CD19 | LT19 | PE | Human | mouse IgG1, κ | Miltenyi |
| CD19 | LT19 | VioBlue | Human | mouse IgG1, κ | Miltenyi |
| CD28 | CD28.2 | Pacific Blue | Human | mouse IgG1, κ | BioLegend |
| CD45RA | HI100 | APC | Human | mouse IgG2b, κ | BioLegend |
| CD45RO | UCHL1 | FITC | Human | mouse IgG2a, κ | Miltenyi |
| CD45 | HI30 | APC | Human | mouse IgG1, κ | BioLegend |
| CD62L | DREG-56 | PE | Human | mouse IgG1, κ | BioLegend |
| CD80 | 2D10 | APC | Human | mouse IgG1, κ | BioLegend |
| CD270 (HVEM) | 122 | PE | Human | mouse IgG1, κ | BioLegend |
| CD272 (BTLA) | MIH26 | PE | Human | mouse IgG2a, κ | BioLegend |
| CD274 (PD-L1) | 29E.2A3 | Biotin | Human | mouse IgG2b, κ | BioLegend |
| CD279 (PD-1) | PD1.3.1.3 | PE | Human | mouse IgG2b, κ | Miltenyi |
| c-Myc | SH1-26E7.1.3 | FITC | Human | mouse IgG1, κ | Miltenyi |
| c-Myc | SH1-26E7.1.3 | Biotin | Human | mouse IgG1, κ | Miltenyi |
| EGFR | C225 (Cetuximab) | Biotin | Human | Human IgG1, κ | ImClone LLC |

| Specificity | Clone | Conjugate | Reactivity | Isotype | Supplier |
|---|---|---|---|---|---|
| EGFR | C225 (Cetuximab) | AF647 | Human | human IgG1, κ | ImClone LLC |
| HER2 | 4D5-8 (Trastuzumab) | Biotin | Human | murine IgG1, κ | Roche |
| HLA-A*0201 | BB7.2 | PE | Human | mouse IgG2b, κ | BioLegend |
| ROR1 | 2A2 | PE | Human | mouse IgG2b, κ | Miltenyi |
| ROR1 | 2A2 | APC | Human | mouse IgG2b, κ | Miltenyi |

**Table 2.10: Reagents for flow cytometry.**

| Reagent | Conjugate | Supplier |
|---|---|---|
| 7-AAD | - | BD Biosciences |
| MHC I HLA-A*0201 pp65 NLVPMVATV Streptamer® | Streptamer® | IBA Lifesciences |
| Soluble recombinant human ROR1 protein | AF647 | Dr. J. Huppa |
| Strep-Tactin® | PE | IBA Lifesciences |
| Streptavidin | PE | BioLegend |

**Table 2.11: Antibodies for western blot.**

| Specificity | Clone/Isotype | Conjugate | Dilution | Supplier |
|---|---|---|---|---|
| NFATc2 | D43B1 / Monoclonal rabbit IgG | - | 1:500 | Cell Signaling |
| NF-κB p65 | D14E12 / Monoclonal rabbit IgG | - | 1:1000 | Cell Signaling |
| Lamin A/C | 4C11 / Monoclonal mouse IgG2a, κ | - | 1:1000 | Cell Signaling |
| α-Tubulin | 11H10 / Monoclonal rabbit IgG | - | 1:2000 | Cell Signaling |
| Mouse IgG Ab | Polyclonal goat | HRP | 1:2000 | Bio-Rad |
| Rabbit IgG Ab | Polyclonal goat | HRP | 1:2000 | Bio-Rad |

## 2.7 Molecular-weight size marker

**Table 2.12: Molecular weight and DNA standards.**

| Name | Supplier, Location |
|---|---|
| 1 kb DNA ladder | NEB, Frankfurt am Main |
| Precision Plus Protein™ Kaleidoscope™ Prestained Standard | Bio-Rad, Munich |

## 2.8 Reagents, enzymes and commercial kits

**Table 2.13: Reagent, enzymes and commercial kits.**

| Name | Supplier, Location |
|---|---|
| Anti-biotin MicroBeads | Miltenyi, Bergisch Gladbach |
| Anti-human CD28 Fab Streptamer® | Stage Cell Therapeutics, Planegg |
| Anti-human CD3 pure functional grade (clone OKT3) | Miltenyi, Bergisch Gladbach |
| Anti-MHC I HLA-A*0201 pp65 NLVPMVATV Streptamer® | Stage Cell Therapeutics, Planegg |
| Anti-PE MicroBeads | Miltenyi, Bergisch Gladbach |
| AscI | NEB, Frankfurt am Main |
| BamHI-HF® | NEB, Frankfurt am Main |
| BspEI | NEB, Frankfurt am Main |
| BstBI | NEB, Frankfurt am Main |
| Buffer IS (10x) | IBA Lifesciences |
| CalPhos™ Mammalian Transfection Kit | Takara, Saint-Germain-en-Laye, France |
| CutSmart® Buffer | NEB, Frankfurt am Main |
| DC™ Protein Assay Kit II | Bio-Rad, Munich |
| D-Biotin (50 mM) | Stage Cell Therapeutics, Planegg |
| Deoxynucleotide (dNTP) Solution Mix (10 mM each NT) | NEB, Frankfurt am Main |
| Dynabeads® Human T-Activator CD3/CD28 | Thermo Fisher Scientific, Darmstadt |
| Effectene® Transfection Reagent Kit | Qiagen, Hilden |
| Gel Loading Dye Purple (6X) | NEB, Frankfurt am Main |
| HindIII-HF® | NEB, Frankfurt am Main |
| Human $CD4^+$ T-Cell Isolation kit | Miltenyi, Bergisch Gladbach |
| Human $CD8^+$ T-Cell Isolation kit | Miltenyi, Bergisch Gladbach |
| Human $CD8^+$ Memory T-Cell Isolation kit | Miltenyi, Bergisch Gladbach |
| Human IFNγ ELISA Max™ Deluxe Kit | BioLegend, London, UK |
| Laemmli Sample Buffer (4x) | Bio-Rad, Munich |
| LB Agar plates with 100 µg/mL carbenicillin | TEKnova, Hollister, CA, USA |
| LB medium (1x) | Thermo Fisher Scientific, Darmstadt |
| Midori Green Advance DNA stain | Nippongenetics, Düren |
| NEBuffer™ 3.1 | NEB, Frankfurt am Main |
| NheI-HF® | NEB, Frankfurt am Main |

| Name | Supplier, Location |
|---|---|
| NotI-HF® | NEB, Frankfurt am Main |
| NucleoBond® Xtra Maxi EF Kit | Macherey-Nagel, Düren |
| NucleoSpin® Gel and PCR Clean-up Kit | Macherey-Nagel, Düren |
| NucleoSpin® Plasmid Kit | Macherey-Nagel, Düren |
| One Shot™ TOP10 chemically competent E. coli | Thermo Fisher Scientific, Darmstadt |
| P3 Primary Cell 4D-Nucleofector® X Kit | Lonza, Cologne |
| PepTivator® CMV pp65 premium grade | Miltenyi, Bergisch Gladbach |
| Phusion® High-Fidelity DNA polymerase | NEB, Frankfurt am Main |
| Platinum® Taq DNA polymerase | Thermo Fisher Scientific, Darmstadt |
| PureLink™ Genomic DNA Mini Kit | Thermo Fisher Scientific, Darmstadt |
| Purified mouse anti-human CD28 (clone 28.2) | BD Biosciences, Heidelberg |
| Recombinant human IL-2 (PROLEUKIN® S) | Novartis, Basel, Switzerland |
| Recombinant human ROR1 protein | Sino Biological, Chesterbrook, PA, USA |
| SE Cell Line 4D-Nucleofector® X Kit | Lonza, Cologne |
| Strep-Tactin® multimer backbone | Stage Cell Therapeutics, Planegg |
| T4 DNA Ligase | NEB, Frankfurt am Main |
| T4 DNA Ligase Buffer (10x) | NEB, Frankfurt am Main |
| TGX Stain-Free™ FastCast™ Acrylamide Kit | Bio-Rad, Munich |
| TOPO TA Cloning® Kit | Thermo Fisher Scientific, Darmstadt |
| Trans-Blot® Turbo™ RTA Mini PVDF Transfer Kit | Bio-Rad, Munich |
| Transfer Buffer (5x) | Bio-Rad, Munich |
| Tris/Glycine/SDS Buffer (10x) | Bio-Rad, Munich |
| Trypan blue solution 0.4% | Thermo Fisher Scientific, Darmstadt |

## 2.9 Buffer

**Table 2.14: Antibody incubation buffer.**

| Ingredient | Volume (f.c.) |
|---|---|
| BSA | 5 g (5% w/v) |
| Sodium azide (1.5 M) | 200 µL (3 mM) |
| TBS-T | 100 mL |

**Table 2.15: Blocking buffer.**

| Ingredient | Volume (f.c.) |
|---|---|
| Skimmed milk powder | 5 g (5% w/v) |
| TBS-T | 100 mL |

**Table 2.16: Blotting buffer.**

| Ingredient | Volume (f.c.) |
|---|---|
| Transfer Buffer 5x concentrate | 200 mL (1x) |
| Ethanol absolute | 200 mL (20% v/v) |
| $dH_2O$ | 600 mL |

**Table 2.17: Buffer IS.**

| Ingredient | Volume (f.c.) |
|---|---|
| Buffer IS 10x concentrate | 50 mL (1x) |
| EDTA (0.5 M) | 1 mL (1 mM) |
| $dH_2O$ | 450 mL |

**Table 2.18: FACS buffer.**

| Ingredient | Volume (f.c.) |
|---|---|
| DPBS | 500 mL |
| Fetal Calf Serum (heat inactivated) | 2.5 mL (0.5% v/v) |
| EDTA (0.5 M) | 2 mL (2 mM) |
| Sodium azide (1.5 M) | 0.5 mL (1.5 mM) |

**Table 2.19: MACS® buffer.**

| Ingredient | Volume (f.c.) |
|---|---|
| DPBS | 500 mL |
| Fetal Calf Serum (heat inactivated) | 2.5 mL (0.5% v/v) |
| EDTA (0.5 M) | 2 mL (2 mM) |

**Table 2.20: NP-40 lysis buffer.**

| Ingredient | Volume (f.c.) |
|---|---|
| DPBS | 500 mL |
| NP-40 | 2.5 mL (0.5%) |

**Table 2.21: PBS/EDTA buffer.**

| Ingredient | Volume (f.c.) |
|---|---|
| DPBS | 500 mL |
| EDTA (0.5 M) | 2 mL (2 mM) |

**Table 2.22: SDS running buffer.**

| Ingredient | Volume (f.c.) |
|---|---|
| Tris/Glycine/SDS Buffer 10x concentrate | 100 mL (1x) |
| $dH_2O$ | 900 mL |

**Table 2.23: Sucrose buffer.**

| Ingredient | Volume (f.c.) |
|---|---|
| Sucrose | 20 g (20% w/v) |
| $dH_2O$ | 100 mL |
| Mixed and sterilized with 0.22 µm PES-membrane filter | |

**Table 2.24: TAE buffer.**

| Ingredient | Volume (f.c.) |
|---|---|
| TRIS-acetate-EDTA (TAE) 50x concentrate | 20 mL (1x) |
| $dH_2O$ | 980 mL |

**Table 2.25: TBS-5 buffer.**

| Ingredient | Volume (f.c.) |
|---|---|
| TRIS - HCl pH 7.8 (1 M) | 5 mL (50 mM) |
| NaCl (5 M) | 2.6 mL (130 mM) |
| KCl (1 M) | 1 mL (10 mM) |
| $MgCl_2$ (1 M) | 0.5 mL (5 mM) |
| $H_2O$ (culture grade) | 100 mL |
| Mixed and sterilized with 0.22 µm PES-membrane filter | |

## 2.10 Chemicals and solutions

**Table 2.26: Chemicals and solutions.**

| Name | Supplier, Location |
|---|---|
| 2-Mercaptoethanol 98% pure | Bio-Rad, Munich |
| 2-Mercaptoethanol (50 mM) | Thermo Fisher Scientific, Darmstadt |
| Album Fraction V (Bovine Serum Albumin, BSA) | AppliChem, Darmstadt |
| Ammonium Persulfate (APS) | Bio-Rad, Munich |
| Ampicillin Sodium Salt | AppliChem, Darmstadt |
| Biocoll separating solution | Merck, Darmstadt |
| Carbenicillin Ready Made Solution (100 mg/mL) | Sigma-Aldrich, Steinheim |
| D-Luciferin firefly, Potassium Salt | Biosynth, Staad, Switzerland |
| Dimethyl sulfoxide (DMSO) | AppliChem, Darmstadt |
| DMEM medium with 4.5 g/L glucose and 25 mM HEPES | Thermo Fisher Scientific, Darmstadt |
| Dulbecco's Phosphate-Buffered Saline (DPBS, no calcium, no magnesium) | Thermo Fisher Scientific, Darmstadt |
| Ethylenediaminetetraacetic acid (EDTA) (0.5 M) | Thermo Fisher Scientific, Darmstadt |
| Ethanol absolute | AppliChem, Darmstadt |
| Fetal Calf Serum (heat inactivated) | Thermo Fisher Scientific, Darmstadt |
| GlutaMAX Supplement (100x) | Thermo Fisher Scientific, Darmstadt |
| Human serum | DRK-Blutspendedienst |
| IMDM medium with 25 mM HEPES and L-glutamine | Thermo Fisher Scientific, Darmstadt |
| Ionomycin calcium salt | Sigma-Aldrich, Steinheim |
| Isopropyl alcohol | Sigma-Aldrich, Steinheim |
| Magnesium chloride ($MgCl_2$) | Carl Roth, Karlsruhe |
| Methanol | Sigma-Aldrich, Steinheim |
| Nonidet P-40 (NP-40) | AppliChem, Darmstadt |
| PBD-tween tablets | Millipore, Billerica |
| Penicillin/Streptomycin (10000 U/mL) | Thermo Fisher Scientific, Darmstadt |
| Phorbol 12-myristate 13-acetate (PMA) | Sigma-Aldrich, Steinheim |
| Polybrene (10 mg/mL) | Merck, Darmstadt |
| Potassium chloride (KCl) | AppliChem, Darmstadt |
| Protease Inhibitor Cocktail for mammalian cells, DMSO solution | Sigma-Aldrich, Steinheim |

| Name | Supplier, Location |
|---|---|
| RPMI 1640 medium with 25 mM HEPES and L-glutamine | Thermo Fisher Scientific, Darmstadt |
| Skimmed milk powder (Sucofin) | TSI, Zeven |
| Sodium azide ($NaN_3$) pure | AppliChem, Darmstadt |
| Sodium chloride (NaCl) | Carl Roth, Karlsruhe |
| Sucrose analytical grade | Serva, Heidelberg |
| Tetramethylethylenediamine (TEMED) | Bio-Rad, Munich |
| TRIS-acetate-EDTA (TAE) 50x | Sigma-Aldrich, Steinheim |
| TRIS ultrapure | Carl Roth, Karlsruhe |
| Trypsin EDTA (0.05%), phenol red | Thermo Fisher Scientific, Darmstadt |
| Tween-20 | AppliChem, Darmstadt |
| Water cell culture grade | AppliChem, Darmstadt |
| Water molecular biology grade | AppliChem, Darmstadt |
| UltraPure™ Agarose | Thermo Fisher Scientific, Darmstadt |

## 2.11 Consumables

**Table 2.27: Consumables.**

| Name | Supplier, Location |
|---|---|
| Cell culture flasks 25 and 75 $cm^2$ surface area | Corning, Kaiserslautern |
| Centrifuge tubes thinwall 38.5 mL | Beckman Coulter, Krefeld |
| Conical glass flask 500 mL | DWK Life Sciences, Wertheim am Main |
| Dish Nunclon™ Delta 10 cm | Thermo Fisher Scientific, Darmstadt |
| Falcon® tube conical bottom 175 mL | Corning, Kaiserslautern |
| Filter tips 2.5, 10, 20, 200 and 1000 µL | Sarstedt, Nümbrecht |
| Flow cytometry tubes 5 mL | Sarstedt, Nümbrecht |
| Glass plates and 10-well combs 1 mm | Bio-Rad, Munich |
| Half-area plate 96-well | Corning, Kaiserslautern |
| Leucosep™ tubes 50 mL | Greiner Bio-One, Frickenhausen |
| MACS® separation LS columns | Miltenyi, Bergisch Gladbach |
| PCR Single Cap Soft Strips 0.2 mL | Biozym, Hessisch Oldendorf |
| Plates flat bottom 6-, 12-, 24-, 48- and 96-well | Corning, Kaiserslautern |
| Plate round bottom 96-well | Corning, Kaiserslautern |

| Name | Supplier, Location |
|---|---|
| SafeSeal micro tubes 1.5 and 2 mL | Sarstedt, Nümbrecht |
| Serological pipettes 2, 5, 10, 25 and 50 mL | Greiner Bio-One, Frickenhausen |
| Sterile Syringe Filter 0.45 µm | Sarstedt, Nümbrecht |
| Sterile filtration vacuum tube 50 mL 0.45 µm | Merck, Darmstadt |
| Sterile syringe 20 mL | B. Braun, Melsungen |
| Suspension TC-plate 12-well | Sarstedt, Nümbrecht |
| Tubes conical bottom 15 and 50 mL | Greiner Bio-One, Frickenhausen |
| Tubes with ventilation cap 13 mL | Sarstedt, Nümbrecht |
| Vacuum Filter PES 0.22 µm | Sarstedt, Nümbrecht |
| White flat bottom plate 96-well | Corning, Kaiserslautern |

## 2.12 Equipment

**Table 2.28: Equipment.**

| Name | Supplier, Location |
|---|---|
| 4D-Nucleofector™ X Unit | Lonza, Cologne |
| Biological safety cabinet Herasafe™ KS | Thermo Fisher Scientific, Darmstadt |
| Cell Sorter FACSAria™ III | BD Biosciences, Heidelberg |
| Centrifuge Heraeus™ Megafuge™ 40R | Thermo Fisher Scientific, Darmstadt |
| $CO_2$ incubators Heracell™ 150i and 240i | Thermo Fisher Scientific, Darmstadt |
| DynaMag™-15 magnet | Thermo Fisher Scientific, Darmstadt |
| Flow cytometer FACSCanto™ II | BD Biosciences, Heidelberg |
| Freezing container Mr. Frosty™ | Thermo Fisher Scientific, Darmstadt |
| Electrophoresis chamber system | Febikon, Wermelskirchen |
| Gel imaging system ChemiDoc™ MP | Bio-Rad, Munich |
| Heating block neoBlock 1 | neoLab, Heidelberg |
| Ice maker | Scotsman, Vernon Hills, IL, USA |
| Irradiator Faxitron CP-160 | Faxitron Bioptics, Tucson, AZ, USA |
| Liquid nitrogen container LS 6000 | Taylor-Wharton, Borehamwood, UK |
| Microcentrifuge Fresco 17 | Thermo Fisher Scientific, Darmstadt |
| Microscope Primo Vert | ZEISS, Jena |
| Mini-PROTEAN® Tetra Vertical Electrophoresis | Bio-Rad, Munich |

| Name | Supplier, Location |
|---|---|
| Multimode multiplate reader Infinite® 200 PRO | TECAN, Männedorf, Switzerland |
| Orbital Compact Digital Microplate shaker | Thermo Fisher Scientific, Darmstadt |
| PCR Mastercycler® ep Gradient S | Eppendorf, Hamburg |
| Pipette controller accu-jet® pro | Brand, Wertheim am Main |
| Pipettes Research plus 2.5, 10, 20, 200 and 1000 µL | Eppendorf, Hamburg |
| Plate washer HydroSpeed™ | TECAN, Männedorf, Switzerland |
| Power supply E802 | Consort, Turnhout, Belgium |
| Power supply PowerPac™ Basic | Bio-Rad, Munich |
| Refrigerator -4 and -20 °C | Liebherr, Bulle, Switzerland |
| Rocking shaker DRS-12 | neoLab, Heidelberg |
| Shaker incubator | INFORS HT, Basel, Switzerland |
| Trans-Blot® Turbo™ Transfer System | Bio-Rad, Munich |
| Ultra-low temperature freezer -80 °C FORMA 900 | Thermo Fisher Scientific, Darmstadt |
| Ultracentrifuge Sorvall™ WX80 | Thermo Fisher Scientific, Darmstadt |
| Ultrasonic processor UP50H | Hielscher Ultrasonics, Teltow |
| UV transilluminator | neoLab, Heidelberg |
| Water bath | Memmert, Schwabach |

## 2.13 Software

**Table 2.29: Software.**

| Software | Application | Company, Location |
|---|---|---|
| Excel | Data management | Microsoft, Redmond, WA, USA |
| FACS Diva | Flow cytometry | BD Biosciences, Heidelberg |
| FlowJo X 10.0.7 | Flow cytometry analysis | Tree Star Inc. Ashland, OR, USA |
| GraphPad Prism 6 | Statistical analysis | La Jolla, CA, USA |
| iControl | Luminescence and protein analysis | TECAN, Männedorf, Switzerland |
| Image Lab | Protein analysis | Bio-Rad, Munich |

# 3 Methods

## 3.1 Cell biological methods

### 3.1.1 Isolation of PBMCs

Peripheral blood mononuclear cells (PBMCs) were isolated from healthy donor peripheral blood by Ficoll-Paque density gradient centrifugation. First, 50 mL Leucosep™ tubes were equilibrated with room temperature Biocoll separating solution. Then, donor blood was mixed with room temperature DPBS to final volume of 35 mL, carefully added to a Leucosep™ tube and centrifuged at 310 x g for 15 minutes at 22 °C (acceleration level 9, break level 2). The buffy coat, which accumulated above the filter, was removed and washed twice with 4 °C cold PBS/EDTA buffer by centrifugation at 220 x g for 10 minutes at 4 °C. PBMCs were resuspended in MACS® buffer or culture medium dependent on the downstream application.

### 3.1.2 Isolation of primary T cells

Untouched $CD4^+$ bulk, $CD8^+$ bulk or $CD8^+$ $CD45RO^+$ $CD45RA^-$ memory T cells were isolated by Miltenyi MACS® MicroBeads Technology, according to the manufacturer's instructions. PBMCs were labeled with antibodies and MicroBeads from the respective kits and a maximum of $1x10^8$ cells were loaded into one LS column for magnetic separation. Isolated T cells were resuspended in T cell medium + 50 U/mL recombinant human IL-2.

### 3.1.3 Culture of primary T cells and cell lines

Human primary T cells were generally cultured in T cell medium supplemented with 50 U/mL recombinant human IL-2. Depending on the density, $0.5\text{-}4.0x10^6$ T cells were grown in 48- or 24-well plates and for expansion in 25 $cm^2$ cell culture flasks. Half-medium changes were performed by removing half of the stale medium and adding the same amount of fresh T cell medium supplemented with 50 U/mL recombinant human IL-2 per total volume. Tumor cell lines BW5147, K562, JeKo-1 and TM-LCL were cultured with tumor cell medium in 25 or 75 $cm^2$ cell culture flasks. These cells were split twice the week at a ratio of 1:10 with fresh tumor cell medium. NF-κB/NFAT reporter cells were a kind gift from the lab of Dr. Peter Steinberger (Medizinische Universität Wien, Austria) and were cultured with reporter medium in 24-well plates, split twice the week at a ratio of 1:5 with fresh reporter

medium. Lenti-X™ and Platinum A cells were cultured with adherent cell line medium in 75 $cm^2$ cell culture flasks. At a confluency of 90%, cells were detached from the flasks by incubation with Trypsin EDTA (0.05%) and split at a 1:20 ratio with fresh adherent cell line medium. All cells were cultured in incubators at 37 °C with 5% $CO_2$ and 97% relative humidity. For long term storage, cells were resuspended in freezing medium, frozen for 24 hours at -80 °C in freezing containers and then transferred to liquid nitrogen containers.

### 3.1.4 Immunophenotyping by flow cytometry

In general, $2x10^5$ cells were transferred to 5 mL flow cytometry tubes, washed with 2 mL FACS buffer by centrifugation at 200 x g for 4 minutes at 4 °C and incubated with mAbs for 25 minutes at 4 °C. CMV-specific T cells were additionally washed with buffer IS and stained with MHC I Streptamer® according to the manufacturer's instructions. For staining PBMCs and T cells, mAbs specific for CD4, CD8, CD45RA and CD45RO were used, and dead cells were excluded by viability staining with 7-AAD. NF-κB/NFAT reporter cells were stained with mAbs specific for CD3, CD28, CD45, CD80, PD-1 and BTLA. CARs on the surface of T cells and reporter cells were either directly detected by staining the N-terminal c-Myc tag or via soluble recombinant human ROR1 protein, or were indirectly detected by staining transduction markers EGFRt or HER2t. Tumor cell lines (BW5147, K562) were analyzed with mAb specific for CD14 (stem domain of mbOKT3), CD19, ROR1, HLA-A*0201, PD-L1 and HVEM. Flow cytometry measurements were performed on a BD FACSCanto™ II and data were analyzed with FlowJo software (Tree Star).

### 3.1.5 Production of retrovirus and transduction

One day before transfection, $4x10^6$ Platinum A cells were transferred to 7 mL adherent cell line medium without antibiotics and added to a 10 cm dish. The Effectene® Transfection Reagent Kit (Qiagen) was used according to the manufacturer's instructions for transfection of 2 µg retroviral transfer vector (LZRS-pBMN-Z) comprising the gene of interest. The transfection mix was taken up in 3 mL adherent cell line medium and added dropwise to Platinum A cells. After one day, the medium was exchanged with tumor cell medium. On the second day, the retroviral supernatant was cleaned from cell debris through a syringe with 0.45 µm filter, and 10 µg/mL polybrene was added. $0.25x10^6$ cells were resuspended in the retroviral supernatant, centrifuged at 800 x g for 45 minutes at 32 °C (acceleration level 9, break level 1) and then incubated at 37 °C. One day later, the procedure was repeated with the same cells.

### 3.1.6 Cytotoxicity assay

$5x10^3$ target cells expressing firefly luciferase were mixed with effector T cells at various effector to target (E:T) ratios and added to a white flat bottom 96-well plate in triplicates. D-luciferin substrate was added to the co-culture to a final concentration of 0.15 mg/mL in 200 µL final volume. After 2- and 4-hours incubation, the luminescence signal was measured by a multiplate reader and specific lysis was calculated with following formula:

$$\text{Lysis (\%)} = \frac{\text{Mean (target cells + UTD effector cells) - Single value (target cells + CAR effector cells)}}{\text{Mean (target cells + UTD effector cells)} \times 100}$$

### 3.1.7 Production of lentivirus

Lentivirus was produced in Lenti-X™ cells plated at a density of $6x10^6$ per 10 cm dish in adherent cell line medium without antibiotics and incubated at 37 °C for 6 hours to allow settlement. Then, transfection was performed with the CalPhos™ Mammalian Transfection Kit (Takara), according to the manufacturer's instructions. In detail, 15 µg lentiviral transfer vector (epHIV7) comprising the gene of interest was diluted with 10 µg pCHGP-2, 1 µg pCMV-Rev2 and 2 µg pCMV-G helper vectors in $CaCl_2$ solution and added to an equal volume of 2x HEPES-buffered saline (HBS). After 20 minutes incubation at room temperature, the mixture was added dropwise to a plate previously seeded with Lenti-X™ cells and incubated at 37 °C overnight. Next day, the transfected cells were washed twice with pre-warmed DPBS, and fresh adherent cell line medium was added. Two days later, lentiviral supernatant from three plates was harvested, centrifuged at 2160 x g for 15 min at 8 °C and filtered through a sterile 0.45 µm vacuum filter to remove cellular debris. The filtered supernatant was transferred to a centrifuge tube and underlaid with 20% sucrose buffer. After ultracentrifugation at 138510 x g for 2 hours at 4 °C, the viral pellet was dissolved in 200 µL TBS-5 buffer for 3 hours at 4 °C and aliquoted in 25 µL fractions. Lentiviral particles were frozen on dry ice and then stored at -80 °C for long time.

### 3.1.8 Lentivirus titer analysis

Titration to determine the titer of the lentiviral particles was performed using Jurkat cells. In detail, $2.5x10^5$ cells were added in 250 µL tumor cell medium per well of a 48-well plate and mixed with 5 µg/mL polybrene to neutralize the charge of the cell membrane. Different volumes of the lentiviral particles (0.5, 1, 2, 5 and 10 µL) were added per well and incubated for 4 hours at 37 °C. Then, the volume in each well was filled to 1 mL with fresh tumor cell medium and the infected cells were cultured for another 48 hours. The expression of the transgene was analyzed by flow cytometry and

the lentivirus titer was calculated as transforming units per µL (TU/µL) using the following equation based on the percentage of transgene-positive cells:

$$\text{Viral titer (TU/µL)} = \frac{\text{Cell count at time of transduction} \times (\text{\% positive cells} / 100)}{\text{Volume of virus added (µL)}}$$

### 3.1.9 Lentiviral transduction of primary T cells

About 0.5-1.0x$10^6$ isolated $CD4^+$ bulk, $CD8^+$ bulk or $CD8^+$ memory T cells were seeded in 1 mL T cell medium + 50 U/mL recombinant human IL-2 in per well of a 48-well plate and activated with anti-CD3/CD28 Dynabeads® at a cell to bead ratio of 1:1. Next day, two-thirds of the medium were removed, and lentiviral particles supplemented with 5 µg/mL polybrene were added at a multiplicity of infection (MOI) of 5. T cells were spinoculated by centrifugation at 800 x g for 45 min at 32 °C and then incubated for 4 hours at 37 °C. Afterwards, the volume was filled to 1 mL with pre-warmed T cell medium + 50 U/mL recombinant human IL-2. Transduced T cells were incubated at 37 °C and half-medium changes were performed with pre-warmed T cell medium + 50 U/mL recombinant human IL-2 every second day. The anti-CD3/CD28 Dynabeads® were removed using the DynaMag™-15 magnet (Thermo Fisher Scientific) on day 6 post-transduction and T cells were transferred to larger flat bottom plates or tissue culture flasks and analyzed by flow cytometry.

### 3.1.10 Lentiviral transduction of CMV-specific stimulated T cells

PBMCs from healthy donors (HLA-A*0201 positive, CMV serum positive) were screened for $CD8^+$ memory T cells expressing a CMV-TCR that recognizes the MHC class I presented CMV pp65 peptide NLVPMVATV by flow cytometry. About 0.5-1.0x$10^6$ isolated $CD8^+$ memory T cells were resuspended in 350 µL T cell medium + 50 U/mL recombinant IL-2 and added to one well of a 48-well plate. 3 µg Strep-Tactin® multimer backbone was pre-incubated with 0.5 µg anti-CD28-Fab Streptamer® and 0.5 µg anti-MHC I HLA-A*0201 pp65 NLVPMVATV Streptamer® for 20 minutes at 4 °C, the mixture was added to one well and incubated at 37 °C overnight. Next day, the CMV-specific stimulated T cells were transduced with lentiviral particles according to the lentiviral transduction protocol for primary T cells (see Chapter 3.1.9) with minor modifications. After transduction and during culture, only pre-warmed T cell medium + 50 U/mL recombinant human IL-2 was added instead of performing half-medium changes to avoid dilution of the CMV-TCR stimulating reagent. On day 8 upon transduction, the CMV-TCR stimulating reagent was removed by incubating the cells with 20 µL D-Biotin (50 mM) per well for 10 minutes at 37 °C. Cells were centrifuged twice at 200 x g for 6 minutes at 8 °C, resuspended in T cell medium + 50 U/mL recombinant human IL-2 and analyzed by flow cytometry.

### 3.1.11 Lentiviral transduction of cell lines

Transduction of NF-κB/NFAT reporter cells and tumor cell lines BW/5147 and K562 was performed by adding $0.25x10^6$ cells in 250 µL appropriate culture medium to one well of a 48-well plate. Lentiviral particles supplemented with 5 µg/mL polybrene were added at a MOI of 3 to the cells and incubated for 4 hours at 37 °C. Then, the volume was filled to 1 mL with the appropriate pre-warmed culture medium, the transduced cells were incubated at 37 °C for 2 days and analyzed by flow cytometry.

### 3.1.12 Nucleofection of reporter cells with Sleeping Beauty transposons

NF-κB/NFAT reporter cells were nucleofected with the 4D-Nucleofector™ X Unit and nucleofection kit SE (Lonza), according to the manufacturer's instructions. In brief, 5 µg of the Sleeping Beauty transposon donor vector (pT2/HB) encoding the CAR and 2.5 µg SB100X MC vector were added per $2x10^6$ reporter cells and nucleofection was performed with program CL-120. Afterwards, the nucleofected cells were immediately mixed with reporter medium, incubated at 37 °C for 4 hours and half of the medium exchanged. Two days later, cells were analyzed by flow cytometry.

### 3.1.13 Enrichment of transgene-positive cells

Tumor cell lines, reporter cells and primary T cells were enriched for transgene surface expression by MACS® MicroBeads technology (Miltenyi) or by FACS. For magnetic bead selection, cells were stained with biotin-labeled anti-EGFR, anti-HER2 or anti-c-Myc mAbs, or with PE-labeled anti, CD19, anti-HLA-A*0201 or anti-ROR1 mAbs. After incubation with anti-biotin or anti-PE MicroBeads, according to the manufacturer's instructions, cells were added to LS columns for positive selection and then collected in the appropriate cell culture medium for expansion. For FACS, cells were stained with AF647-labeled soluble recombinant human ROR1 protein and biotin-labeled anti-EGFR mAb + streptavidin-PE. Cells were sorted by the Cell Sorting core facility at the Institute for Virology and Immunobiology Würzburg using a FACSAria™ III (BD Biosciences).

### 3.1.14 Antigen-independent expansion of T cells

Following enrichment, CAR-positive T cells were expanded by a rapid expansion protocol (REP) with irradiated feeder cells and anti-CD3 mAb (OKT3).[123] In brief, $5x10^4$ T cells were incubated with $30x10^6$ irradiated PBMCs (30 Gy), $5x10^6$ irradiated TM-LCL (80 Gy) and 30 ng/mL OKT3 in T cell medium. Next day, the T cell medium was supplemented with 50 U/mL recombinant human IL-2. On day 4,

T cells were washed by centrifugation at 200 x g for 6 minutes at 22 °C and resuspended in fresh T cell medium + 50 U/mL recombinant human IL-2. Half-medium changes were performed every second day, and the T cell phenotype was analyzed between day 8 and 10 by flow cytometry.

### 3.1.15 Antigen-dependent expansion of CMV-specific T cells

Following CMV-specific stimulation and enrichment, CAR-positive T cells were expanded by antigen-dependent stimulation of the HLA-A*0201 restricted CMV-TCR. K562 cells expressing HLA-A*0201 were resuspended in plain RPMI 1640 medium, irradiated with 80 Gy and incubated with 600 ng/mL PepTivator® CMV pp65 (Miltenyi) at 37 °C for 2 hours. T cells were mixed with pp65 pulsed K562/HLA-A*0201 cells at a 3:1 ratio in T cell medium + 50 U/mL recombinant human IL-2 and incubated at 37 °C. Half-medium changes were performed every second day and the T cell phenotype was analyzed between day 8 and 10 by flow cytometry.

### 3.1.16 Stimulation of primary T cells by plate-coated proteins

12-well suspension plates were pre-coated with 0.6 µg/mL recombinant human ROR1 protein or 2.5 µg/mL anti-CD3 mAb (OKT3) per well and incubated at 4 °C overnight. Next day, the wells were washed twice with DPBS, $5x10^6$ T cells were added to 1 mL T cell medium per well and OKT3-stimulated T cells were supplemented with 6 µg/mL anti-CD28 mAb. For control, T cells were stimulated with 120 ng/mL PMA and 3 µg/mL ionomycin. After 2 hours cells were harvested for lysate preparation.

### 3.1.17 Reporter cell assay

Reporter cells and stimulator cells (BW5147, K562, JeKo-1) were washed with DPBS by centrifugation at 200 x g for 6 minutes at 22 °C and resuspended in reporter medium. Additionally, K562 and JeKo-1 cells were pre-stained with eFluor 670 dye (Thermo Fisher Scientific, Darmstadt, Germany), according to the manufacturer's instructions. Then, $5x10^4$ reporter cells were mixed with $2x10^4$ stimulator cells in a final volume of 100 µL and added to round bottom 96-well plates in duplicates. After a 24-hour incubation at 37 °C, the co-cultures were harvested, and reporter cells were distinguished from murine BW5147 stimulator cells by detection of human CD45 and from human cell lines (K562 and JeKo-1) by detection of eFluor 670 dye via flow cytometry. Reporter gene activation was analyzed by measuring the geometric mean fluorescence intensity (MFI) of cyan fluorescent protein (CFP) or green fluorescent protein (GFP).

### 3.1.18 Cytokine secretion assay and ELISA

$5x10^4$ effector T cells were mixed with $12.5x10^4$ target cells and added to a round bottom 96-well plate in triplicates with final volume of 200 µL tumor cell medium. For control, T cells were stimulated with 25 ng/mL PMA and 1 µg/mL ionomycin. After 24 hours incubation, 100 µL supernatant was collected from each well and IFNγ concentration was analyzed by ELISA (BioLegend), according to manufacturer's instructions with minor modifications. In detail, 25 µL supernatant was analyzed in a 96-well half-area plate using a quarter of the reagent quantity described in the instructions. Absorbance at 570 and 450 nm was measured by a multiplate reader, and IFNγ concentration was calculated based on a standard curve with 5-parameter logistic curve-fitting algorithm.

## 3.2 Molecular methods

### 3.2.1 Description of encoding elements and DNA vectors

All constructs used in this study were synthesized with codon optimization by GeneArt (Thermo Fisher Scientific, Regensburg, Germany) and cloned either into the retroviral transfer vector LZRS-pBMN-Z, lentiviral transfer vector epHIV7 or Sleeping Beauty transposon donor vector pT2/HB[124] using restriction sites for BamHI, BspEI, HindIII, NheI or NotI. The vectors epHIV7 and pT2/HB contained the EF1 promoter and a Kozak sequence (5'-GCCGCCACC-3') upstream of the integration site for the gene of interest. Gene expression for vector LZRS-pBMN-Z was driven by the 5' LTR sequence.

For CAR constructs, the signal peptide of GM-CSF receptor subunit α (UniProtKB P15509; AA 1-22) was selected to enable transport and integration of the receptors into the membrane. The CD19-specific scFv was generated by fusing $V_H$ and $V_L$ domains of the antibody FMC63 via a Whitlow linker and addition of two c-Myc tags (EQKLISEEDL) at the N-terminus.[125] Similarly, the $V_H$ and $V_L$ domains of antibodies R12 and R11 were coupled via a $(G_4S)_3$ linker resulting in ROR1-specific scFvs.[126] The spacer domains were mainly derived from IgG4-Fc and IgG1-Fc molecules (consisting of hinge and/or CH2 and/or CH3 domains),[48,127] but also from the CD8α-chain (UniProtKB P01732; AA 135-182) or from the extracellular part of PD-1 (UniProtKB Q15116; AA 146-170). The transmembrane domains originated from CD28 (UniProtKB P10747; AA 154-179), CD8α-chain (UniProtKB P01732; AA 183-203) or PD-1 (UniProtKB Q15116; AA 171-191). For the intracellular signaling domains of the CARs, the domains of CD3ζ (UniProtKB P20963; AA 52-164), 4-1BB (UniProtKB Q07011; AA 214-255), CD28 (UniProtKB P10747; AA 180-220) or PD-1 (UniProtKB Q15116; AA 192-288) were selected. If indicated,

the CAR coding sequences were separated by a viral T2A peptide from the transduction markers EGFRt[34] or HER2t (a kind gift from Dr. Karen Spratt, Seattle Children's, WA, USA).

For the expression of human ROR1 (UniProtKB Q01973) and human CD19 (UniProtKB P15391), full-length sequences were synthesized and cloned into the lentiviral transfer vector epHIV7. The α-chain of MHC class I molecule HLA-A*0201 (UniProtKB P01892) was cloned from the construct HLA-A0201-Aug'07 into the retroviral backbone LZRS-pBMN-Z. The reporter genes for NF-κB/NFAT reporter cells were generated in the lab of Dr. Peter Steinberger (Medizinische Universität Wien, Austria) and encoded enhanced versions of CFP and GFP, response elements for NF-κB (5'-TGGGGACTTTCCGC-3') and NFAT (5'-TGGAGGAAAAACTGTTTCATACAGAAGGCG-3') and a minimal promoter (5'-TAGAGGGTATATAATGGAAGCTCGATTTCCAG-3'). Both reporter gene cassettes were cloned into the self-inactivating retroviral vector pSIRV.[128]

### 3.2.2 ROR1-CAR scFv library construction

The ROR1-CAR scFv library was based on a library derived from the ROR1-specific R11 scFv, which was generated in the lab of Dr. Christoph Rader (The Scripps Research Institute, Florida, USA). Using NNK doping strategy (N = A, C, G, or T; K = G or T) for site-restricted mutagenesis of the $V_H$ CDR3 region of R11, 12 nucleotides encoding amino acids STYY that are involved in ROR1 kringle domain binding were mutated.[129] In detail, PCR of the right arm of the R11 scFv template DNA was performed using the degenerated forward primer 1 binding to the R11 $V_H$ CDR3 region that covers the four amino acids with NNK codons to introduce mutations, and the reverse primer 2 binding in the IgG1-Fc spacer domain. A second PCR was performed with forward primer 3 and reverse primer 4 to amplify the left arm of the scFv including the signal peptide, the $V_L$ and the residual $V_H$ domain to obtain an amplicon with overlapping sequence to the right arm amplicon. PCR products were recovered by gel purification and the complete scFv was fused by overlapping PCR using forward R11 scFv primer 3 and reverse R11 scFv primer 2. Then, the scFv mutants were cloned via restriction sites AscI and BstBI into the Sleeping Beauty transposon donor vector pT2/HB upstream of a CD28 transmembrane domain and intracellular CD3ζ and 4-1BB domains by GeneArt (Thermo Fisher Scientific, Regensburg, Germany) to generate the ROR1-CAR scFv library. Library accuracy analysis confirmed a correctness of 91% with 74 out of 81 clones containing four sense codons in the correct reading frame.

### 3.2.3 General cloning procedure of vector constructs

Approximately 1 µg vector DNA was digested with 0.5 µL restriction enzymes in 1x CutSmart® or NEBuffer™ 3.1 at 37 °C for 30-60 minutes. After heat inactivation at 65 °C for 20 minutes, the digestion mix was supplemented with 6x Gel Loading Dye Purple and loaded to a 1% agarose gel containing Midori Green Advance DNA stain. DNA fragments were separated by electrophoresis at 120 V for 80 minutes and visualized by UV light. DNA was removed from the gel and purified by the NucleoSpin® Gel and PCR Clean-up Kit (Macherey-Nagel), according to the manufacturer's instructions. Vector insert and backbone were mixed in a volume ratio of 4:1 in 1x ligase buffer with 1 µL T4 DNA ligase and incubated at 16 °C overnight.

### 3.2.4 Amplification of vector DNA by bacteria

One Shot™ TOP10 chemically competent E. coli (Thermo Fisher Scientific) were transformed according to the manufacturer's instructions with vector DNA using heat shock at 42 °C for 45 seconds. Transformed bacteria were added to 200 µL SOC medium, briefly incubated at 37 °C, and then 40 µL of the bacterial solution was plated on an LB agar plate with 100 µg/mL carbenicillin. After incubation at 37 °C overnight, bacterial clones were picked and grown in 5 mL LB medium supplemented with 50 µg/mL carbenicillin at 37 °C overnight. Vector DNA was isolated using the NucleoSpin® Plasmid Kit (Macherey-Nagel), according to the manufacturer's instructions, and the vector DNA sequence was validated by analytical restriction enzyme digestion and Sanger sequencing (GATC, Konstanz, Germany). In order to produce vector DNA on a large-scale, bacterial clones were grown in 170 mL LB medium supplemented with 100 µg/mL ampicillin at 37 °C overnight. DNA was isolated with the NucleoBond® Xtra Maxi EF Kit (Macherey-Nagel), according to the manufacturer's instructions, and finally eluted in 500 µL endotoxin-free $H_2O$.

### 3.2.5 Genomic DNA isolation and PCR

To analyze the sequence of the $V_H$ CDR3 region of the R11 scFv of the ROR1-CAR scFv library, approximately $2x10^6$ cells were harvested and washed twice with cold DPBS by centrifugation at 200 x g for 4 minutes at 4 °C. Genomic DNA was isolated with the PureLink™ Genomic DNA Mini Kit (Thermo Fisher Scientific), according to the manufacturer's instructions, and eluted in 80 µL genomic elution buffer. The scFv sequence was amplified with forward CAR panel epHIV7 primer and reverse CAR28tm library primer by mixing 100 ng genomic DNA with Phusion® High-Fidelity DNA polymerase

(NEB), according to the manufacturer's instructions. The following thermocycler setting was applied for PCR:

| | | | |
|---|---|---|---|
| Initial denaturation | 98°C | 1 min | |
| Denaturation | 98°C | 20 sec | |
| Annealing | 64°C | 30 sec | 30 cycles |
| Extension | 72°C | 1 min | |
| Final extension | 72°C | 5 min | |

The amplified fragments were separated by electrophoresis and the desired PCR amplicon was isolated and purified with the NucleoSpin® Gel and PCR Clean-up Kit (Macherey-Nagel), according to the manufacturer's instructions. Then, 3'-overhangs were added to the amplified DNA by incubation with Platinum® Taq DNA polymerase (Thermo Fisher Scientific) and 0.2 mM dNTPs at 72 °C for 20 minutes. Finally, the DNA amplicons were cloned with the TOPO TA Cloning® kit (Thermo Fisher Scientific), according to the manufacturer's instructions, and single scFv fragments were analyzed by sequencing with reverse CAR28tm library primer.

## 3.3 Protein biochemistry methods

### 3.3.1 Lysis and fractionation of primary T cells

T cells were stimulated as described in Chapter 3.1.16 and lysed according to the REAP fractionation protocol with minor modifications.[130] In detail, T cells were resuspended, transferred to 2 mL micro tubes and centrifuged at 800 x g for 30 seconds at 4 °C. The cell pellet was washed once with cold DPBS and was then disrupted with 150 µL cold NP-40 lysis buffer supplemented with 1x Protease Inhibitor Cocktail. After 10 minutes incubation on ice, the lysate was centrifuged at 13000 x g for 1 minute at 4 °C, and the supernatant containing the cytosolic fraction was removed and mixed with 4x Laemmli Sample buffer. The remaining nuclear pellet was washed once with cold NP-40 lysis buffer and once with cold DPBS by centrifugation at 13000 x g for 1 minute at 4 °C. Subsequently, the nuclear pellet was dissolved in 1x Laemmli Sample buffer supplemented with 1x Protease Inhibitor Cocktail and disrupted by sonication with a 0.5 second cycle at an amplitude of 80% for a total of 10 seconds. To reduce foaming, the nuclear fraction was centrifuged at 13000 x g for 10 minutes at 4 °C, and both lysate fractions were stored on ice until protein quantification (see Chapter 3.3.2). Then,

the lysates were supplemented with 2-Mercaptoethanol at a volume ratio of 40:1, heated at 90 °C for 5 minutes and stored at -80 °C.

### 3.3.2 Protein quantification according to Lowry assay

Protein concentration was quantified with the DC™ Protein Assay Kit (Bio-Rad) in a flat bottom 96-well plate, according to the manufacturer's instructions. In brief, 5 µL lysate sample was mixed with 25 µL reagent A' and 200 µL reagent B in duplicates. For the standard curve, a 2.175 mg/mL BSA stock in 1x Laemmli Sample buffer was serially diluted 8 times and added in duplicates. After incubation at room temperature for 15 minutes, the absorbance was measured at 750 nm with a multiplate reader and concentration was determined based on the standard curve.

### 3.3.3 SDS polyacrylamide gel electrophoresis (SDS-PAGE)

10% SDS polyacrylamide gels with 1 mm thickness and 10-well comb were prepared with the TGX Stain-Free Fast Cast Acrylamide Kit (Bio-Rad) using 10% APS and TEMED, according to the manufacturer's instructions. Gels were loaded with lysate containing 10-15 µg protein and the Precision Plus Protein™ Kaleidoscope™ Prestained Standard (Bio-Rad) was applied to monitor running and protein size. The proteins were separated by electrophoresis in 1x Tris/Glycine/SDS buffer for 60 minutes at 150 V using the Mini-PROTEAN® Tetra Vertical Electrophoresis device (Bio-Rad).

### 3.3.4 Western blot

Protein transfer was performed with the Trans-Blot® Turbo™ RTA Mini PVDF Transfer Kit and the Trans-Blot® Turbo™ Transfer System (both Bio-Rad) using the High MW program, according to the manufacturer's instructions. After washing blotted membranes twice with TBS-T buffer, they were incubated with blocking buffer for 2 hours at room temperature. Next, the membranes were incubated overnight at 4 °C in antibody incubation buffer supplemented with antibodies for NFATc2, NF-κB p65, α-Tubulin or Lamin A/C. The membranes were washed 3 times with TBS-T buffer and further incubated with HRP-linked anti-mouse or anti-rabbit IgG antibodies in blocking buffer for 1 hour at room temperature. After 3 washes with TBS-T buffer, the membranes were incubated with Clarity Western ECL substrate and protein bands visualized at different time points using the ChemiDoc™ MP gel imaging system (Bio-Rad).

## 3.4 Statistical analyses

If not further specified in the text, in the figure legend or in the table legend, the data regarding nuclear enrichment of NF-κB and NFAT, normalized NF-κB and NFAT activation, activation kinetics of NF-κB and NFAT, CAR-T cell cytotoxicity and CAR-T cell IFNγ secretion show the mean values of at least n = 3 experiments and the error bars represent the standard deviation (SD). All statistical analyses were performed with GraphPad Prism software. To calculate the statistical significance and to control the Type I error rate at 5%, the ANOVA hypothesis test was used to compare and analyze multiple groups in each data set. For this, it was assumed that the data of each group were normally distributed, and the variances were equal (homogeneity of variances). One-way ANOVA was used to calculate statistical significance of data sets with one variable using the Holm-Sidak post hoc test for multiple comparisons. Two-way ANOVA was used to calculate statistical significance of data sets with two variables using the Holm-Sidak post hoc test for multiple comparisons. Significance is indicated by the p-value as follows: *p < 0.05; **p < 0.01; ***p < 0.001; ****p < 0.0001; ns = not significant.

# 4 Results

## 4.1 A CAR-screening platform based on NF-κB and NFAT activation

We assumed that the transcription factors NF-κB and NFAT, both induced by distinct T cell signaling pathways, could serve as indicators of CAR-mediated activation. Consequently, we first analyzed the activation of these transcription factors upon CAR stimulation in primary T cells. Next, we assumed that CAR-mediated NF-κB and NFAT activation can be measured using a quantitative readout without primary T cells, which we consider a key requirement for a CAR-screening platform. We developed a reporter cell line based on Jurkat cells that indicated the activation of NF-κB and NFAT through integrated reporter genes encoding the fluorophores CFP and GFP, respectively.[128,131] We demonstrated NF-κB and NFAT reporter gene induction upon stimulation of ROR1- and CD19-specific CARs, and then we defined the optimal readout time of CFP and GFP signal intensity.

### 4.1.1 NF-κB and NFAT activation in primary T cells

We speculated that CAR stimulation induces translocation of the key transcription factors NF-κB and NFAT into the nucleus of primary T cells.

To verify this, we used a prototypic ROR1-specific CAR, whose scFv is based on the antibody R12 and comprises intracellular signaling domains of CD3ζ and 4-1BB (ROR1-CAR-zBB).[38] First, $CD4^+$ and $CD8^+$ T cells of healthy donors were isolated, stimulated with CD3/CD28 Dynabeads®, and transduced with a lentivirus containing the ROR1-CAR gene. $CAR^+$ T cells co-expressed a truncated version of EGFR (EGFRt), which was used to enrich positively transduced T cells to over 95% purity by MACS® MicroBeads technology. The CD4 and CD8 expression of the T cells was analyzed by flow cytometry and showed clear populations of $CD4^+$ (91.3%) and $CD8^+$ (97.5%) T cells (Figure 4.1A). Moreover, we directly stained the ROR1-specific CAR with soluble ROR1 protein linked to the fluorophore AF647. All $EGFRt^+$ T cells bound ROR1 protein and demonstrated a proportional expression of CAR and EGFRt. Next, we stimulated ROR1-specific CAR-T cells with immobilized ROR1 protein for 120 minutes to analyze the activation of NF-κB and NFAT. TCR-dependent stimulation of CAR-T cells by CD3 and CD28 antibodies, or unspecific stimulation by PMA and ionomycin (P/I) served as positive controls. T cells were disrupted and the cell lysate was divided into a cytosolic and a nuclear fraction to detect the translocation of NF-κB and NFAT after separation through SDS-Page and western blot (Figure 4.1B). Lamin A/C and α-Tubulin as marker proteins of nuclear and cytosolic fraction, respectively, confirmed high purity of the separation. We observed similar amounts of NF-κB and NFATc2 in the cytosolic

fraction of stimulated as well as unstimulated samples. In contrast, in the nuclear fraction, both transcription factors were only present after T cell stimulation. Here, triggering of the CAR with ROR1 protein caused translocation of NF-κB and NFATc2 into the nucleus to the same degree as triggering of the TCR complex via CD3/CD28 Dynabeads® or P/I. Quantitative analysis confirmed an accumulation of NF-κB and NFATc2 after CAR stimulation with comparable levels in $CD4^+$ and $CD8^+$ T cells (Figure 4.1C).

In summary, these data show that both transcription factors are activated upon CAR stimulation and migrate into the nucleus, an essential event also observed upon TCR stimulation.

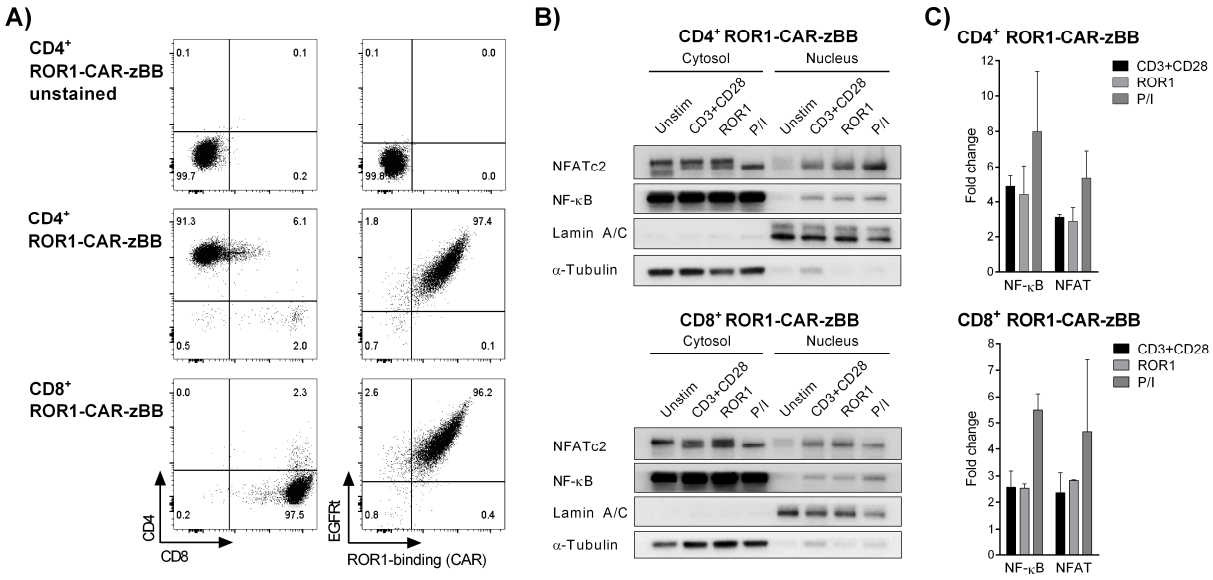


**Figure 4.1: Detection of NF-κB and NFAT in primary $CD4^+$ and $CD8^+$ ROR1-CAR-T cells after stimulation.**

**A)** Phenotype of $CD4^+$ and $CD8^+$ ROR1-CAR-T cells. Staining was performed with anti-EGFR mAb to detect the EGFRt transduction marker, and AF647-labeled soluble ROR1 protein to detect the CAR. **B)** Representative western blot detecting NF-κB and NFATc2 in the nuclear and cytosolic fraction of ROR1-CAR-T cells after 120 minutes stimulation with anti-CD3/anti-CD28 mAbs (CD3+CD28), immobilized ROR1 protein (ROR1) or PMA and ionomycin (P/I). Lamin A/C and α-Tubulin served as loading controls for the nuclear and cytosolic fraction, respectively. **C)** Nuclear enrichment of NF-κB and NFATc2 quantified by densitometric analysis of western blots (n = 3 donors for $CD4^+$ and n = 2 donors for $CD8^+$ ROR1-CAR-T cells). Data were normalized to corresponding loading controls and presented as fold change ± SD relative to unstimulated T cells.

## 4.1.2 Generation of NF-κB/NFAT reporter cells

We considered that the activation of NF-κB and NFAT is also detectable in the human T cell lymphoma line Jurkat and can be quantified more accurately using inducible reporter genes encoding fluorophores than using western blot.

Consequently, we developed a Jurkat based reporter cell line, which stably integrated two reporter genes with inducible expression of CFP or GFP (Figure 4.2A). These genes contain a response element that allows specific binding of transcription factors NF-κB or NFAT, and a minimal promotor

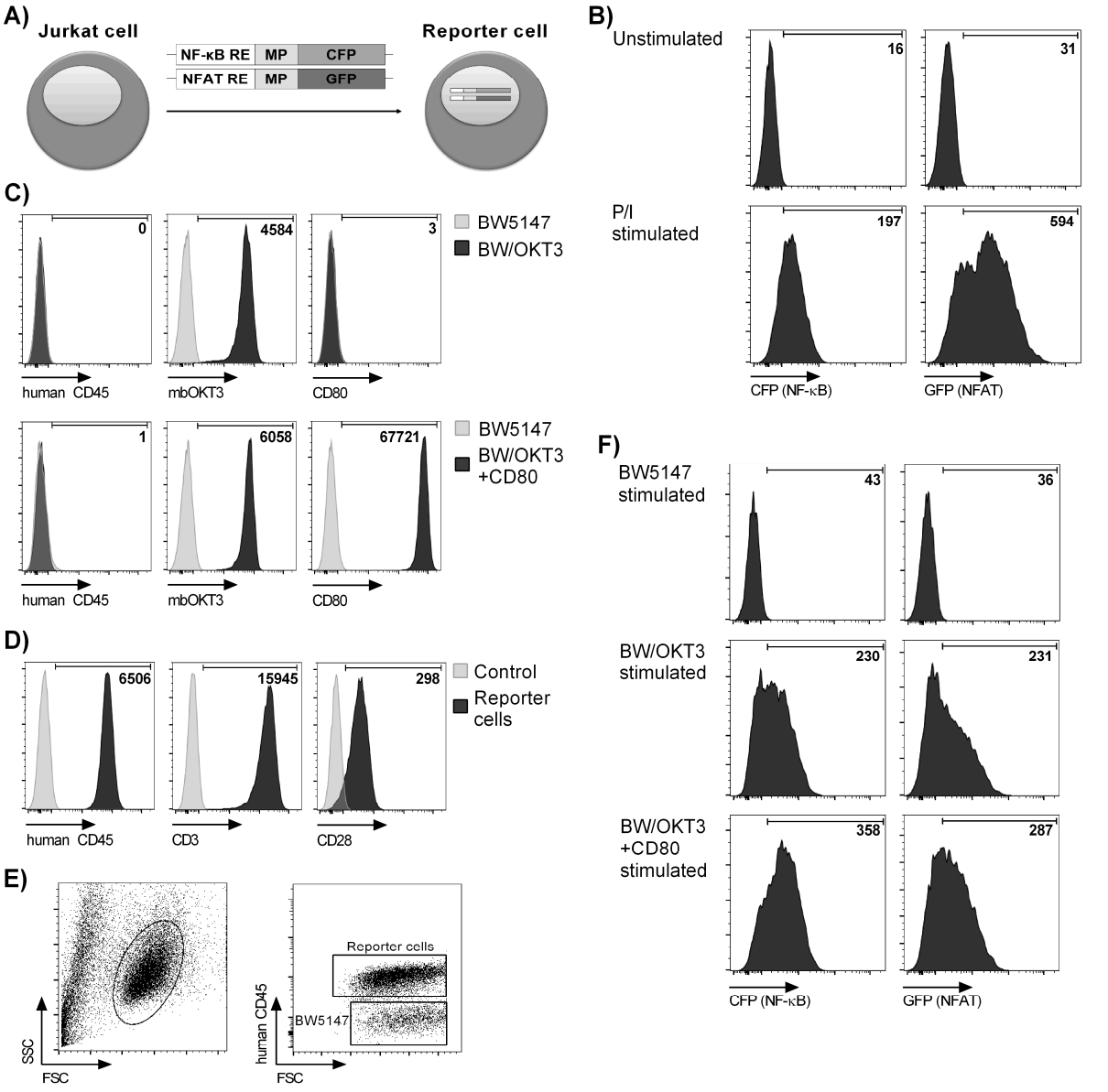


**Figure 4.2: Analysis of Jurkat cells with stably integrated NF-κB and NFAT reporter genes.**

**A)** Schematic representation of a Jurkat-derived reporter cell with NF-κB-inducible cyan fluorescent protein (CFP) reporter gene and NFAT-inducible green fluorescent protein (GFP) reporter gene. RE = response element; MP = minimal promoter. **B)** MFI of CFP and GFP after stimulation of reporter cells with PMA and ionomycin (P/I). **C)** Phenotype of BW5147 cells after modification with a membrane-bound anti-CD3-scFv (BW/OKT3) or additional human CD80 (BW/OKT3+CD80). Membrane-bound OKT3 (mbOKT3) was detected by its CD14 stem domain. The level of surface expression on BW/OKT3 and BW/OKT3+CD80 cells is shown as MFI minus the MFI of native BW5147 cells. **D)** Analysis of surface molecules on reporter cells shown as MFI minus the MFI of unstained cells (control). **E)** Distinction of reporter cells and BW5147 cells after co-culture by detection of human CD45 during flow cytometry. **F)** MFI of CFP and GFP after stimulation of reporter cells with BW/OKT3 or BW/OKT3+CD80 at a 2.5:1 ratio for 24 hours.

that is inactive by default. Therefore, the cells are termed NF-κB/NFAT reporter cells or just reporter cells in the present study. Binding of NF-κB or NFAT to their corresponding response element initiates the expression of CFP or GFP, respectively. Fluorescence can then be analyzed by flow cytometry and indicates cellular activation. As proof of concept, we performed stimulation with PMA and ionomycin for 24 hours, and we detected a strong and uniform increase of CFP and GFP signals in reporter cells (MFI of 197 and 594) in comparison to unstimulated reporter cells (MFI of 16 and 31; Figure 4.2B).

Next, we established a stimulator cell line that could be used in conjunction with NF-κB/NFAT reporter cells to trigger activation through cell-cell interaction. We selected the mouse thymoma cell line BW5147, which expresses murine activating and inhibitory ligands that do not cross-react with human receptors to prevent interference with reporter cell activation. Further, BW5147 cells do not express human CD45 in contrast to reporter cells (Figure 4.2C and D), which allows their separation during flow cytometry analysis (Figure 4.2E). To use BW5147 as a stimulator cell line for positive controls in co-culture experiments, they were modified to express a membrane-bound anti-CD3 scFv derived from mAb OKT3 (referred to as BW/OKT3 cells) that engages CD3 on reporter cells (Figure 4.2C and D). As anticipated, 24-hours co-culture of reporter cells with BW/OKT3 cells resulted in high-level CFP and GFP reporter gene signal (MFI of 230 and 231; Figure 4.2F). Additionally, to demonstrate that reporter gene activation corresponds to the strength of the input stimulus, we modified BW/OKT3 cells with human CD80 (referred to as BW/OKT3+CD80, Figure 4.2C) to engage the co-stimulatory molecule CD28 on reporter cells (Figure 4.2D). Stimulation of reporter cells with BW/OKT3+CD80 further increased the NF-κB and NFAT reporter signal (MFI of 358 and 287; Figure 4.2F).

In aggregate, these results show that reporter cells enable the analysis of NF-κB and NFAT activation by measuring the fluoresce signal of CFP and GFP and that murine BW5147 cells can be employed for the stimulation of reporter cells. Further, the data show that the signal intensity of CFP and GFP reflects variable stimulation intensities triggered by CD3 and co-stimulatory receptors like CD28.

### 4.1.3 Expression of ROR1- and CD19-specific CARs in reporter cells

To investigate the applicability of NF-κB/NFAT reporter cells for the analysis of CAR constructs, we next modified them with CARs of different specificity.

We used CAR constructs specifically targeting ROR1 (ROR1-CAR-zBB, targeting the R12 epitope) or CD19 (CD19-CAR-zBB, targeting FMC63 epitope) and comprising an IgG4-Fc spacer and a CD28 transmembrane domain connected to intracellular 4-1BB and CD3ζ signaling domains.[48] Reporter cells were transduced with lentivirus to stably integrate one of the CAR genes into their

genome (Figure 4.3A). After transduction, CAR$^+$ cells (referred to as CAR reporter cells) were enriched through our transduction marker EGFRt, which was included in both CAR genes, and CAR expression was analyzed via flow cytometry. Of the CAR reporter cells transduced with the ROR1-CAR-zBB construct, approximately 94% expressed the CAR as quantified by detection of EGFRt and direct staining of the CAR using soluble ROR1 protein (Figure 4.3B). Similarly, CAR reporter cells transduced with the CD19-CAR-zBB construct were more than 95% positive for CAR expression as confirmed by staining of EGFRt and the N-terminal c-Myc tag of the CD19-targeting scFv. For both constructs, the intensity of EGFRt and CAR expression correlated, showing that the transduction marker was an adequate surrogate for CAR expression in CAR reporter cell lines. In addition, CAR expression was stable and detectable for weeks after transduction and enrichment.

In summary, these data illustrate the readily integration of CAR constructs with different specificities into reporter cells and the high purity of the resulting CAR-positive cell population after lentiviral transduction and subsequent enrichment.

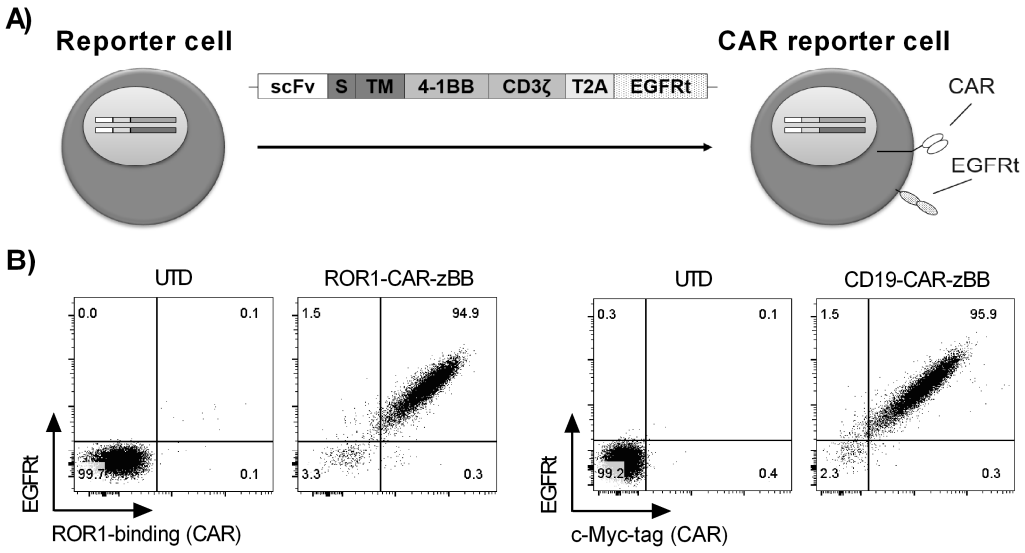


**Figure 4.3: Transduction of reporter cells with ROR1- and CD19-specific CAR constructs.**

**A)** Schematic representation of a reporter cell equipped with a second generation CAR and referred to as CAR reporter cell. scFv = single-chain fragment variable; S = spacer; TM = transmembrane domain. **B)** ROR1- and CD19-CAR expression after transduction and EGFRt-based enrichment. Staining of the EGFRt transduction marker was performed with EGFR mAb. The ROR1-CAR was directly stained with AF647-labeled soluble ROR1 protein and CD19-CAR was directly detected by its N-terminal c-Myc tag. UTD = untransduced.

### 4.1.4 CAR-mediated NF-κB and NFAT activation in reporter cells

We reasoned that NF-κB/NFAT reporter cells modified with ROR1- and CD19-specific CARs show reporter gene activation when stimulated with the respective antigen-expressing target cells.

We co-cultured ROR1-CAR-zBB and CD19-CAR-zBB reporter cells with murine BW5147 cells expressing either ROR1 (BW/ROR1) or CD19 (BW/CD19) and analyzed reporter signal after 24 hours. Stimulation of ROR1-CAR induced strong CFP and GFP reporter signals (MFI of 256 and 146) in comparison to unstimulated reporter cells (MFI of 24 and 49; Figure 4.4A). Similarly, CD19-CAR stimulation resulted in increased NF-κB and NFAT reporter activation (MFI of 204 and 162; Figure 4.4B).

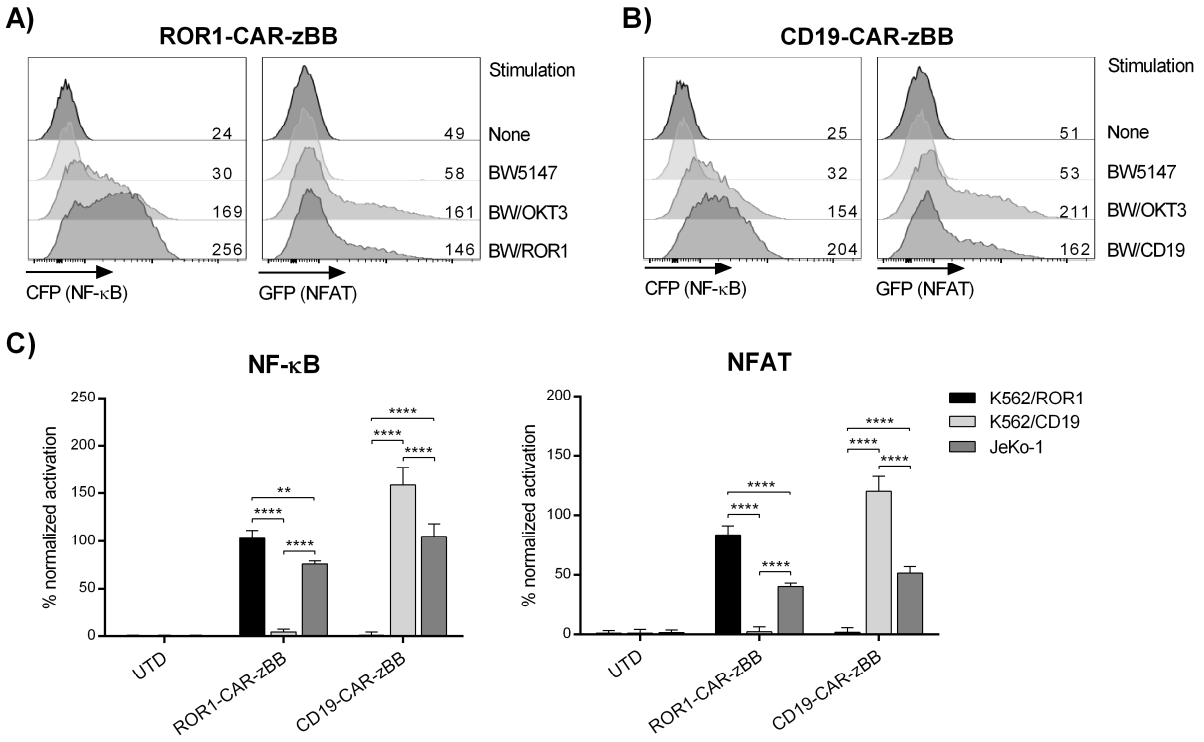


**Figure 4.4: Antigen-specific stimulation of ROR1-CAR-zBB and CD19-CAR-zBB reporter cells.**

**A, B)** MFI of CFP and GFP after stimulation of ROR1-CAR-zBB and CD19-CAR-zBB reporter cells with BW/ROR1 or BW/CD19 at a 2.5:1 ratio for 24 hours. As positive control, CAR reporter cells were stimulated with BW/OKT3 cells, as negative control with native BW5147 cells. **C)** NF-κB and NFAT activation of ROR1-CAR-zBB and CD19-CAR-zBB reporter cells co-cultured with human K562 cells expressing either ROR1 (K562/ROR1) or CD19 (K562/CD19), or JeKo-1 cells expressing both antigens. The activation in percent ± SD was calculated by normalizing CAR stimulation to the positive control (stimulation with BW/OKT3). Statistical significance (n = 3) was determined using two-way ANOVA with Holm-Sidak post hoc test; **p < 0.01; ****p < 0.0001.

As a positive control, we stimulated ROR1-CAR-zBB and CD19-CAR-zBB reporter cells with BW/OKT3, and we observed strong CFP and GFP reporter signals, indicating robust activation of reporter genes independent of CAR expression. In contrast, co-culture with native BW5147 cells did not activate the CAR reporter cells, which highlights the specificity of both ROR1- and CD19-CARs to their antigens. Further, we analyzed if ROR1-CAR-zBB and CD19-CAR-zBB reporter cells respond to their respective antigen on human cancer cell lines. Indeed, co-culture with JeKo-1 lymphoma cells (ROR1+ CD19+) and K562 cells transduced to express ROR1 (K562/ROR1) or CD19 (K562/CD19) resulted in significant, high-level NF-κB and NFAT reporter signal (Figure 4.4C).

Collectively, these data demonstrate that CAR reporter cells respond to their respective antigen with specific and readily detectable NF-κB and NFAT reporter signal. In addition to murine BW5147 cells, human cell lines can also be used to stimulate CAR reporter cells.

### 4.1.5 Kinetics of NF-κB and NFAT reporter gene activation

We anticipated that the kinetics of NF-κB and NFAT reporter gene activation upon CAR stimulation includes signal increase, plateau and decrease, suggesting that an optimal time window for signal analysis could be determined.

We incubated ROR1-CAR-zBB reporter cells with BW/ROR1 or BW/OKT3 cells to specifically stimulate CAR or TCR, and we detected reporter fluorescence periodically by flow cytometry. ROR1-CAR-induced CFP and GFP signal was first detectable after 4 hours and significantly increased after 6 hours of stimulation (Figure 4.5A). The reporter gene signal was further increased at 24 hours and reached its maximum at 48 hours. At 72 and 96 hours, the reporter signal was decreased but still higher than baseline signal (1 hour) and the signal obtained with native BW5147 cells that were included in the assay as a reference. Interestingly, stimulation with BW/OKT3 cells followed similar kinetics, but the NF-κB signal was much lower compared to stimulation with BW/ROR1 cells, likely because the CAR contained a 4-1BB co-stimulatory domain that augmented NF-κB activation. We also incubated untransduced reporter cells with BW/ROR1 or BW/OKT3 cells to monitor CAR-independent reporter gene activation and potential alterations in activation kinetics after CAR gene transfer (Figure 4.5B). At no time during stimulation with BW/ROR1 did we observe an increase of NF-κB or NFAT reporter signals compared to stimulation with native BW5147 cells, and the activation kinetics of untransduced reporter cells with BW/OKT3 cells was similar to the stimulation of CAR reporter cells.

In conclusion, these data show that NF-κB and NFAT reporter gene activation is already detectable after 6 hours, increases over time, and reaches its peak after 24 to 48 hours after CAR stimulation. To provide a rapid turnaround time to deliver results in CAR-screening campaigns, reporter signal quantification after 24 hours was deemed optimal to allow accurate quantification of CAR signaling.

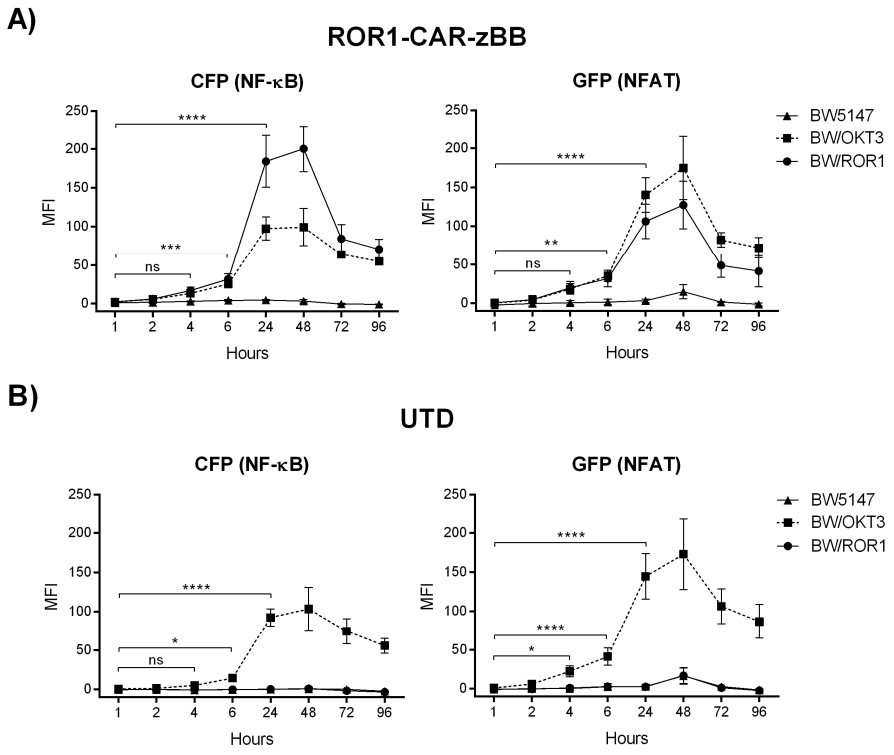


**Figure 4.5: Analysis of NF-κB and NFAT reporter signal in ROR-CAR-zBB reporter cells over time.**

**A, B)** Kinetics of NF-κB and NFAT reporter activation of ROR1-CAR-zBB reporter cells or untransduced (UTD) reporter cells. Reporter cells were co-cultured with native BW5147, BW/OKT3 or BW/ROR1 cells up to 96 hours and MFI ± SD of CFP and GFP were measured. Statistical significance (n = 4) was determined using two-way ANOVA with Holm-Sidak post hoc test; *p < 0.05; **p < 0.01; ***p < 0.001; ****p < 0.0001; ns = not significant.

### 4.1.6 Interim summary

In summary, the data from Chapter 4.1 show that CAR-specific stimulation of primary T cells triggered the translocation of NF-κB and NFAT into the nucleus, suggesting that both transcription factors can serve as indicators for CAR activation. By establishing a reporter cell line with inducible reporter genes, the activation of NF-κB and NFAT could be determined in a quantitative and robust manner. The reporter cells were modified with CARs of two different specificities (ROR1 and CD19) and induced strong NF-κB and NFAT signals upon antigen engagement, thus allowing analysis of CAR stimulation without the use of primary T cells. In addition, reporter gene induction was detectable after only 6 hours, with an optimum at 24 hours to provide a rapid turnaround time to deliver results in CAR-screening campaigns. These results meet the first and second aim of the study by validating NF-κB and NFAT as indicators of CAR activation and establishing a CAR-screening platform. Since it is based on reporter cells with quantitative readout of NF κB and NFAT activation, it is also referred to as NF-κB/NFAT reporter cell platform.

## 4.2 Small-scale screening campaigns to validate the CAR-screening platform

We anticipated that the NF-κB/NFAT reporter cell platform enables identification of optimal design parameters for extracellular and intracellular CAR modules. In this way, reporter cells should facilitate screening campaigns with CAR libraries to retrieve lead candidates with superior functionality for follow-up experiments in primary T cells. Accordingly, we generated a small panel of CAR constructs that differed in spacer length to identify the optimal spacer domain for targeting the R11 epitope of ROR1.[38,48] We further assumed that intracellular signal modules of CARs, which significantly affect the functionality of CAR-T cells,[65] will also affect NF-κB and NFAT activation in reporter cells. Therefore, we developed a library of CAR constructs with signal modules including CD3ζ, CD28 and 4-1BB domains, and we analyzed the reporter gene activation to identify the combination of domains generating the highest signal.

### 4.2.1 Expression of a ROR1-CAR spacer library in reporter cells

Because CAR binding and stimulation depends, among others, on steric determinants affecting the ability of the CAR to access membrane proximal and distal epitopes, we considered that this is reflected by the activation of NF-κB and NFAT reporter genes. Therefore, we decided to validate the reporter cells with a previously published CAR spacer library with known function in primary T cells.[48]

This library was composed of three ROR1-specific CARs containing an scFv derived from the antibody R11 and intracellular signaling domains of CD3ζ and 4-1BB (Figure 4.6A). The CARs differed, however, in extracellular spacer length, with a short spacer based on the hinge domain of IgG4-Fc (12 AA), an intermediate spacer with additional IgG4-Fc CH3 domain (119 AA), and a long spacer with IgG4-Fc hinge plus CH2 and CH3 domains (229 AA). NF-κB/NFAT reporter cells were transduced with the R11 ROR1-CAR constructs and $CAR^+$ cells were enriched to >87% purity (Figure 4.6B), which is comparable to purities obtained with primary T cells after transduction and enrichment.[38,48] We confirmed uniform expression of each CAR construct by detecting the transduction marker EGFRt, and staining with soluble ROR1 protein suggested that all CARs were equally capable of binding ROR1.

These results show comparable expression levels of the three CAR spacer variants in reporter cells, which is necessary for a subsequent robust comparison of reporter gene activation.

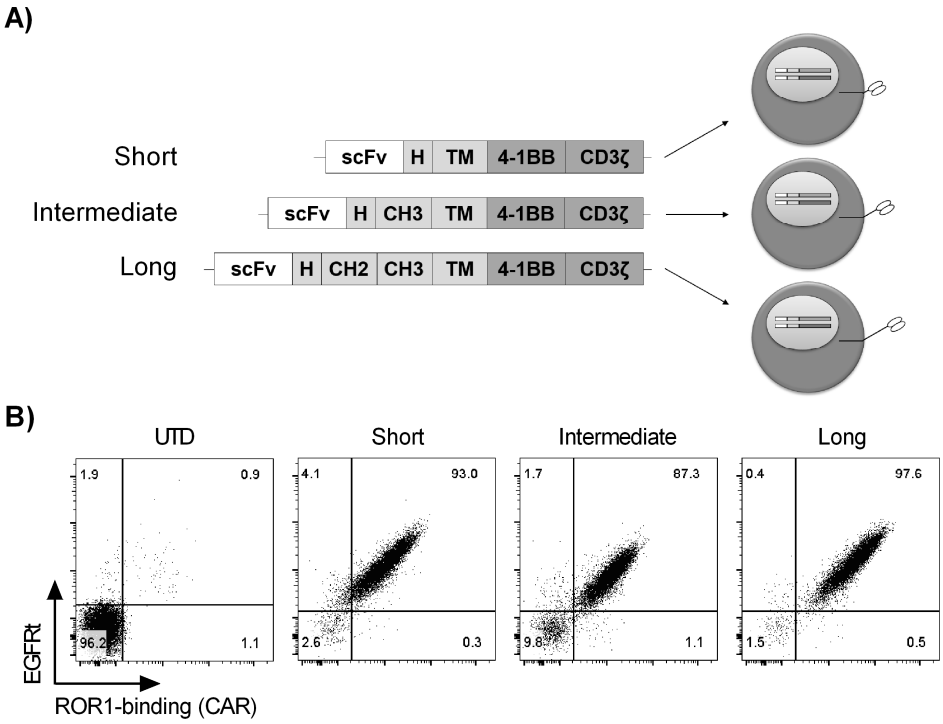


**Figure 4.6: Integration of the ROR1-CAR spacer library into reporter cells.**

**A)** Schematic representation of ROR1-CAR constructs with short, intermediate and long spacer domains derived from IgG4-Fc. scFv = single-chain fragment variable recognizing R11 epitope; H = hinge; CH = constant heavy domain; TM = transmembrane domain. **B)** CAR expression in reporter cells after transduction of the CAR spacer library and EGFRt enrichment. Staining was performed with anti-EGFR mAb to detect the EGFRt transduction marker, and AF647-labeled soluble ROR1 protein to detect the CAR. UTD = untransduced.

## 4.2.2 Identifying the optimal spacer for targeting the ROR1 R11 epitope

We anticipated that the reporter cells expressing the CAR with optimal spacer length for targeting the R11 epitope of ROR1 would generate the highest reporter gene signals after stimulation.

Therefore, we stimulated NF-κB/NFAT reporter cells modified with the ROR1-CAR spacer library by BW/ROR1 cells for 24 hours, and we analyzed NF-κB and NFAT activation via flow cytometry. Figure 4.7A shows highly increased CFP and GFP signals (MFI of 164 and 158) for reporter cells expressing the ROR1-CAR variant with long spacer domain in comparison to untransduced reporter cells (MFI of 22 and 32). We did not observe increased reporter gene signal for ROR1-CARs with short or intermediate spacer length. Positive control by stimulation with BW/OKT3 cells revealed a similar activation profile for all CAR reporter cells irrespective of CAR expression. In addition, we normalized CAR stimulation to the positive control, enabling better comparison and statistical analyses between individual experiments (Figure 4.7B). Again, a strong increase in NF-κB and NFAT activation for the

ROR1-CAR variant with long spacer was observed, which differed significantly from reporter cells expressing the short and intermediate spacer design.

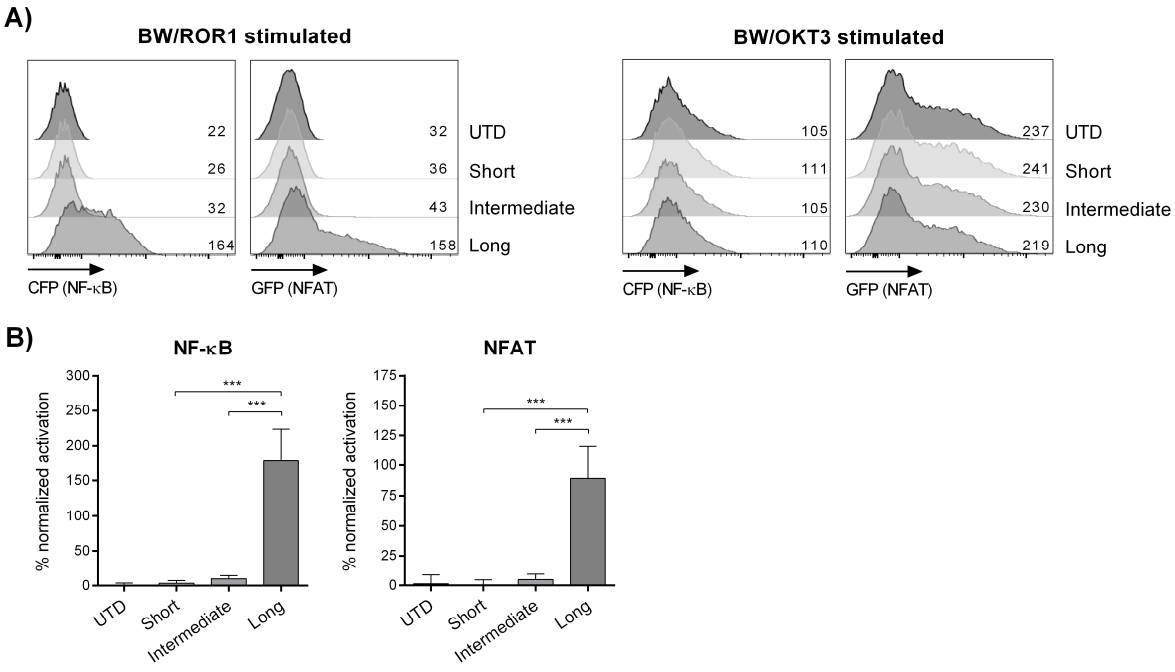


**Figure 4.7: NF-κB and NFAT activation of reporter cells expressing the ROR1-CAR spacer library.**

**A)** MFI of CFP and GFP after stimulation of ROR1-CAR spacer library-modified reporter cells with BW/ROR1 or BW/OKT3 cells at a 2.5:1 ratio for 24 hours. UTD = untransduced. **B)** NF-κB and NFAT activation in percent ± SD of BW/ROR1 stimulated ROR1-CAR reporter cells normalized to the positive control (stimulation with BW/OKT3). Statistical significance (n = 3) was determined using one-way ANOVA with Holm-Sidak post hoc test; ***p < 0.001.

In conclusion, reporter cells distinguished functional from non-functional constructs in the ROR1-CAR spacer library and identified the CAR lead candidate with long spacer design to optimally target the membrane proximal R11 epitope. These data are consistent with a previously published study showing optimal antitumor function of this CAR design in primary $CD8^+$ T cells, thus highlighting the platform's potential to accurately analyze spacer designs.[48]

### 4.2.3 Expression of a ROR1-CAR library with different signal modules in reporter cells

Many studies have illustrated the major influence of the CAR intracellular signal module on activation and functionality of primary T cells.[63,65] Therefore, we anticipated this influence would also be reflected by NF-κB and NFAT signals from reporter cells modified with a CAR library comprising different intracellular signal modules.

The library consisted of four CAR variants, each containing an scFv based on the ROR1-specific antibody R12, short IgG4-Fc spacer, and CD28 transmembrane domain (Figure 4.8A). However, in one CAR, the intracellular signal module included only a CD3ζ domain (ROR1-CAR-z). Two other CAR constructs had either a CD28 (ROR1-CAR-z28) or a 4-1BB (ROR1-CAR-zBB) co-stimulatory domain besides the CD3ζ domain. A fourth CAR contained both co-stimulatory domains in addition to CD3ζ in the signal module (ROR1-CAR-z28BB). Thus, the library included three different generations of CAR constructs. NF-κB/NFAT reporter cells were transduced with the variants of the ROR1-CAR library and enriched to >90% purity (Figure 4.8B). We observed uniform expression of each CAR construct by staining for EGFRt and direct staining with soluble ROR1 protein, which also indicated equal binding capacity of all CARs to ROR1.

In summary, the reporter cells expressed all four CAR variants from the library at similar levels, which is crucial for the robust comparison of reporter gene activation.

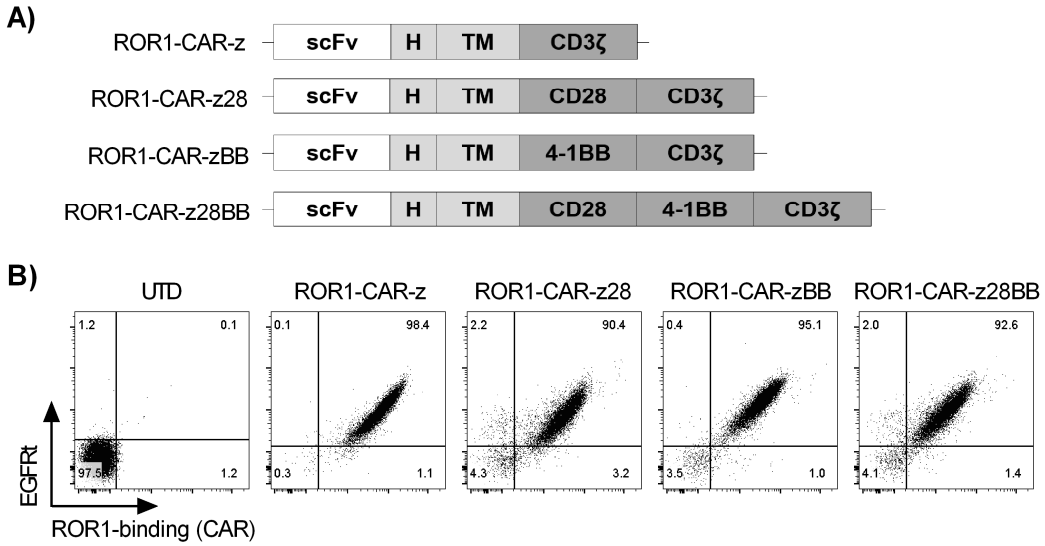


**Figure 4.8: Integration of the ROR1-CAR library with different signal modules into reporter cells.**

**A)** Schematic representation of the ROR1-CAR library with different signal modules, including first generation (ROR1-CAR-z), second generation (ROR1-CAR-z28; ROR1-CAR-zBB) and third generation (ROR1-CAR-z28BB) CARs. scFv = single-chain fragment variable recognizing R12 epitope; H= hinge; TM = transmembrane domain. **B)** CAR expression in reporter cells after transduction of the CAR library and EGFRt enrichment. Staining was performed with anti-EGFR mAb to detect the EGFRt transduction marker, and AF647-labeled soluble ROR1 protein to detect the CAR. UTD = untransduced.

### 4.2.4 Identifying signal modules with high reporter gene activation

We assumed that the co-stimulatory domains of the CAR signal modules would influence signal transduction and intensity, and that the platform would reflect this through its reporter genes. For

example, as recently demonstrated in a study, the 4-1BB domain in CARs induces strong NF-κB activation in comparison to the CD28 domain.[114]

Therefore, we stimulated the reporter cells expressing a first, second or third generation ROR1-CAR with BW/ROR1 cells for 24 hours, and we examined NF-κB and NFAT activation via detection of CFP and GFP. Interestingly, we observed similar levels of NFAT-induced GFP expression in all CAR reporter cells with an average fluorescence intensity of 157.0 ± 17.3 (Figure 4.9A). In contrast, NF-κB-induced CFP expression varied remarkably, with high deviations in fluorescence intensity between the four CAR constructs (average fluorescence intensity of 145.5 ± 52.5), indicating highest CFP signal for the ROR1-CAR with 4-1BB signal module (ROR1-CAR-zBB). Positive control stimulation with BW/OKT3 cells showed similar CFP and GFP signals (average fluorescence intensity of 128.0 ± 24.0 and 197.3 ± 19.7) for all reporter cells independent of the CAR library variant.

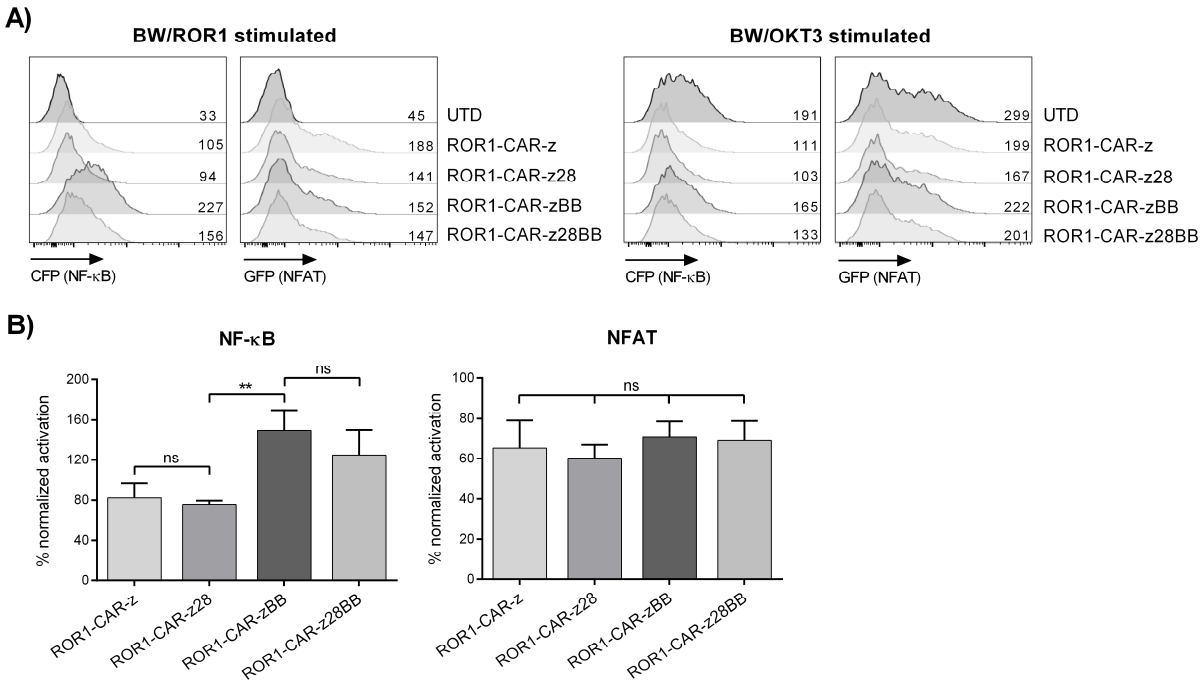


**Figure 4.9: NF-κB and NFAT activation of reporter cells expressing the ROR1-CAR library with different signal modules.** **A)** MFI of CFP and GFP after stimulation of reporter cells expressing a first, second or third generation ROR1-CAR with BW/ROR1 or BW/OKT3 cells at a 2.5:1 ratio for 24 hours. UTD = untransduced. **B)** NF-κB and NFAT activation in percent ± SD of BW/ROR1 stimulated ROR1-CAR reporter cells normalized to the positive control (stimulation with BW/OKT3). Statistical significance (n = 3) was determined using one-way ANOVA with Holm-Sidak post hoc test; **p < 0.01; ns = not significant.

For statistical evaluation, we repeated the experiments (n = 3) and normalized NF-κB and NFAT activation (Figure 4.9B). No statistical difference in NFAT activation was observed between the four CAR library variants. However, NF-κB activation differed remarkably, showing significantly stronger induction of the ROR1-CAR-zBB compared to the ROR1-CAR-z28. Notably, the NF-κB signal of the ROR1-CAR-z28 was as weak as the NF-κB signal of the ROR1-CAR-z (comprising no co-stimulatory

domain). Along with this, the CD28 domain in the ROR1-CAR-z28BB construct failed to enhance NF-κB activation compared to the ROR1-CAR with 4-1BB domain.

In aggregate, the reporter cell analyses of the ROR1-CAR library with different signal modules suggest that CAR constructs with 4-1BB co-stimulatory domain have a stronger impact on NF-κB activation than constructs with CD28 co-stimulatory domain. In contrast, NFAT activation is not affected, indicating that NFAT-inducing signaling pathways are not augmented by any of the co-stimulatory domains in this CAR library.

### 4.2.5 Reporter gene activation after stimulation of endogenous CD28 in CAR reporter cells

Our observation that the CD28 co-stimulatory domain in the CAR signal module does not enhance NF-κB activation contradicts T cell studies showing increased NF-κB activation by the CD28 receptor.[93,101] This prompted us to stimulate the endogenous CD28 receptor in CAR reporter cells to assess whether it amplifies the NF-κB signal in the presence of CARs.

Accordingly, we challenged CAR reporter cells with BW/OKT3 and compared the reporter signal to stimulation with BW/OKT3+CD80 cells, which trigger the native CD28 receptor of reporter cells. Untransduced as well as CAR transduced reporter cells showed significantly increased NF-κB reporter activation when the native CD28 receptor was triggered (Figure 4.10), excluding a negative impact of CAR expression on native CD28 stimulation. In contrast, we observed slightly increased but not significant NFAT activation after co-culture with BW/OKT3+CD80 cells, suggesting that CD28 has a minor impact on NFAT-inducing signaling pathways.

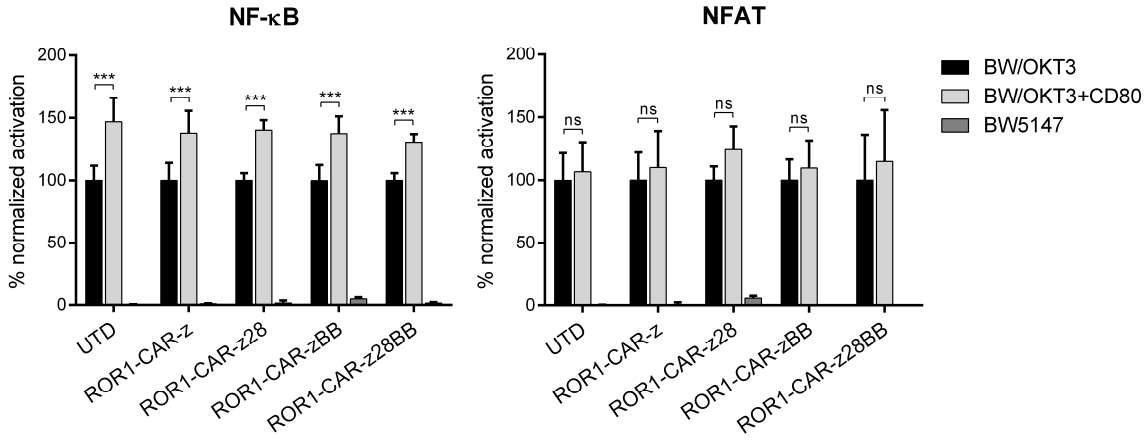


**Figure 4.10: NF-κB and NFAT activation upon stimulation of the native CD28 receptor of reporter cells.**

NF-κB and NFAT activation in percent ± SD of BW/OKT3+CD80 stimulated ROR1-CAR reporter cells normalized to the positive control (stimulation with BW/OKT3). Statistical significance (n = 3) was determined using two-way ANOVA with Holm-Sidak post hoc test; ***p < 0.001; ns = not significant. UTD = untransduced.

This experiment suggests that the CD28 domain in the CAR framework is suboptimal to trigger NF-κB-inducing signaling pathways, since the CD28 receptor can still augment NF-κB activation. Thus, the variations in NF-κB signaling observed with reporter cells may explain the different behavior of these CAR signal modules in T cells and support studies correlating 4-1BB with higher viability, central memory differentiation and less exhaustion.[69,70,114]

### 4.2.6 Interim summary

In summary, the data from Chapter 4.2 demonstrate that the NF-κB/NFAT reporter cell platform can be used to screen for optimal design parameters of extracellular and intracellular CAR modules. The analyses of a CAR spacer library showed significant activation of NF-κB and NFAT reporter genes by the CAR with long IgG4-Fc spacer, which means that this spacer domain is optimal for mediating ROR1 binding at its R11 epitope. Further analyses of a library comprising ROR1-CARs with different signal modules revealed that the 4-1BB co-stimulatory domain highly amplified the NF-κB signal, while the CD28 co-stimulatory domain in the CAR framework has lost its NF-κB inducing capacity. In the context of current literature, the high NF-κB activity may explain some advantages of CAR-T cells with 4-1BB co-stimulation regarding better viability and enhanced respiratory capacity. These results meet the third aim of the study by demonstrating in small-scale screening campaigns that the reporter cells identify CAR modules that provide optimal function in primary T cells, thus validating the accuracy and significance of the CAR-screening platform. In addition, because of the standardized analysis using the platform, the results can be obtained more rapidly than with primary T cells.

## 4.3 A large-scale screening campaign with a CAR scFv library

Because reporter cells enabled small-scale screening campaigns to identify optimal design parameters of CAR modules, we reasoned that a higher number of constructs could also be evaluated with our CAR-screening platform. For convenient implementation of a large-scale screening campaign, however, it is not possible to generate single CAR constructs and integrate them separately into reporter cells. Instead, we used a ROR1-specific CAR library whose constructs were generated by mutations of the R11-derived scFv and which were integrated into reporter cells as a pool of CAR constructs (n = $1.05x10^6$). Through a pre-enrichment and screening strategy, reporter cell clones expressing functional ROR1-CAR variants were isolated by NF-κB and NFAT signals and their CAR sequences analyzed to identify lead candidates.

### 4.3.1 Nucleofection of the ROR1-CAR scFv library and enrichment of reporter cells

We anticipated that a CAR library of many constructs, of which only a few are functional, could be used for a large-scale screening campaign to identify lead candidates. We considered the mutagenesis of the scFv antigen-binding region to be most appropriate for constructing such a CAR library, as mutations in this domain could produce a large number of constructs with altered affinity to the antigen, which is expected to strongly affect CAR functionality. For the ROR1-specific R11 scFv, for example, it can be assumed that mutations in regions important for epitope binding would cause a substantial loss of specificity and affinity.

For this purpose, we generated a library based on this R11 scFv by introducing nucleotide changes in its $V_H$ CDR3 domain using PCR-based site-restricted mutagenesis with NNK primers (Figure 4.11A). It was recently shown by crystal structure that this region is highly important for binding the ROR1 kringle domain.[129] We calculated that random mutagenesis of 12 defined nucleotides encoding the amino acids STYY would generate a total of $1.05x10^6$ $(NNK)_4$ nucleotide sequence variants, resulting in approximately $2x10^5$ distinct amino acid sequence variants. From the $1.05x10^6$ nucleotide sequence variants, only six would still encode the wild type (WT) amino acid sequence. Our PCR-based mutagenesis was not expected to re-generate the WT nucleotide sequence, which we, however, confirmed to be present in our library prior to initiating the screening campaign. To generate the final ROR1-CAR scFv library, we integrated the R11 scFv library into the pT2/HB Sleeping Beauty transposon donor vector upstream of a long IgG1-Fc spacer, CD28 transmembrane domain and intracellular signaling domains of CD3ζ and 4-1BB. The library was transferred into $64,6x10^6$ reporter cells via nucleofection to ensure that each of the $1.05x10^6$ nucleotide sequence variants was integrated at least

once. The nucleofection resulted in approximately 2.7% EGFRt-positive cells, of which only a small fraction (≤ 0.3%) was still capable of binding soluble ROR1 protein (Figure 4.11B, top panel).

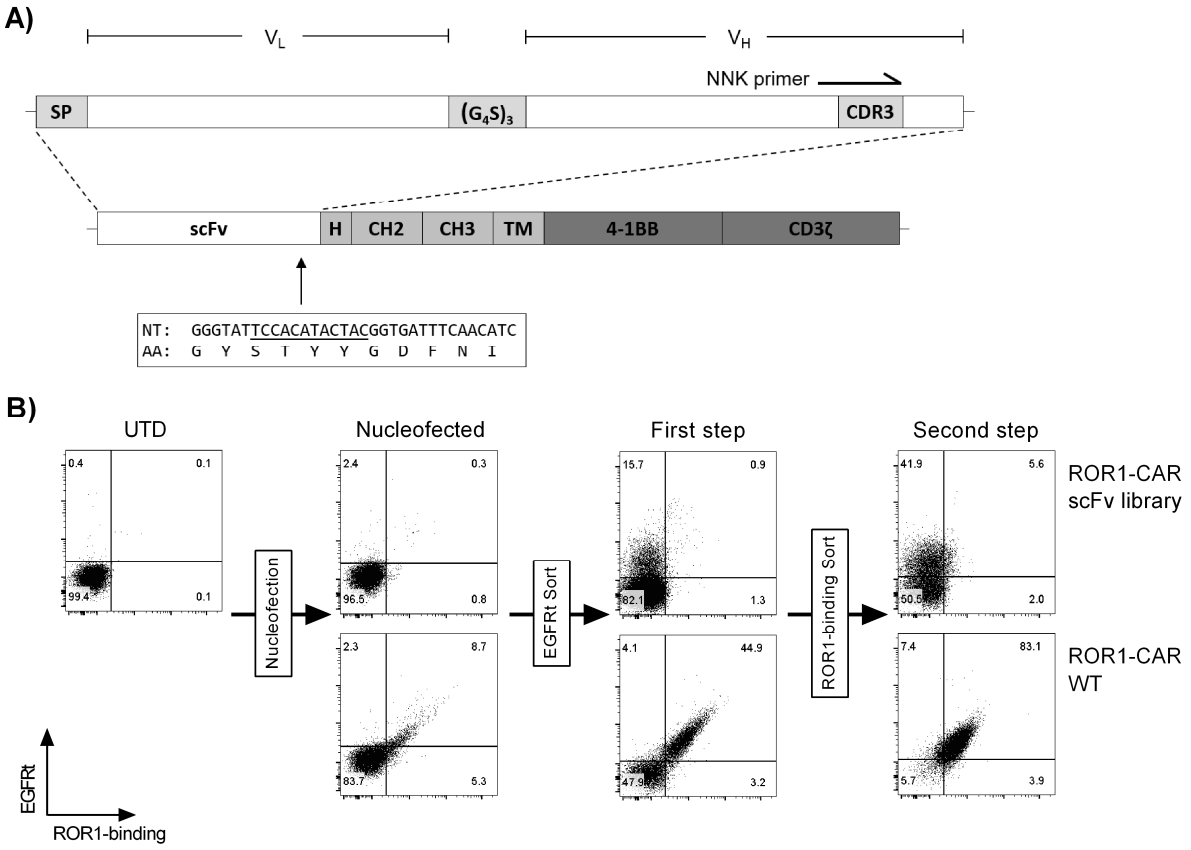


**Figure 4.11: Generation of reporter cells expressing the ROR1-CAR scFv library.**

**A)** Schematic representation of the ROR1-CAR scFv library, which is derived from the ROR1-specific R11 scFv mutated with NNK primers in the complementarity-determining region 3 (CDR3). The mutants were integrated into a CAR framework with long IgG1-Fc spacer, CD28 transmembrane and 4-1BB + CD3ζ signaling domains. The nucleotide (NT) and amino acid (AA) sequence of the CDR3 region are depicted and the 12 randomly mutated nucleotides are underlined. SP = signal peptide; scFv = single-chain fragment variable; H= hinge; CH = constant heavy domain; TM = transmembrane. **B)** EGFRt and ROR1-specific CAR expression of ROR1-CAR scFv library and R11 ROR1-CAR WT reporter cells after nucleofection and subsequent EGFRt-based magnetic bead enrichment (first step) and flow cytometry-based sorting with AF647-labeled soluble ROR1 protein (second step). UTD = untransduced.

To reduce the amount of non-nucleofected reporter cells and reporter cells that encoded nucleotide variants comprising a stop codon, we performed two sequential sorting steps enriching for CAR reporter cells that expressed EGFRt (first step) and bound ROR1 protein (second step). This increased the population of interest (double positive, i.e. $EGFRt^+$ and binding to ROR1 protein) to 5.6%. In contrast, nucleofection with the wild type CAR (R11 ROR1-CAR WT), which we used as reference, resulted in approximately 8.6% cells that bound ROR1 protein and expressed EGFRt (Figure 4.11B, bottom panel). Further, the same pre-enrichment strategy as for the ROR1-CAR scFv

library finally produced 83.1% double-positive R11 ROR1-CAR WT cells, which was to be expected as the WT is a high-affinity CAR.

In summary, these data show that the mutagenesis of R11 scFv generated a library containing many different CARs of which only a minority was capable of binding ROR1. Furthermore, the number of EGFRt$^+$ reporter cells that showed specific binding to ROR1 could be increased by the pre-enrichment strategy.

### 4.3.2 Stimulation of reporter cells expressing the ROR1-CAR scFv library

We speculated that the pre-enrichment steps, which increased the number of reporter cells expressing a ROR1-binding CAR, also increased the number of cells showing reporter gene signals upon antigen-specific stimulation.

Therefore, we compared nucleofected ROR1-CAR scFv library reporter cells with first and second step pre-enriched ROR1-CAR scFv library reporter cells after 24-hours stimulation with BW/ROR1 cells (Figure 4.12, top panel). Nucleofected cells as well as first step pre-enriched reporter cells showed very little NF-κB or NFAT signal. However, after the second step of pre-enrichment, the number of positive cells with CFP and GFP signal was clearly increased to 3.5%. In contrast, reporter cells nucleofected with the R11 ROR1-CAR WT already showed 8.8% CFP$^+$ GFP$^+$ cells after stimulation with BW/ROR1 due to the high functionality of the CAR (Figure 4.12, bottom panel). The pre-enrichment finally increased the fraction of cells with CFP and GFP signal up to 16.5%.

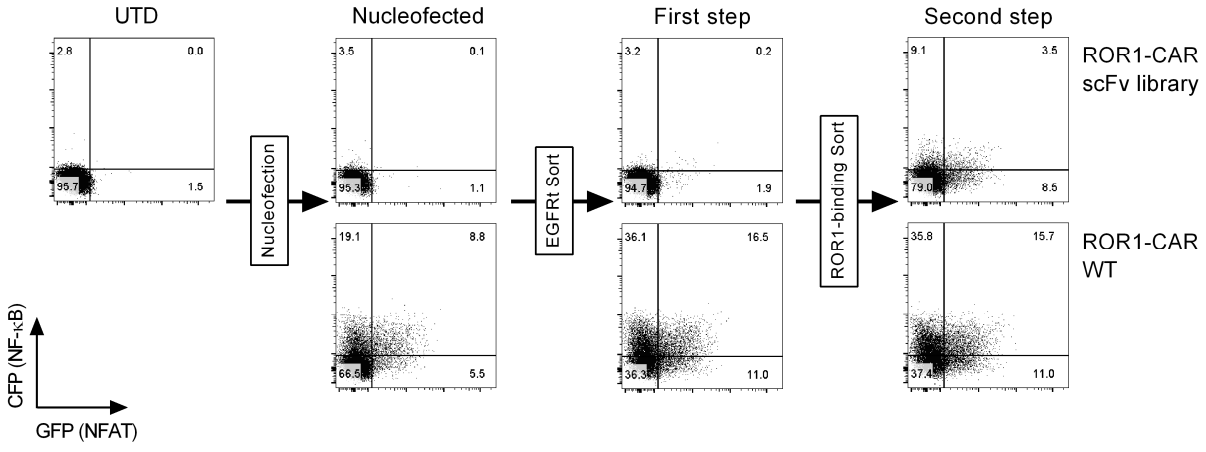


**Figure 4.12: Stimulation of ROR1-CAR scFv library modified reporter cells before and after pre-enrichment.**

Reporter gene induced CFP and GFP expression after stimulation with BW/ROR1 cells at a 2.5:1 ratio for 24 hours. For the analysis, reporter cells after nucleofection with the ROR1-CAR scFv library or R11 ROR1-CAR WT were used, which were then pre-enriched in two steps. UTD = untransduced.

In aggregate, the results demonstrate that the pre-enrichment strategy increased the number of reporter cells expressing a CAR that could be stimulated by ROR1, as shown by the elevated NF-κB and NFAT reporter signals.

### 4.3.3 Single-cell sorting based on NF-κB and NFAT reporter signals

Since we sought to identify new functional ROR1-specific CARs, we considered it necessary to isolate single reporter cell clones from the pre-enriched population and analyze the NF-κB and NFAT signals in a follow-up screening campaign.

We incubated the pre-enriched ROR1-CAR scFv library cells with lethally irradiated BW/ROR1 cells, and we sorted for single cells with highest level of CFP and GFP expression by FACS (Figure 4.13A). From this sorting campaign, a total of 100 cell clones were re-analyzed for reporter activity upon stimulation with BW/ROR1 cells, and the 25 clones with strongest CFP and GFP signal were selected. Of these, 10 clones had to be excluded from further analysis due to insufficient expansion or unspecific reactivity, which left 15 clones for detailed analysis. Figure 4.13B depicts representatively the stimulation of 7 out of these 15 clones with $CFP^+$ $GFP^+$ cells in a range between 10.8% and 35.8%, while stimulation of R11 ROR1-CAR WT reporter cells resulted in 19.6% $CFP^+$ $GFP^+$ cells. Calculation of the normalized reporter gene activation for all 15 clones showed that in 11 clones the signal of at least one of the two reporter genes was significantly lower (* ↓) than the reference set by reporter cells expressing the R11 ROR1-CAR WT (Figure 4.13C). In 4 of the 15 clones (#45, #54, #70 and #80), the reporter signal was similar (ns) or higher (* ↑) compared to the reference.

Altogether, the data suggest that the four clones with a comparable or higher reporter signal than the ROR1-CAR WT should be examined more closely. It is conceivable that these clones express either the WT ROR1-CAR, or a ROR1-CAR variant with altered specificity and/or affinity to ROR1, which apparently did not considerably influence reporter gene activation.

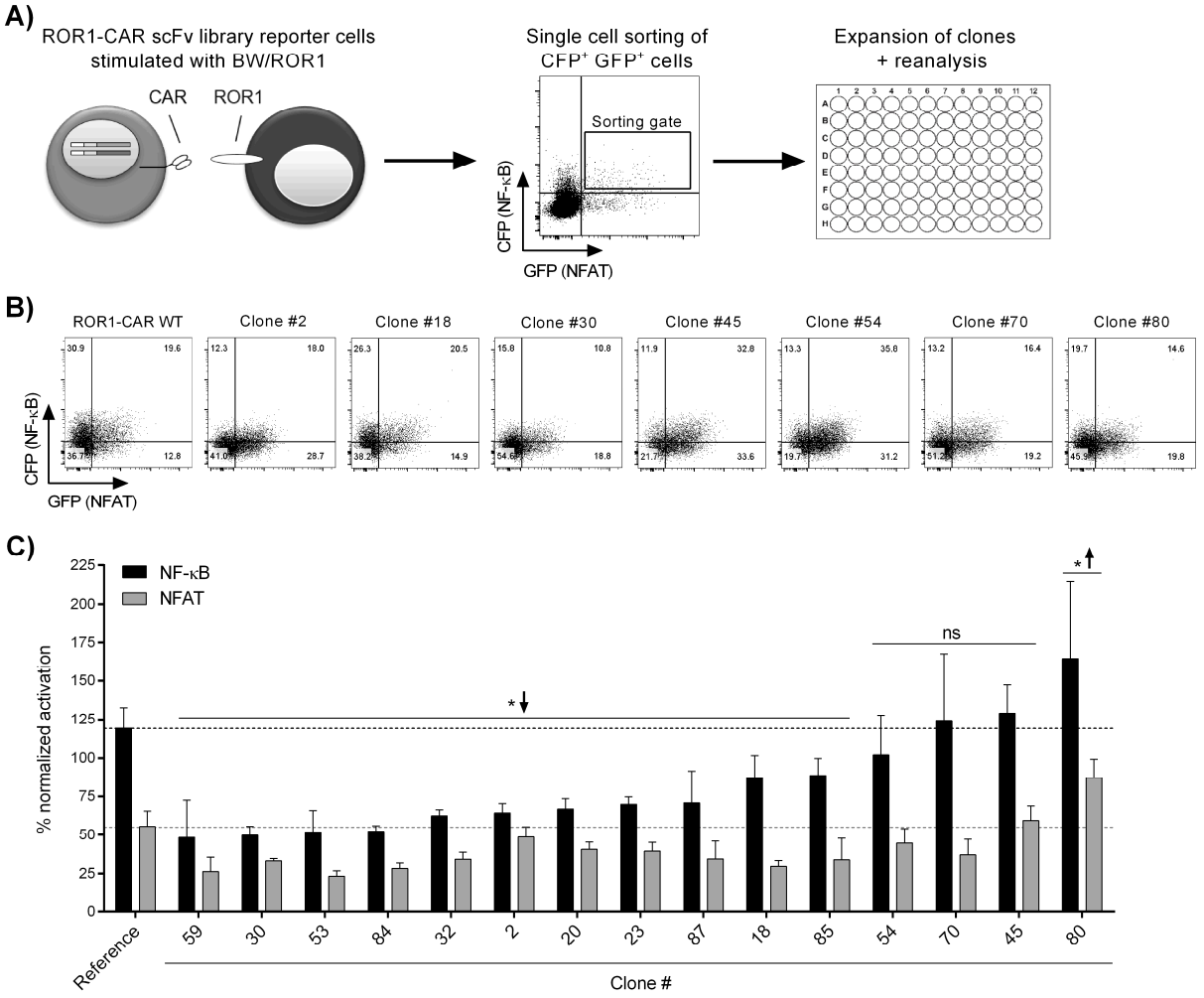


**Figure 4.13: Analysis of single cell clones isolated from ROR1-CAR scFv library reporter cells based on NF-κB- and NFAT.** **A)** Schematic representation of the single-cell sorting approach, showing isolation of $CFP^+$ $GFP^+$ clones after stimulation of ROR1-CAR scFv library reporter cells with BW/ROR1. Cell clones were expanded and then re-analyzed for reporter gene activation. **B)** CFP and GFP expression of representative cell clones stimulated with BW/ROR1 cells at a 2.5:1 ratio for 24 hours. **C)** NF-κB and NFAT activation in percent ± SD of BW/ROR1 stimulated ROR1-CAR scFv library clones normalized to the positive control (stimulation with BW/OKT3). Stimulation of the R11 ROR1-CAR WT was used as reference for NF-κB (black line) and NFAT (grey line) reporter induction. Statistical significance (n = 3) was determined in comparison to the reference (ROR1-CAR WT) using two-way ANOVA with Holm-Sidak post hoc test. ↑ = higher; ↓ = lower; *p < 0.05; ns = not significant.

### 4.3.4 Analysis of CAR sequences obtained from reporter cells with high NF-κB and NFAT signals

To identify the CARs expressed by the clones selected for NF-κB and NFAT signals in the screening campaign, we decided to analyze their scFv sequences containing possible mutations.

We isolated the genomic DNA of the 15 clones and amplified the scFv sequence by PCR, resulting in DNA fragments of about 1500 bp (Figure 4.14). As it was anticipated that our gene transfer method

could result in genomic integrations of more than one CAR variant, we cloned the amplified DNA fragments into TOPO TA vectors to analyze transformed bacterial clones for single scFv sequences.

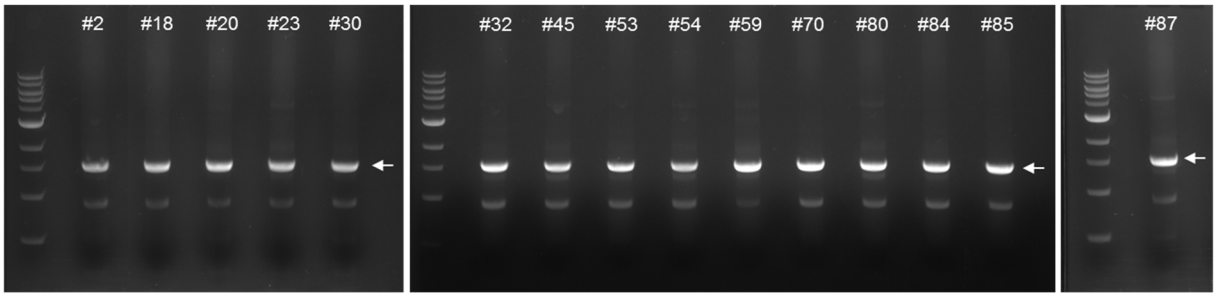


**Figure 4.14: Isolation of scFv fragments from clones with high reporter signal.**

Separation of PCR-amplified scFv fragments by gel electrophoresis. The 1500 bp fragment (arrow) was isolated and used for further analysis. An unspecific fragment was detected at 800 bp.

Being particularly interested in the clones with the highest reporter signal, we focused on clones #45, #54, #70 and #80 for analysis. Indeed, in clones #45, #70 and #80, we detected more than two $V_H$ CDR3 nucleotide sequences (Table 4.1). In each of the three clones, there was at least one nucleotide sequence that encoded a novel and unique CDR3 amino acid sequence; however, we also detected the scFv nucleotide sequence of the R11 ROR1-CAR WT. In clone #80, in which we detected the highest reporter signal, we also detected the highest level of CAR expression as assessed by staining for EGFRt. This observation provides an explanation for the higher reporter signal compared to clones #45, #54, #70 and WT reference. Analysis of clone #54 revealed only a single nucleotide sequence that was distinct from the WT scFv nucleotide sequence. Upon translation into the amino acid sequence, we found that this nucleotide sequence also encoded the WT amino acid motif STYY.

**Table 4.1: Detailed analysis of CDR3 sequences in the 4 clones with highest reporter signal.***

| Library Clone | EGFRt [MFI] | NF-κB act. [%] | NFAT act. [%] | CDR3 nucleotide sequences | Amino acid sequences |
|---|---|---|---|---|---|
| #45 | 394 | 129.0 ± 18.3 | 59.3 ± 9.3 | 5'-TCCACATACTAC-3' (WT) | STYY (WT) |
| | | | | 5'-GATACGTATTAG-3' | DTY– |
| | | | | 5'-ACGTTGAATTCG-3' | TLNS |
| | | | | 5'-GATCCGCCGCAT-3' | DPPH |
| #54 | 353 | 101.9 ± 25.8 | 44.5 ± 9.4 | 5'-TCGACTTATTAT-3' (non-WT) | STYY (WT) |
| #70 | 208 | 124.3 ± 43.2 | 36.9 ± 10.2 | 5'-TCCACATACTAC-3' (WT) | STYY (WT) |
| | | | | 5'-TAGCGTGCTCCT-3' | –RAP |
| #80 | 599 | 164.5 ± 49.9 | 87.1 ± 12.0 | 5'-TCCACATACTAC-3' (WT) | STYY (WT) |
| | | | | 5'-TAGTTTACGGCT-3' | –FTA |
| | | | | 5'-GTGTGGGTTACG-3' | VWVT |
| | | | | 5'-ACGCCGCTGCCT-3' | TPLP |
| | | | | 5'-ATGACTGGGTAG-3' | MTG– |
| | | | | 5'-CAGGCTTGGATG-3' | QAWM |
| | | | | 5'-ATGAGTATGATT-3' | MSMI |
| Reference (ROR1-CAR WT) | 288 | 119.1 ± 13.4 | 55.5 ± 9.9 | 5'-TCCACATACTAC-3' (WT) | STYY (WT) |

* NF-κB act. and NFAT act. correspond to normalized CAR activation, which is indicated as percentage ± SD. Stop codons are displayed as – in the amino acid sequence.

Since we found several ROR1-CAR scFv library variants in clones #45 and #80, which did not contain a stop codon and thus should be expressed on the cell surface, we assessed whether one of these variants was functional besides the ROR1-CAR WT. Thus, we isolated their scFv sequences, and we cloned them into the CAR framework of the pT2/HB Sleeping Beauty transposon donor vector. After nucleofection of the CAR variants and EGFRt-dependent enrichment, we detected EGFRt on >91% of reporter cells, but none of the variants were capable of binding soluble ROR1 protein (Figure 4.15A). Similarly, reporter cells expressing the ROR1-CAR variants and stimulated with BW/ROR1 cells did not show NF-κB or NFAT reporter gene activation (Figure 4.15B), suggesting that the reporter signal in clones #45 and #80 was induced by the ROR1-CAR with the WT $V_H$ CDR3 sequence. Moreover, we preliminary analyzed several of the remaining eleven clones, which had shown significantly lower reporter gene signal compared to the reference. We only detected multiple novel CAR-encoding nucleotide sequence variants that did not encode the WT $V_H$ CDR3 amino acid sequence. However, analysis of these CAR variants with reporter cells showed neither binding to soluble ROR1 protein nor activation by BW/ROR1 stimulation (data not shown).

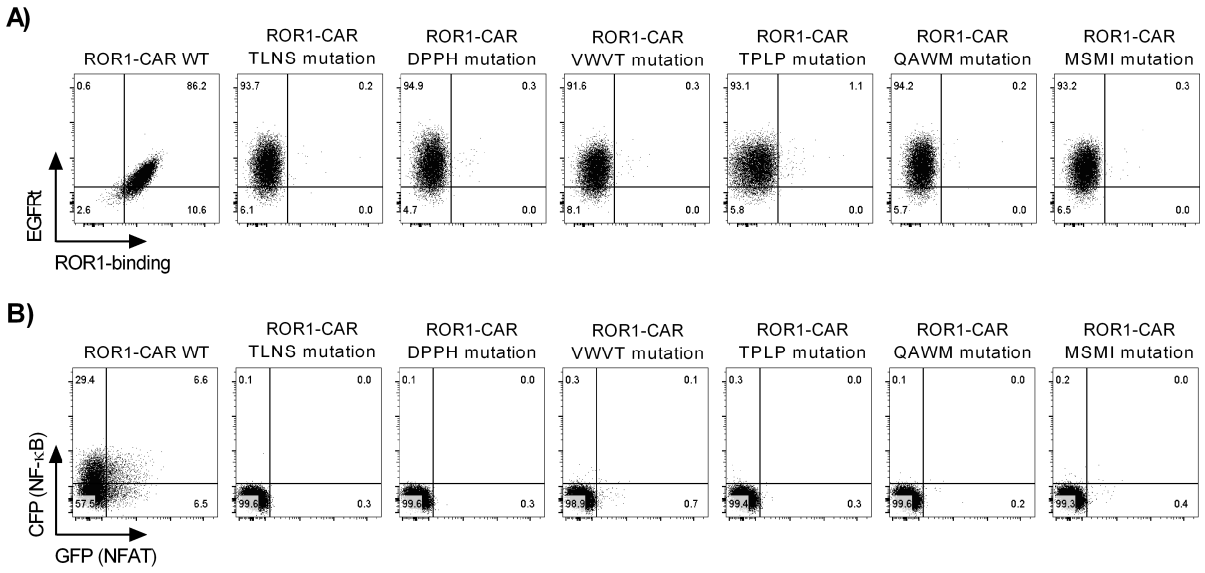


**Figure 4.15: Analysis of ROR1-CAR variants found in clones with highest reporter signal.**

**A)** EGFRt and ROR1-specific CAR expression of reporter cells expressing the ROR1-CAR WT or ROR1-CAR scFv library variants that were found in clones #45 and #80. **B)** CFP and GFP expression of reporter cells expressing the ROR1-CAR WT or ROR1-CAR scFv library variants after stimulation with BW/ROR1 cells at a 2.5:1 ratio for 24 hours.

In conclusion, the data demonstrate the utilization of the platform for large-scale screening campaigns with libraries of >1x10$^6$ CAR constructs. We detected the R11 ROR1-CAR WT sequence in those clones with highest NF-κB and NFAT signals, and we retrieved one out of six possible nucleotide sequence variants encoding the WT $V_H$ CDR3. Since none of the other novel CAR variants identified in

in the clones with highest reporter gene activity showed functionality, it is likely that only the WT CAR triggered the NF-κB and NFAT signals.

### 4.3.5 Interim summary

In summary, the data from Chapter 4.3 show the potential of the CAR-screening platform for the analysis of complex CAR libraries with high sample numbers that presumably cannot be handled in screening campaigns with primary T cells. For our large-scale screening campaign, we used a CAR library with $1.05x10^6$ variants that differed by mutations in the CDR3 region of the R11 scFv, which we anticipated would alter their specificity and affinity. Through a pre-enrichment and screening strategy, the platform identified cell clones with high NF-κB and NFAT signals that expressed the functional WT ROR1-CAR. Further, a nucleotide sequence variant of the WT ROR1-CAR was retrieved, suggesting that mutations of the CDR3 region encoding for non-WT ROR1-CAR variants were incapable to augment NF-κB and NFAT induction. These results meet the fourth aim of the study by demonstrating the implementation of a large-scale screening campaign with a complex CAR library in the NF-κB/NFAT reporter cell platform.

## 4.4 CAR-library screening of constructs with inhibitory signal module

The screening campaign from Chapter 4.2.4 showed that intracellular signal modules comprising stimulatory domains can be analyzed by NF-κB/NFAT reporter cells. This prompted us to assume that signal modules with inhibitory domains could also be investigated, for example in logic gates together with activating CARs.[83] In this way, the platform should enable the analysis of strategies that are expected to improve the selectivity of CAR-T cells for the prevention of on-target off-tumor toxicities, thereby demonstrating its potential to test novel CAR approaches. First, we studied inhibitory receptors with the NF-κB/NFAT reporter cell platform to evaluate its readout, and then we generated an iCAR library of constructs with inhibitory signal module. The inhibitory capacity of iCARs to neutralize reporter gene activation was finally analyzed in different logics gates, and the results were verified in primary human T cells.

### 4.4.1 Analysis of inhibitory receptors using reporter cells

Studies have previously shown that reporter genes are capable of measuring the suppressive effects of inhibitory receptors.[128,131] Therefore, we aimed to reproduce these observations with the reporter cells and demonstrate the reduction of NF-κB and NFAT signals by inhibitory receptors.

The reporter cells were activated by stimulator cells through the TCR complex and the resulting NF-κB and NFAT signals were compared to reporter cells additionally stimulated by an inhibitory receptor (Figure 4.16A). As inhibitory receptors, we used PD-1 and BTLA, which are well-known for their inhibitory potential on T cells and were supposed to interfere with the activation of reporter genes. Reporter cells transduced with PD-1 or BTLA showed uniform expression of the receptors (Figure 4.16B). To trigger PD-1 and BTLA on reporter cells, we equipped BW/OKT3 cells with the corresponding ligands PD-L1 and HVEM, respectively, and assessed their expression (Figure 4.16C). Then, we stimulated PD-1 or BTLA reporter cells with BW/OKT3, and we compared the ensuing reporter activation to stimulation with BW/OKT3 cells expressing the ligand of the inhibitory receptor. PD-1 reduced the MFI of NF-κB from 525 to 346 (approx. 1.5-fold) and the MFI of NFAT from 238 to 127 (approx. 1.8-fold) (Figure 4.16D). Similarly, BTLA decreased the MFI of NF-κB from 514 to 235 (approx. 2.1-fold) and the MFI of NFAT from 133 to 73 (approx. 1.8-fold).

In summary, these data demonstrate the platform's ability to evaluate the suppressive effects of inhibitory receptors on NF-κB and NFAT activation. This suggests that the platform also enables the analysis of CARs with inhibitory signal modules.

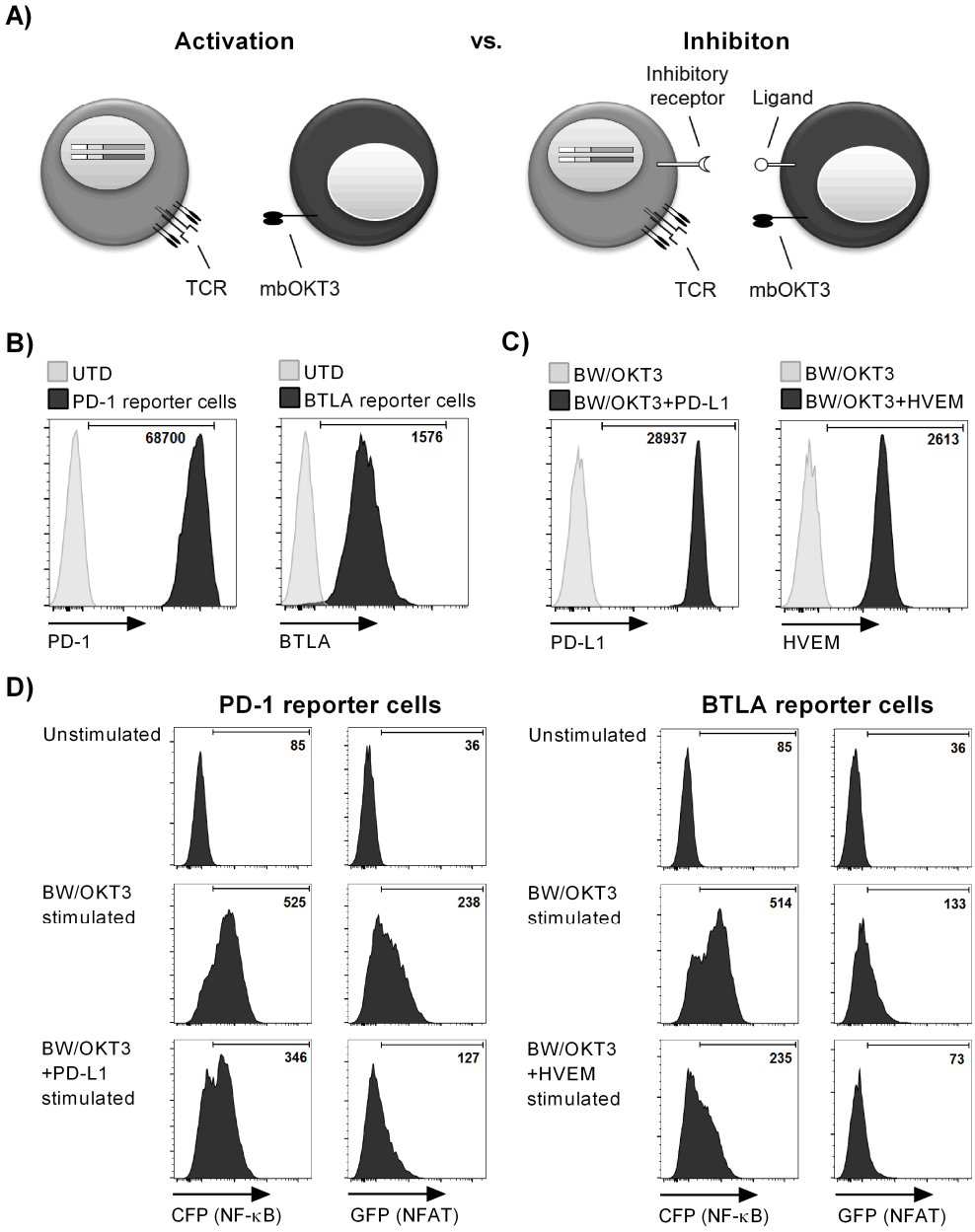


**Figure 4.16: Inhibition of NF-κB and NFAT through inhibitory receptors PD-1 and BTLA.**

**A)** Schematic representation of NF-κB/NFAT reporter cells expressing an inhibitory receptor and stimulated via TCR engagement and interaction of the inhibitory receptor with its ligand. **B)** Expression of inhibitory receptors on reporter cells. Numeric values represent the MFI of transduced cells minus the MFI of untransduced (UTD) reporter cells. **C)** Expression of ligands on BW/OKT3 cells that interact with the cognate inhibitory receptor. Numeric values represent the MFI of transduced cells minus the MFI of BW/OKT3. **D)** MFI of CFP and GFP after stimulation of PD-1 and BTLA reporter cells with BW/OKT3, BW/OKT3+PD-L1 or BW/OKT3+BTLA at a 2.5:1 ratio for 24 hours.

## 4.4.2 Challenging CD19-iCARs in logic gates in reporter cells

Because we anticipated that the platform allows the analysis of CARs with inhibitory capacity on reporter gene activation, we decided to challenge an iCAR library with TCR or CAR stimulation. For this,

two logic gate settings, consisting of either iCAR and CAR or iCAR and TCR, should be employed and transferred to reporter cells.

The iCAR library contained three constructs with a signal module from the intracellular part of PD-1 (Figure 4.17), as studies have shown a strong inhibitory effect of the PD-1 receptor in T cells.[132] We selected CD19 as target antigen for the iCARs, because it is effectively recognized by the FMC63-derived scFv and could be implemented in a logic gate to avoid the elimination of healthy B cells. Further, to assess the impact of spacer design on iCAR expression and inhibitory function, the constructs differed in spacer and transmembrane domains. iCAR 101 contained the hinge and transmembrane domain of PD-1, iCAR 102 contained the spacer domain of IgG4-Fc and the transmembrane domain of CD28, and iCAR 103 contained the hinge and transmembrane domain of CD8α. A c-Myc tag was attached to the N-terminus of the CD19-targeting scFv to allow direct analysis of iCAR expression and enrichment of iCAR$^+$ cells.

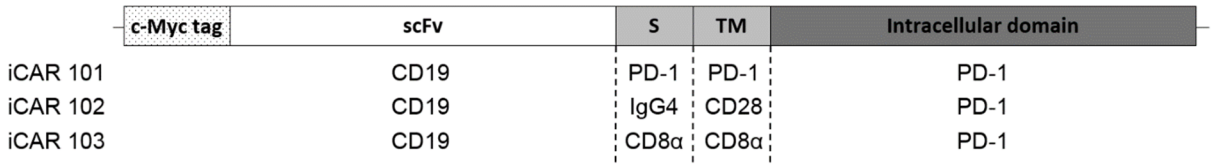


**Figure 4.17: Constructs of the CD19-iCAR library with intracellular inhibitory domain of PD-1.**
Schematic representation of iCAR constructs that targeted CD19 by the FMC63-derived scFv. All iCAR constructs contained the intracellular domain of PD-1 but differed in the spacer and transmembrane domain. The c-Myc tag was included at the N-terminus of the scFv for detection and enrichment. scFv = single-chain fragment variable; S = spacer; TM = transmembrane domain.

To analyze the efficacy of inhibitory signal modules in reporter cells, we first decided to challenge the iCARs by stimulation of the TCR complex. BW/OKT3 cells served as 'on-tumor' cells, while CD19 equipped BW/OKT3+CD19 cells served as 'off-tumor' cells (Figure 4.18A). We transduced NF-κB/NFAT reporter cells with the CD19-iCAR constructs and enriched iCAR$^+$ cells, and we detected high and similar iCAR expression for all constructs, suggesting that the choice of spacer and transmembrane domains did not affect iCAR expression (Figure 4.18B). In addition, the iCAR target antigen CD19 was highly expressed on BW/OKT3+CD19 cells as confirmed by flow cytometry (Figure 4.18C). Then, we challenged CD19-iCAR reporter cells with BW/OKT3 on-tumor cells, and we compared the reporter signal to stimulation with BW/OKT3+CD19 off-tumor cells. For both, NF-κB and NFAT, we observed a slight decrease of the activation, however, this was not significant and independent of the design of the iCAR constructs (Figure 4.18D).

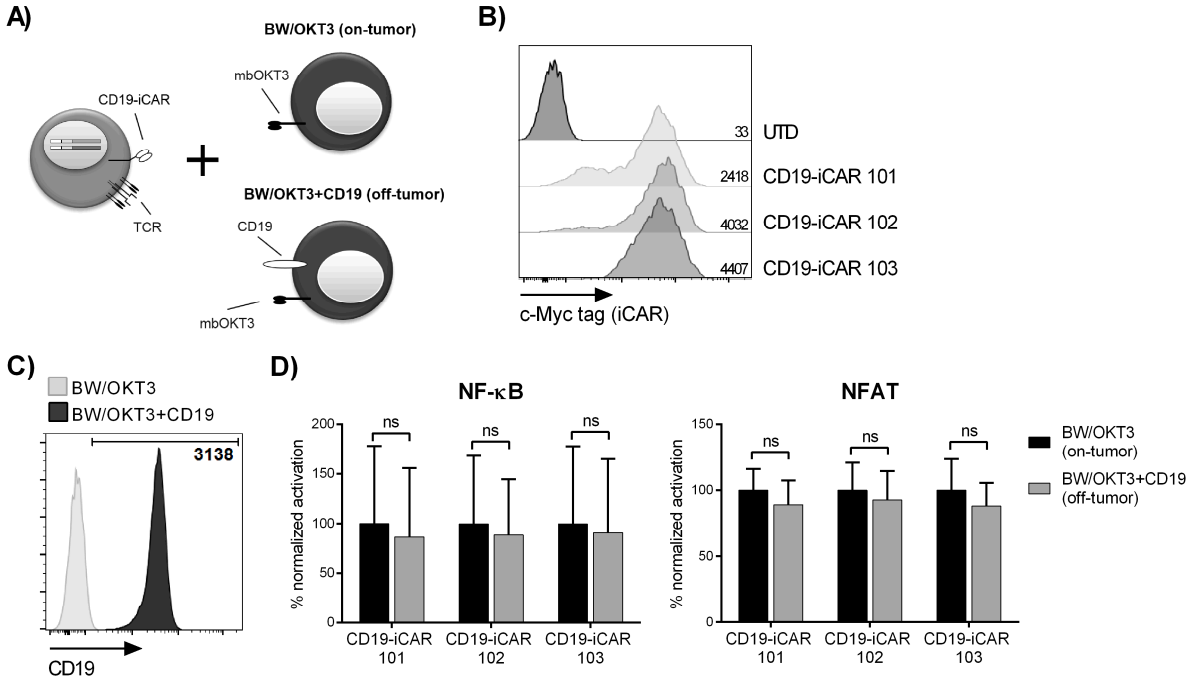


**Figure 4.18: NF-κB and NFAT reporter activation after challenging CD19-iCARs with TCR stimulation in reporter cells.**
**A)** Schematic representation of the experimental setup with CD19-iCAR reporter cells challenged with BW/OKT3 on-tumor or BW/OKT3+CD19 off-tumor cells. **B)** iCAR expression after transduction and enrichment of reporter cells with the CD19-iCAR library. Staining was performed with anti-c-Myc mAb to detect the c-Myc tag of CD19-iCARs. Numeric values represent the MFI of transduced cells. UTD = untransduced. **C)** Expression of CD19 on BW/OKT3+CD19 cells. Numeric value represents the MFI of BW/OKT3+CD19 minus the MFI of BW/OKT3. **D)** NF-κB and NFAT activation in percent ± SD of BW/OKT3+CD19 stimulated CD19 iCAR reporter cells normalized to the positive control (stimulation with BW/OKT3). Statistical significance (n = 3) was determined using two-way ANOVA with Holm-Sidak post hoc test; ns = not significant.

Next, we decided to challenge the iCARs in another logic gate with an activating CAR, for which we chose ROR1-CAR-zBB with R12-derived scFv. Here, BW/ROR1 cells served as 'on-tumor' cells and CD19-equipped BW/ROR1+CD19 cells served as 'off-tumor' cells (Figure 4.19A). NF-κB/NFAT reporter cells were transduced with ROR1-CAR-zBB and CD19-iCARs and double-positive reporter cells ($CAR^+$ $iCAR^+$) were enriched via EGFRt and c-Myc tag. Flow cytometry analysis revealed >70% CAR and iCAR-positive cells after enrichment (Figure 4.19B). Furthermore, BW5147 cells were transduced with ROR1 and CD19 resulting in high surface expression of both proteins (Figure 4.19C). When we stimulated ROR1-CAR-zBB + CD19-iCAR reporter cells with BW/ROR1+CD19 off-tumor cells, we detected a slight decrease of NF-κB and NFAT activation in comparison to the stimulation with BW/ROR1 on-tumor cells (Figure 4.19D). However, this reduction was not significant, and the different spacer and transmembrane domains did not improve the inhibitory function of the iCARs.

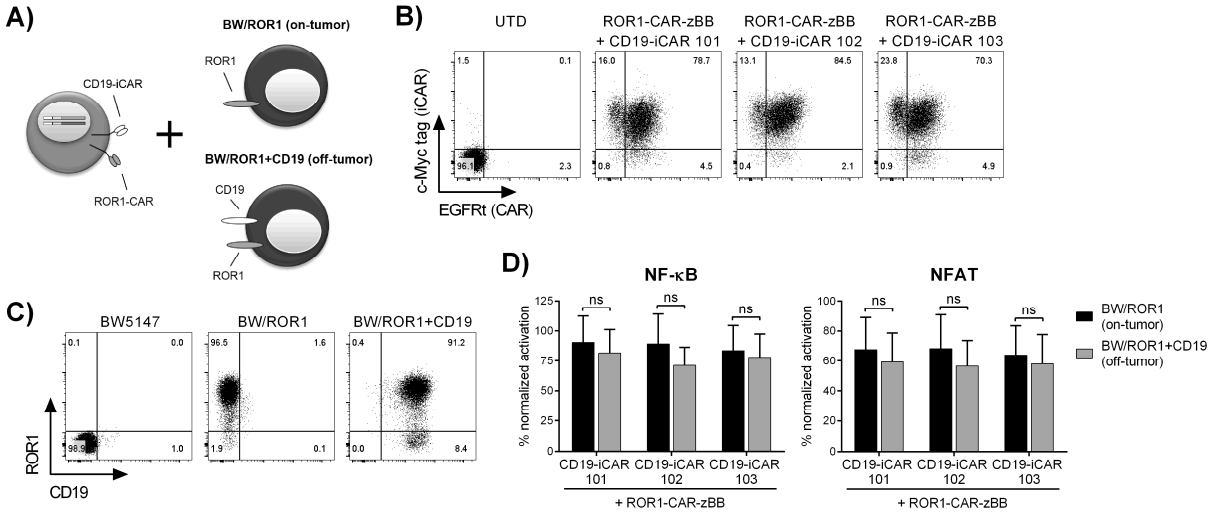


**Figure 4.19: NF-κB and NFAT reporter activation after challenging CD19-iCARs with CAR stimulation in reporter cells.**
**A)** Schematic representation of the experimental setup with ROR1-CAR + CD19-iCAR reporter cells challenged with BW/ROR1 on-tumor or BW/ROR1+CD19 off-tumor cells. **B)** Expression of ROR1-CAR-zBB and CD19-iCARs by reporter cells after transduction and enrichment. Staining was performed with anti-EGFR mAb to detect the EGFRt transduction marker of the ROR1-CAR-zBB and with anti-c-Myc mAb to detect the c-Myc tag of CD19-iCARs. UTD = untransduced. **C)** Expression of ROR1 and CD19 on BW5147 cells after transduction. **D)** NF-κB and NFAT activation in percent ± SD of stimulated ROR1-CAR-zBB + CD19-iCAR reporter cells normalized to the positive control (stimulation with BW/OKT3). Statistical significance (n = 4) was determined using two-way ANOVA with Holm-Sidak post hoc test; ns = not significant.

Taken together, these results demonstrate that the inhibitory signal modules of the CD19-iCARs were not able to significantly reduce the reporter signal induced by TCR or ROR1-CAR stimulation. Furthermore, the spacer and transmembrane domains had no influence on the inhibitory capacity of the iCAR constructs to neutralize reporter gene activation in both logic gates.

### 4.4.3 Verification of the reporter cell results with CD19-iCARs in primary T cells

To verify the significance of the results obtained with the NF-κB/NFAT reporter cell platform, we aimed to reproduce the CD19-iCAR logic gate experiments in primary T cells.

First, we tested the logic gate of CD19-iCAR and ROR1-CAR by challenging T cells with K562/ROR1 on-tumor and K562/ROR1+CD19 off-tumor cells (Figure 4.20A). We isolated $CD8^+$ memory T cells from PBMCs and transduced them to express ROR1-CAR-zBB together with one of the CD19-iCARs. After enrichment via EGFRt and c-Myc tag, we detected >63% ROR1-CAR-zBB$^+$ CD19-iCAR$^+$ T cells by flow cytometry (Figure 4.20B). Additionally, we generated K562/ROR1 and K562/ROR1+CD19 cells, and we confirmed high surface expression for both proteins (Figure 4.20C).

We then co-cultured CAR-T cells with K562/ROR1+CD19 cells at different E:T ratios, and we compared cytotoxicity to co-culture with K562/ROR1 cells. No differences were observed between the killing of on- and off-tumor cells with T cells expressing the CD19-iCAR 101 or CD19-iCAR 103, similar to control T cells expressing only the ROR1-CAR-zBB (Figure 4.20D). Notably, off-tumor cells were eliminated faster than on-tumor cells by T cells expressing the CD19-iCAR 102, maybe due to dimerization of CAR and iCAR through their IgG4-Fc spacers, which may have led to cross-signaling and domination of the ROR1-CAR-zBB. We measured IFNγ secretion after 24-hours co-culture with on- and off-tumor cells but we only observed a minor decrease of IFNγ for T cells expressing the CD19-iCAR 103 and no changes for T cells expressing the CD19-iCAR 101 and CD19-iCAR 102 (Figure 4.20E).

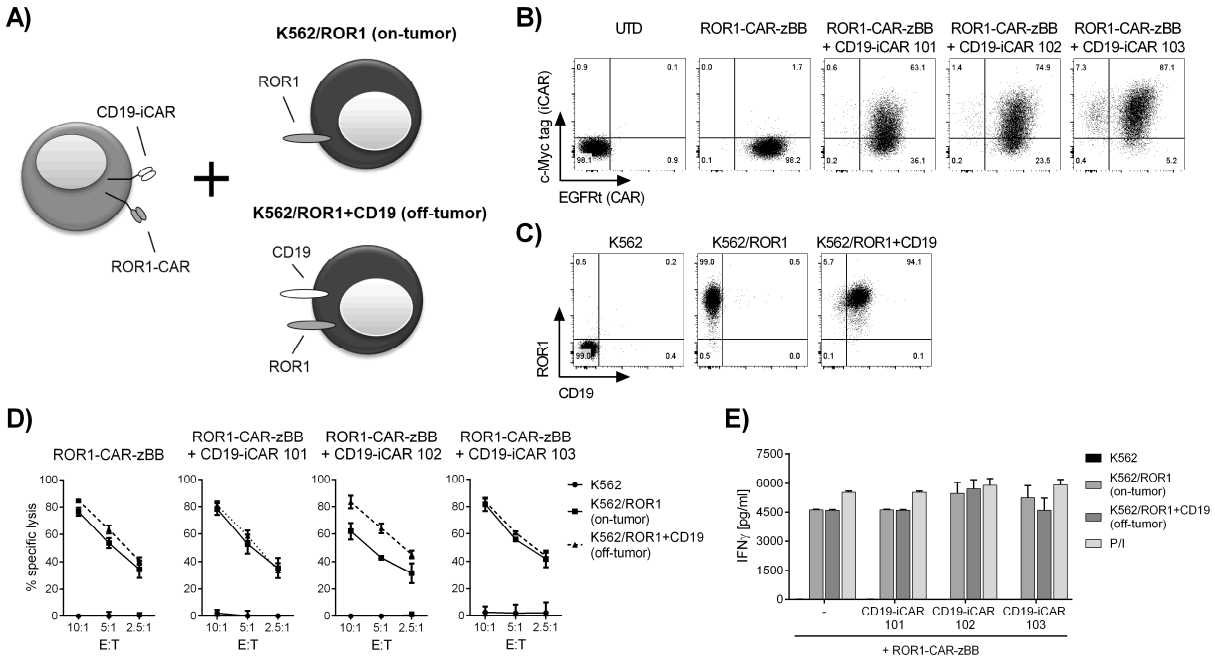


**Figure 4.20: Challenging CD19-iCARs with a ROR1-CAR in primary T cells.**

**A)** Schematic representation of the experimental setup with T cells expressing both ROR1-CAR and CD19-iCAR and challenged with K562/ROR1 on-tumor or K562/ROR1+CD19 off-tumor cells. **B)** Expression of ROR1-CAR-zBB and CD19-iCARs on primary $CD8^+$ T cells on day 8 of expansion. Staining was performed with anti-EGFR mAb to detect the EGFRt transduction marker of the ROR1-CAR, and with anti-c-Myc mAb to detect the c-Myc tag of CD19-iCARs. UTD = untransduced. **C)** Expression of ROR1 and CD19 on K562 cells after transduction. **D)** Specific lysis ± SD (n = 3 technical replicates) of ROR1-CAR-zBB + CD19-iCAR-T cells co-cultured with on- or off-tumor cells at different E:T ratios for 4 hours. T cells expressing only ROR1-CAR-zBB were used as control. **E)** IFNγ secretion ± SD of ROR1-CAR-zBB + CD19-iCAR-T cells co-cultured with on- or off-target cells at a 4:1 ratio for 24 hours. Stimulation with PMA and ionomycin (P/I) and stimulation of T cells expressing only ROR1-CAR-zBB served as controls.

Analogous to the previous experiment, we tested a logic gate consisting of CD19-iCARs and a CMV-specific TCR (CMV-TCR), which recognizes the HLA-A*0201 restricted CMV peptide pp65 with the amino acid sequence NLVPMVATV. The CMV-specific T cells expressing a CD19-iCAR would then be

challenged with K562/HLA-A*0201 on-tumor cells and K562/HLA-A*0201+CD19 off-tumor cells (Figure 4.21A). We isolated CD8$^+$ memory T cells from CMV-serum positive, HLA-A*0201 positive donors, and we specifically stimulated the T cell subset expressing the CMV-TCR. The stimulated T cells were transduced with the CD19-iCAR library and expanded, but only with the CD19-iCAR 102 we achieved a sufficient number of >70% T cells double positive for CMV-TCR and CD19-iCAR (Figure 4.21B). As a control, we generated T cells that only expressed the CMV-TCR (~97.9%). On- and off-tumor cells were prepared by transduction of K562 cells with HLA-A*0201 and CD19, and we confirmed high expression of both proteins by flow cytometry (Figure 4.21C).

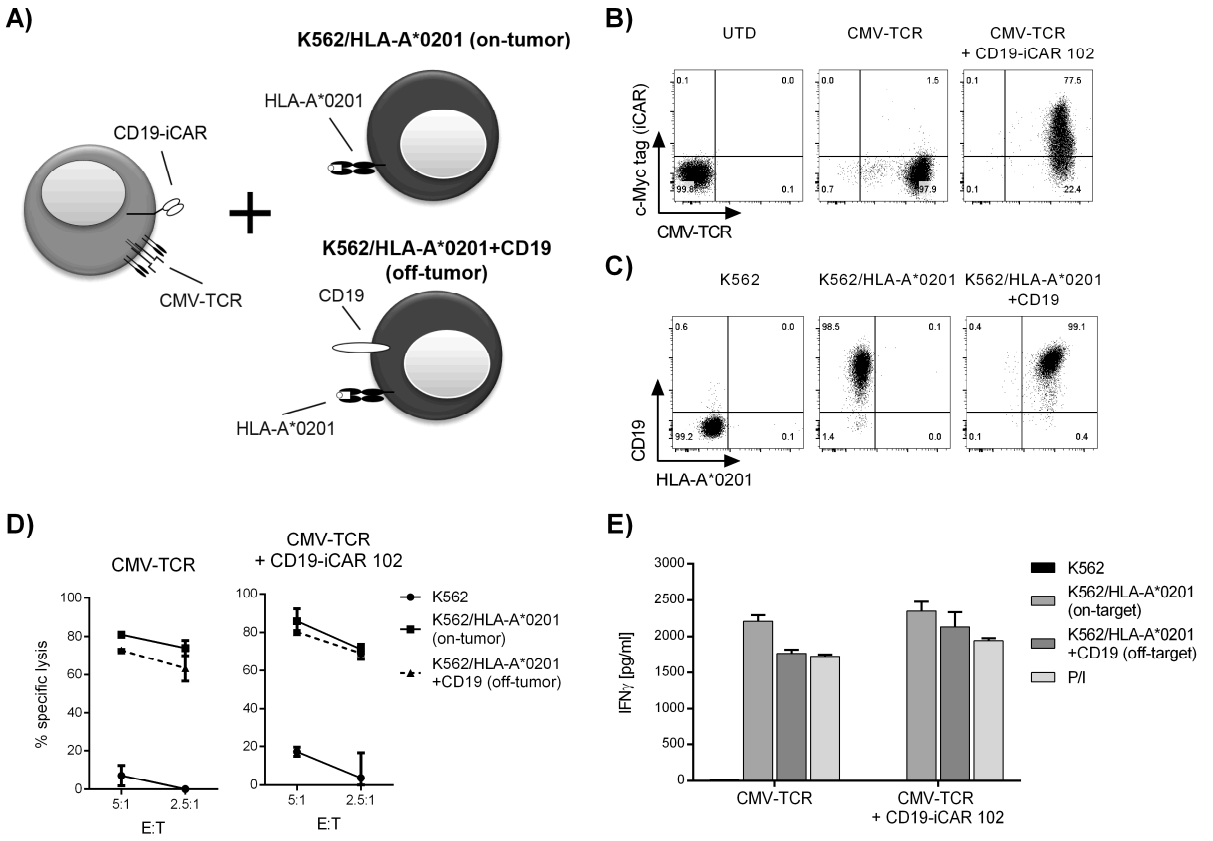


**Figure 4.21: Challenging CD19-iCARs with a CMV-TCR in primary T cells.**

**A)** Schematic representation of the experimental setup with T cells expressing a CMV-specific TCR (CMV-TCR) and a CD19-iCAR and challenged with K562/HLA-A*0201 on-tumor or K562/HLA-A*0201+CD19 off-tumor cells. **B)** Expression of CMV-TCR and CD19-iCARs on primary CD8$^+$ T cells on day 10 of expansion. Staining was performed with anti-EGFR mAb to detect the EGFRt transduction marker of the ROR1-CAR, and with MHC I pp65 NLVPMVATV Streptamer® to detect the CMV-TCR. UTD = untransduced T cells without CMV-specific stimulation. **C)** Expression of HLA-A*0201 and CD19 on K562 cells after transduction. **D)** Specific lysis ± SD (n = 3 technical replicates) of CMV-TCR + CD19-iCAR-T cells co-cultured with on- or off-tumor cells at different E:T ratios for 4 hours. T cells expressing only the CMV-TCR were used as control. **E)** IFNγ secretion ± SD of CMV-TCR + CD19-iCAR-T cells co-cultured with on- or off-target cells at a 4:1 ratio for 24 hours. Stimulation with PMA and ionomycin (P/I) and stimulation of T cells expressing only the CMV-TCR served as controls.

We then co-cultured the T cells with K562/HLA-A*0201 and K562/HLA-A*0201+CD19 cells that were previously pulsed with a pp65 peptide pool, and we analyzed cytotoxicity. CMV-TCR + CD19-iCAR-T cells showed equal lysis of on- and off-tumor cells, and likewise control CMV-TCR-T cells killed both target cell lines similarly (Figure 4.21D). Furthermore, analysis of IFNγ secretion after 24 hours showed only a minor decrease for CMV-TCR + CD19-iCAR-T cells challenged with off-tumor cells in comparison to on-tumor cells (Figure 4.21E). A similar IFNγ reduction was observed with control CMV-TCR-T cells, suggesting a lower overall stimulatory effect of K562/HLA-A*0201+CD19 cells.

In aggregate, the results with primary T cells confirmed the data obtained with the CAR-screening platform, as no inhibitory effect on cytotoxicity or cytokine secretion was observed through logic gates consisting of iCAR and CAR or iCAR and TCR.

### 4.4.4 Inhibition by CD19-iCARs in a logic gate with an activating CD19-CAR

We speculated that several factors could have prevented inhibition by our iCARs in the previous logic gate experiments. These include the density of the target antigens on the cell surface, the expression level of the activating receptors, or different activation kinetics of the activating and inhibitory domains. Moreover, we reasoned that spatial proximity between activating and inhibitory receptors is required to enable their interaction. To address this assumption, we decided to force both receptors into close proximity by targeting only CD19, which has been shown in studies to form nanoclusters on the cell surface.[133]

For the new logic gate, we co-expressed CD19-iCARs with the activating CD19-CAR-zBB, which recognizes the same epitope, in reporter cells to challenge them with $CD19^+$ target cells (Figure 4.22A). To assess whether competitive binding of both CARs to the same antigen could already lead to inhibition, we created a truncated CD19-specific CAR (CD19-tCAR) without intracellular domain as a control. Reporter cells were transduced with the CAR constructs, and enrichment resulted in >86.7% reporter cells expressing the CD19-CAR-zBB together with one of the CD19-iCARs or the CD19-tCAR (Figure 4.22B). Reporter cells only transduced with the CD19-CAR-zBB could be enriched to over 97%. Furthermore, we generated BW/CD19 cells, and we confirmed high expression of CD19 on the cell surface by flow cytometry (Figure 4.22C). We then stimulated the CD19-CAR-zBB + CD19-iCAR reporter cells with BW/CD19 cells, and we compared the reporter signal to stimulation of CD19-CAR-zBB + CD19-tCAR reporter cells and CD19-CAR-zBB reporter cells. The NF-κB and NFAT signal of reporter cells expressing an iCAR significantly decreased relative to reporter cells expressing only the CD19-CAR-zBB (Figure 4.22D). Reporter cells with the CD19-iCAR 103 showed the strongest reporter inhibition of all three iCAR constructs. Importantly, the NF-κB and NFAT activation of

CD19-CAR-zBB + CD19-tCAR reporter cells was comparable to the CD19-CAR-zBB reporter cells, excluding that the observed inhibition with iCARs in reporter cells was due to competitive binding of the receptors.

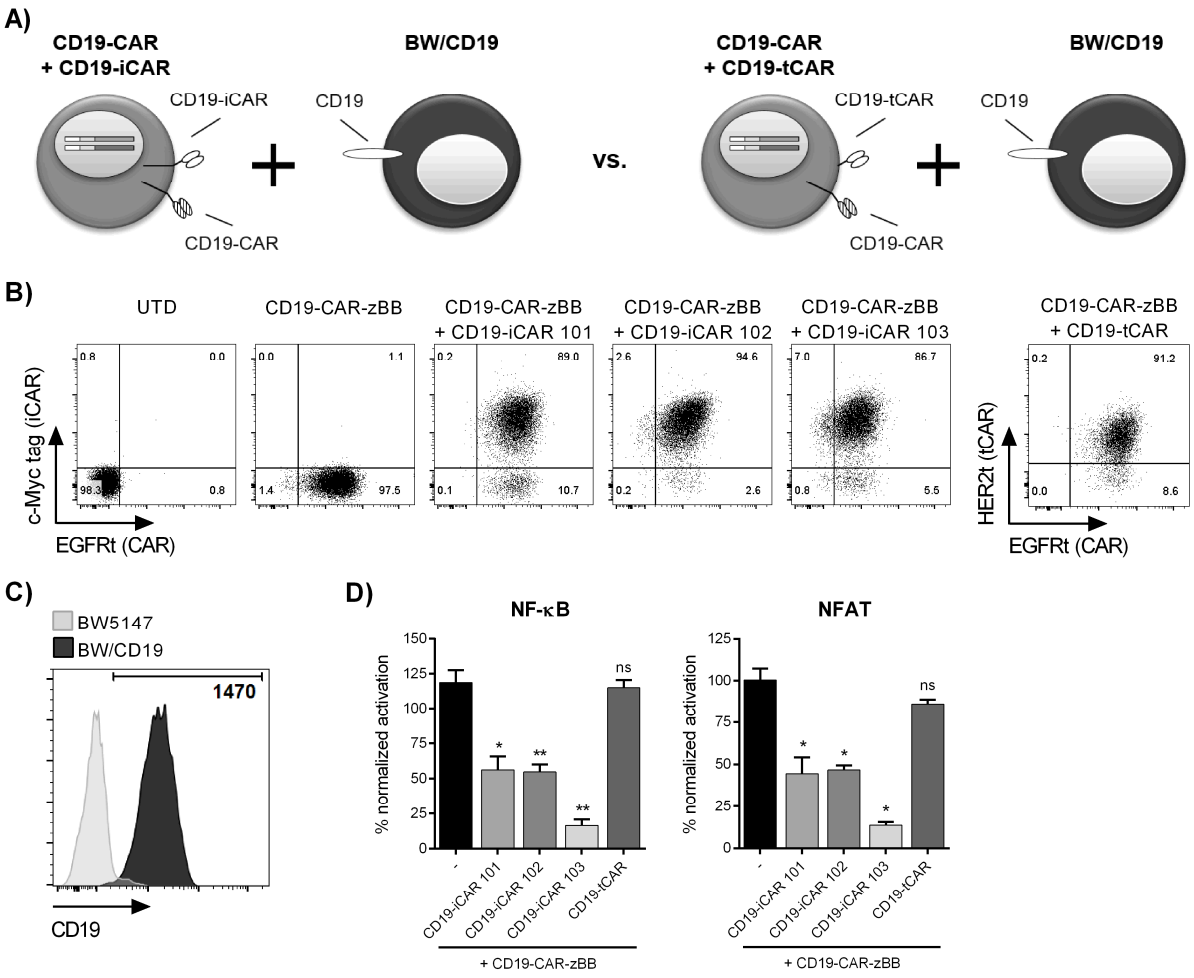


**Figure 4.22: NF-κB and NFAT activation in reporter cells transduced with CD19-CAR and CD19-iCAR.**

**A)** Schematic representation of the experimental setup with CD19-CAR + CD19-iCAR reporter cells challenged with BW/CD19 target cells. Cells equipped with an intracellular truncated version of the CD19-CAR (CD19-tCAR) served as control. **B)** Expression of CD19-CAR-zBB, CD19-iCARs and CD19-tCAR on reporter cells. Staining was performed with anti-EGFR mAb to detect the EGFRt transduction marker of the CD19-CAR-zBB, and with anti-c-Myc mAb to detect the c-Myc tag of CD19-iCARs. The CD19-tCAR was detected by staining of the HER2t transduction marker with anti-HER2 mAb. UTD = untransduced. **C)** Expression of CD19 on BW/CD19 cells. Numeric value represents the MFI of BW/CD19 minus the MFI of native BW5147 cells. **D)** NF-κB and NFAT activation in percent ± SD of BW/CD19 stimulated reporter cells normalized to the positive control (stimulation with BW/OKT3). Statistical significance (n = 3) was determined in comparison to the CD19-CAR-zBB reporter cells using one-way ANOVA with Holm-Sidak post hoc test; *p < 0.05; **p < 0.01; ns = not significant.

We tested the new logic gate in primary T cells to verify the data of the reporter cell screening. $CD8^+$ memory T cells were transduced with the CAR constructs, enriched for CAR expression and analyzed by flow cytometry. We observed >80.3% T cells expressing the CD19-CAR-zBB together with

one of the CD19-iCARs or the CD19-tCAR, and >98% T cells expressing only the CD19-CAR-zBB (Figure 4.23A). In addition, we created K562/CD19 cells, and we detected uniform CD19 expression on the cell surface (Figure 4.23B). Next, we co-cultured the CAR-modified T cells with K562/CD19 at different E:T ratios and analyzed cytotoxicity. After 2 hours, CD19-CAR-zBB-T cells and CD19-CAR-zBB + CD19-tCAR-T cells lysed the target cells equally well. By contrast, T cells with CD19-CAR-zBB + CD19-iCAR showed reduced killing of K562/CD19 cells (Figure 4.23C). Here, the inhibition of cytotoxicity was strongest with CD19-iCARs 101 and 103, and slightly weaker with CD19-iCAR 102. Notably, the iCARs could not completely prevent killing over a long period of time, as inhibition was less distinguishable after 4 hours when compared to the controls. We also analyzed IFNγ secretion after 24-hours co-culture, and we observed CD19-iCAR-mediated inhibition as shown by decreased IFNγ concentrations in the supernatant (Figure 4.23D). However, CD19-CAR-zBB + CD19-tCAR-T cells also slightly reduced IFNγ secretion compared to CD19-CAR-zBB-T cells, which may indicate competitive effects at later time points in primary T cells.

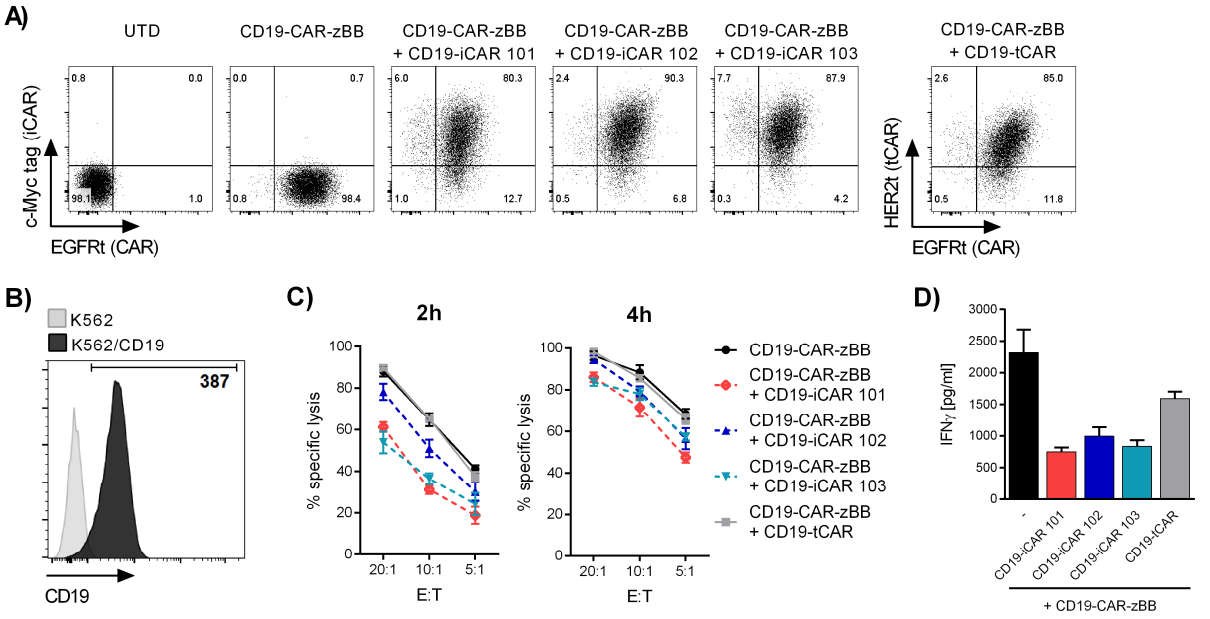


**Figure 4.23: Impact of CD19-CAR and CD19-iCAR on T cell functions.**

**A)** Expression of CD19-CAR-zBB, CD19-iCARs and CD19-tCAR on primary CD8⁺ T cells on day 8 of expansion. Expression of CD19-CAR and CD19-iCAR on transduced CD8⁺ T cells on day 8 of expansion. Staining was performed with anti-EGFR mAb to detect the EGFRt transduction marker of the CD19-CAR-zBB, and with anti-c-Myc mAb to detect the c-Myc tag of CD19-iCARs. The CD19-tCAR was detected by staining of the HER2t transduction marker with anti-HER2 mAb. UTD = untransduced. **B)** Expression of CD19 on K562/CD19 cells. Numeric value represents the MFI of K562/CD19 minus the MFI of native K562 cells. **C)** Specific lysis ± SD (n = 3 technical replicates) of CAR-modified T cells co-cultured with K562/ROR1 cells at different E:T ratios for 2 and 4 hours. T cells expressing only CD19-CAR-zBB or CD19-CAR-zBB + CD19-tCAR served as controls. **D)** IFNγ secretion ± SD of CAR-modified T cells co-cultured with K562/ROR1 cells at a 4:1 ratio for 24 hours. Stimulation of T cells expressing only CD19-CAR-zBB or CD19-CAR-zBB + CD19-tCAR served as controls.

In conclusion, these data demonstrate the capacity of the CD19-iCAR constructs with PD-1 signal modules to reduce reporter gene activation in reporter cells and interfere with cytotoxicity and cytokine secretion in primary T cells. The data suggest that, among others, spatial proximity is required between activating and inhibitory receptors, which was achieved in this experiment by recognition of the same antigen. Inhibition by competitive binding of both receptors as the cause of reduced reporter gene activation was excluded, as a truncated CAR able to compete for antigen had no inhibitory effect. Accordingly, spatial proximity may be an essential factor for creating reasonable and functional logic gates targeting two different antigens.

### 4.4.5 Interim summary and conclusion

In summary, the data from Chapter 4.4 demonstrate that reporter cells enable the analysis of inhibitory receptors as well as CARs with PD-1-derived inhibitory signal module. Although there was no inhibition observed by challenging CD19-iCARs with ROR1-CAR or TCR stimulation, a logic gate of CD19-iCAR and CD19-CAR revealed the inhibitory capacity of the constructs on NF-κB and NFAT activation, and it suggested the requirement of spatial proximity. The observations were further verified by experiments in primary T cells, which supported the significance of reporter cell-based screening campaigns with logic gates. These results meet the fifth aim of the study by screening CARs with inhibitory signal modules in logic gates and emphasize the utility of the NF-κB/NFAT reporter cell platform for the analysis of novel CAR approaches.

In conclusion, all aims of the study have been accomplished by the results presented in this work. Therefore, we accept the hypotheses that the transcription factors NF-κB and NFAT could be used as indicators of CAR stimulation and signaling output of the platform, and that Jurkat cells provide an easy-to-measure, quantitative readout by inducible reporter genes, enabling scalable screening campaigns of CAR libraries for identifying lead candidates with optimal design parameters.

# 5 Discussion

Cancer is a group of diseases that can affect any part of the body and is commonly associated with rapid growth of abnormal cells that may spread throughout the entire organism. It is a leading cause of morbidity and mortality worldwide with an estimated 14.1 million new cases and 8 million cancer-related deaths in 2012. As cancer incidence is highly correlated with age, demographic change is expected to increase the number of cancer cases to over 25 million over the next 20 years.[134] This poses a major challenge for medicine because new therapeutics must be developed to treat cancer more efficiently. Besides standard therapies such as chemotherapy, radiation and surgery, cancer immunotherapies based on immune checkpoint blockade, vaccination or adoptive cell transfer have been established for effective treatment of malignancies.[135] Therapies based on adoptive cell transfer include, among others, the administration of CAR-modified T cells, which has emerged as a potent cancer treatment due to superior antitumor function. Clinical studies with CD19-specific CAR-T cells, for instance, have demonstrated complete and durable remission in patients with B cell malignancies like -B-ALL or NHL.[6] However, other tumor entities, particularly solid tumors, are more difficult to treat with CAR-T cells. To improve the efficacy of CAR-T cell therapy, translational research investigates a rapidly increasing spectrum of target antigens and CAR designs,[73] which often involves extensive testing in preclinical *in vitro* and *in vivo* models to evaluate CAR functionality. This is associated with a high expenditure of time, effort and costs because first donor material must be obtained, then T cells must be isolated and modified with CARs, and finally CAR-T cells must be expanded before starting functional analyses. In addition, when working with primary cells, quality and variability of the donor material significantly influence the experimental outcome, making testing campaigns with multiple runs in one or more laboratories error-prone and difficult to reproduce.

Similar to screening campaigns in pharmaceutical small molecule and antibody discovery,[121,122] a standardized platform that is free of any primary donor material would provide convenient handling and a robust readout to overcome such hurdles, thereby minimizing costs and accelerating CAR-screening campaigns. Therefore, we decided to generate a CAR-screening platform based on the immortalized T cell lymphoma line Jurkat, which was equipped with reporter genes for the transcription factors NF-κB and NFAT as indicators of CAR stimulation. Through the expression of fluorophores from the reporter genes upon CAR stimulation, the platform allows rapid and quantitative analysis of CARs based on signal strength and thus identifies lead candidates with optimal extracellular and intracellular modules that can be analyzed in detail in subsequent tests. Moreover, the NF-κB/NFAT reporter cell platform is scalable for CAR libraries of variable size, enabling its use for high-throughput screening campaigns where large amounts of CARs are analyzed in parallel.

## 5.1 NF-κB and NFAT as indicators of CAR activation

Intensive research on the signaling machinery triggered by the TCR in T cells has shown the involvement of a series of receptors, signaling proteins and secondary messengers. This finally results in the activation of transcription factors that migrate into the nucleus, where they regulate gene expression and initiate specific T cell programs. Among the most important and well-studied transcription factors for T cell activation are the members of the NF-κB and NFAT family.[87,89] Both have a major influence on the development and effector functions of T cells. For instance, NF-κB mediates proliferation and up-regulation of chemokines and cytokines like CXCL6, IL-2 and IL-6,[136,137] and NFAT controls the induction of cytotoxicity and T helper cell differentiation.[138–140] Furthermore, the level of NF-κB and NFAT activation increases with the stimulation strength of TCR and associated co-stimulatory receptors.[98,102]

Because CARs integrate structural and functional elements of the TCR complex and engage TCR-associated signaling molecules upon stimulation, we reasoned that NF-κB and NFAT should serve as indicators of CAR-T cell activation. Indeed, several studies have shown that CAR stimulation activates signaling proteins like ZAP-70, Akt and ERK, which are involved in the regulation of NF-κB and NFAT.[66,105] In addition, inducible reporter gene systems have demonstrated that NF-κB and NFAT are activated in primary T cells and Jurkats upon CAR stimulation.[110,114] Using primary T cells expressing a ROR1-specific CAR, our data support these observations by showing accumulation of NF-κB and NFAT in the nucleus after CAR engagement.

Therefore, it was reasonable to develop the standardized CAR-screening platform based on the detection of activated NF-κB and NFAT. In comparison to effector functions like cytokine secretion or proliferation, which are usually detectable within days after CAR stimulation, the activation of NF-κB and NFAT is detectable within a few hours, allowing for an earlier analysis.[98,141] In addition, since such T cell effector functions are commonly controlled by transcription factors, it could be possible to predict the type and strength of CAR-induced effector functions by analyzing NF-κB and NFAT. To facilitate the analysis of activated transcription factors, we have used inducible reporter genes that eliminate the need for expensive reagents. In contrast, for example, the analysis of cytokine secretion by ELISA usually requires the extensive use of antibodies and buffers. Moreover, the expression of reporter gene-encoded fluorophores enables quantitative analysis of intact cells, e.g. by flow cytometry, providing rapid and automated acquisition of a high number of events from a high number of samples. Unlike reporter genes whose readout relies on luciferase activity, the detection of CFP and GFP allows simultaneous analysis of NF-κB and NFAT and correlation of signals to individual cells. Additionally, fluorescence-based reporter systems require less hands-on time, which makes them more suitable for high-throughput screening than bioluminescence-based reporter systems.

## 5.2 Advantages of Jurkat cells for the CAR-screening platform

We decided to use the human T cell lymphoma line Jurkat as the basis for the CAR-screening platform, since these cells have been widely used as a model system to study TCR signaling down to the molecular level. Although the Jurkat cell line harbors mutations that resulted in malignant transformation, it still comprises the entire downstream signaling machinery of primary T cells.[142,143] However, compared to primary T cells, Jurkats are easier to handle and can be kept in culture indefinitely, which is beneficial for their implementation in a screening platform and renders them an intuitive tool for the analysis of T cell immune receptors. There are several approaches to measure activation of Jurkat cells, e.g. by cytosolic calcium flux, which is experimentally complex to measure, moderately quantitative and provides only a single output.[144,145] Analysis of activation markers like CD25 and CD95 or cytokines like IL-2 and TNFα is also possible, but their expression is often low and detection requires antibodies, making this approach rather inappropriate for platform-based screenings.[146,147]

As recently shown, Jurkat cells equipped with fluorescent reporter genes for the transcription factors NF-κB, NFAT and AP-1 enable quantitative analyses of TCR stimulation in combination with activating and inhibitory ligands.[128,131] In other studies, similar reporter gene-modified cells were used to examine antibody-dependent cell-mediated cytotoxicity, the influence of inhibitory molecules or immune checkpoint modulators, and the signaling of virus- and tumor-specific TCRs.[148–151] In the present study, we show that Jurkat NF-κB/NFAT reporter cells can be used to visualize and quantify antigen-specific CAR stimulation. The reporter cells are easily modified with CARs by viral or non-viral gene transfer, and CAR-positive reporter cells can be enriched to high purity. Furthermore, CAR expression remains stable over a long period of time, enabling long-term CAR-screening campaigns.

To stimulate Jurkat NF-κB/NFAT reporter cells, we used the mouse thymoma cell line BW5147, which only expresses murine activating and inhibitory ligands and can be modified to ectopically express human target antigens.[152] Due to the evolutionary distance between murine and human immune system and the known incompatibility of murine and human MHC and TCR,[153] the presence of cross-reactions is most likely excluded. Accordingly, reporter gene activation in Jurkat cells upon stimulation with untransduced BW5147 cells should not occur, minimizing background signals of NF-κB and NFAT. In addition, we show that reporter cells are easily distinguished from murine BW5147 stimulator cells by detection of human CD45. Alternatively, stimulation with human cell lines that endogenously or ectopically express the CAR target antigen is possible but could be influenced by the interaction of co-stimulatory and inhibitory molecules between Jurkat cells and human target cells.

## 5.3 Rapid identification of CAR lead constructs

In this study, we modified reporter cells with CAR constructs specific for two different antigens. We targeted the human receptor tyrosine kinase ROR1 with scFvs derived from the $V_H$ and $V_L$ domains of the ROR1-specific antibodies R12 and R11, which recognize epitopes at different positions of the protein.[126] ROR1 is an attractive target antigen for CAR-T cells, because it is expressed in several hematologic malignancies, including chronic lymphocytic leukemia and mantle cell lymphoma, and several prevalent epithelial cancers like lung adenocarcinoma and triple negative breast cancer.[154] Further, we targeted the human B cell surface protein CD19 with a CAR comprising an scFv derived from the CD19-specifiv antibody FMC63.[125] CD19-CARs with this scFv are a prime example of highly functional receptors and have demonstrated clinical efficacy in studies with patients suffering from acute lymphoblastic leukemia, Non-Hodgkin lymphoma and chronic lymphocytic leukemia.[155] With the NF-κB/NFAT reporter cells, we show that the stimulation of ROR1- and CD19-specific CARs by target antigen-positive murine and human cell lines induces high-level reporter gene activation. The reporter signal is already detectable 6 hours after CAR stimulation and reaches its maximum after 24 to 48 hours, providing a rapid and highly competitive turnaround time to deliver results. Based on using murine stimulator cells that can potentially be equipped with any human target antigen, it is reasonable to assume that the reporter cell-based screening platform can be employed to rapidly analyze CARs of any specificity, including targets like FLT3, SLAMF7 or mesothelin.[156–158]

We performed several small-scale screening campaigns with the NF-κB/NFAT reporter cell platform to identify CAR lead candidates. In one example, we tested a CAR library of constructs that differed in extracellular spacer length and had been established in previous work, showing that the spacer domain is a critical feature in CAR design. Thus, it was known that the CAR targeting the membrane-proximal R11 epitope in the ROR1 kringle domain requires a long IgG4-Fc spacer for optimal function, including cytotoxicity, cytokine secretion and proliferation.[48] This allowed us to evaluate the output of the CAR-screening platform. The analysis of ROR1-CARs with short, intermediate and long extracellular spacer domain by the reporter cells provided a clear distinction between functional and non-functional constructs. The CAR lead construct against the R11 epitope was readily identified based on specific and high-level NF-κB and NFAT signals. Notably, the screening campaign required less than one-third of the time compared to conventional analyses with primary T cells due to the rapid generation and testing of CAR reporter cells (Figure 5.1). Our data suggest that the screening platform can also analyze other CAR spacer domains, e.g. derived from IgG1-Fc, IgG2-Fc or novel Strep tag,[50,159] to rapidly and reliably identify CAR lead candidates with optimal spacer modules.

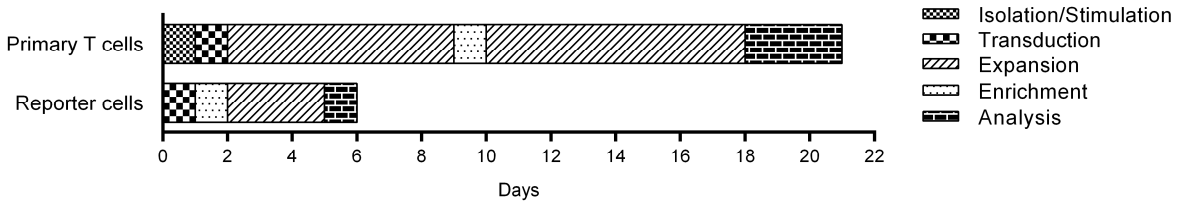


**Figure 5.1: Required time for a CAR-screening campaign in reporter cells and primary T cells.**

Time course of a small-scale screening campaign with CAR reporter cells in comparison to primary human T cells, including approximate time for stimulation, CAR gene modification, cell expansion and final analyses.

In another small-scale screening campaign, we analyzed a library of CAR constructs that differed due to co-stimulatory domains in the intracellular signal module. Here, the reporter cells showed a similar NFAT signal for all CARs, but the NF-κB signal was highly elevated for second and third generation CARs containing the 4-1BB co-stimulatory moiety. In comparison, the first generation CAR that contained no co-stimulatory domain and the second generation CAR with CD28 co-stimulatory domain only showed a low NF-κB reporter signal. Thus, our data support a recent study suggesting enhanced survival of CAR-T cells with 4-1BB co-stimulatory domain compared to CD28 co-stimulatory domain that is driven by higher NF-κB activation.[114] In accordance with this, other CAR studies with 4-1BB co-stimulation observed enhanced *in vivo* persistence and tumor eradication.[69] The higher functionality in these cases could be related to the induction of a transcriptional profile by 4-1BB comprising CARs[71] that includes upregulation of common NF-κB targets like JUNB (memory phenotype)[160] or TNFRSF4 (survival).[161] Consequently, the screening campaign in reporter cells identified the CAR with the 4-1BB signal module as the lead candidate with higher NF-κB signaling intensity compared to the CAR with CD28 signal module.

Interestingly, the CD28 domain in our CARs did not affect NF-κB activation, as the signal for the first generation CAR without co-stimulation and the second generation CAR with CD28 co-stimulation was similar. However, several studies have demonstrated a positive influence of the CD28 receptor on TCR-induced NF-κB activation.[93,101] By stimulating TCR and endogenous CD28 on reporter cells, we confirmed these observations and conclude that the CD28 domain in our signal module was incapable of efficiently activating NF-κB. We assume that steric effects may have prevented complete induction of pathways associated with NF-κB activation, but modifications of the CD28 domain, e.g. by changing its localization in the CAR framework or adding linker amino acids, may help to restore its full capacity to activate NF-κB. However, assuming that NF-κB activation has a positive effect on T cell functions, our observations might contradict studies that have demonstrated enhanced functionality with increased proliferation and prolonged survival of CD28 comprising CARs.[11,25] This suggests that other CD28-induced signaling pathways, including PI3K/Akt that regulates mediators of apoptosis, cell cycle

and transcriptional activity,[162] might compensate for missing NF-κB induction. Accordingly, modified reporter cells that analyze other important T cell transcription factors like AP-1,[136] GATA3[163] or IRF4[164] could be implemented to further improve the informational value of screening campaigns for intracellular signal modules.

## 5.4 Large-scale screening campaigns with reporter cells

In the present study, we aimed to enable a large-scale CAR-screening campaign with the NF-κB/NFAT reporter cell platform to demonstrate scalability, a criterion that is typically required for the screening of therapeutics, such as small molecules, antibodies and other biologics. For instance, antibody development can be based on large naive rabbit antibody repertoires[165] or *in vitro* combinatorial antibody libraries[166] from which lead candidates with high specificity and affinity are identified by *in vitro* display technologies, e.g. using phages or yeast. A previous attempt to combine a large-scale screening process with the development of CARs led to a study that resulted in a CEA-specific CAR after phage display and direct transfer of the scFv into the CAR format.[167] Here, the high-affinity scFv was only selected for further analysis, but affinity of CARs does not necessarily correlate with optimal function[40,43] and could also change when incorporated into the CAR framework.

Instead of first selecting a high-affinity scFv and then transferring it into the CAR framework, we decided to analyze scFv variants directly in the CAR framework and select functional constructs based on the reporter gene signal. This has the advantage that functional scFv variants are not assessed by their affinity but by their functionality in the CAR. Furthermore, our screening platform allows the analysis of multiple CAR constructs in parallel, which presumably cannot be handled in screening campaigns with primary T cells. Therefore, we performed a large-scale screening campaign involving a CAR library with many different scFvs that was generated from the ROR1-specific R11 scFv by site-restricted mutagenesis. Recently, the co-crystal structure of the R11 scFv in complex with the kringle domain of ROR1 demonstrated that the CDR3 region of the $V_H$ domain is crucial for binding.[129] We anticipated that introducing mutations in this region would cause a loss of specificity and affinity in the majority of the $2x10^5$ amino acid variants. Consequently, we challenged the screening platform with the ROR1-CAR scFv library to identify those rare scFv variants in CARs that either contain the WT amino acid sequence or an alternative amino acid sequence that is capable of binding ROR1 and triggering T cell activation. From the screening campaign, we received four reporter cell clones that showed similar or even significantly increased NF-κB and NFAT signals compared to the reference. In three clones, we discovered the WT scFv sequence, which was used as the mutagenesis template to generate the library. The fourth clone contained one of the mutated $V_H$ CDR3 nucleotide sequences

encoding the WT amino acids STYY, occurring in the library with a frequency of only 6 in $1.05x10^6$. The other CAR-encoding nucleotide sequence variants that we found in the four reporter clones were non-functional, suggesting that the NF-κB and NFAT activation was only driven by CARs with the WT sequence. Notably, we detected the largest number of integrated CAR variants in the clone that showed highest EGFRt expression and significantly increased reporter signals compared to the WT reference. Thus, multiple genomic insertions in reporter cells due to the CAR gene transfer remain a technical challenge that complicate library-screening campaigns regarding the identification of functional CARs and the comparison of reporter gene activation between clones. Strategies of targeted gene integration into specific genomic loci are currently emerging and will facilitate future large-scale screening campaigns with CAR libraries where each reporter cell only expresses a single library variant.[168,169]

Several studies have rationally modified the CDR regions of the $V_L$ and $V_H$ domain to modulate binding properties of mAbs and scFvs.[45,46] It is conceivable that such modifications would also alter binding properties of CARs and thus influence the activation and function of CAR-T cells. Consistent with the importance of the $V_H$ CDR3 region of R11 for the binding to ROR1, we have not identified scFv variants from the CAR scFv library with superior functionality over the WT. Indeed, the R11/ROR1 co-crystal structure supports the assumption that the STYY motif is already optimal in terms of paratope/epitope interaction, making the identification of new scFv variants with improved function challenging.[129] Accordingly, the mutagenesis of other stretches in the CDR or framework regions of the $V_H$ domain (the $V_L$ domain of R11 does not interact with ROR1) are likely more suitable for yielding scFv variants with ROR1-binding capacity, which can then be identified in reporter cell-based screenings. It should be noted that due to the selection criteria in this screening campaign – including high NF-κB and NFAT signal, ROR1 binding, expansive growth and specific activation – cell clones that expressed functional CARs with potentially lower affinity were excluded from subsequent sequencing analysis. In future screenings, the selection criteria and cohort size of cell clones should be adjusted to support the identification of novel CAR variants with altered (lower or higher) affinity from CAR scFv libraries. Libraries that contain functional CARs with higher frequency and/or CAR variants that are functionally more similar may require a higher number of sequential pre-enrichments and screening rounds to identify the lead candidates. In particular, the identification of high-affinity CAR variants, which are anticipated to generate a stronger reporter signal compared to the WT, may be fostered by performing a higher number of iterative pre-enrichment steps.

## 5.5 Analysis of inhibitory signal modules with the platform

We assumed that NF-κB/NFAT reporter cells enable screening campaigns of CARs with inhibitory signal modules, which can be used in logic gates with activating receptors to enhance the selectivity of CAR-T cells. For instance, one study with a PSMA-specific inhibitory and a CD19-specific activating CAR showed that only CD19-positive cells were eliminated, but cells that expressed CD19 and PSMA were not affected.[83] The increase in selectivity is particularly intended to prevent on-target off-tumor toxicities in patients when CAR-T cells detect tumor antigens that are also expressed by healthy cells.[73] These toxicities can lead to different adverse events in CAR-T cell therapy depending on the target antigen and tumor entity. The treatment of hematologic malignancies with CD19-specific CAR-T cells, for example, is associated with aplasia of the normal B cell population but can be compensated by immunoglobulin supplementation.[74,75] In contrast, the treatment of solid malignancies, for example with HER2- and CAIX-specific CAR-T cells, carries a high risk of life-threatening complications by damaging healthy lung and liver tissue and may therefore require termination of the treatment.[76,77]

It has previously been shown that the function of inhibitory receptors like PD-1, CTLA-4 and BTLA can be readily assessed via reporter genes in Jurkat cells,[128,131] which prompted us to evaluate iCARs for their inhibitory capacity on NF-κB and NFAT activation. We selected CD19 as target antigen for the iCARs because it is efficiently detected by the FMC63-derived scFv, which has proven high functionality in many CAR-T cell studies. For the activating CAR, we chose the antigen ROR1, which is present on many tumors, including lung and breast cancer, but also on intermediate B cell precursors during maturation.[170] Here, a logic gate of CD19-iCAR and ROR1-CAR was designed to protect the CD19-positive B cell precursors from eradication, thus preserving the healthy B cell population during CAR-T cell therapy of solid tumors. Because we have observed strong inhibition of TCR-mediated stimulation by the PD-1 receptor in NF-κB/NFAT reporter cells, and due to its well-known inhibitory function demonstrated in many studies,[132] the PD-1 intracellular domain was implemented in all constructs of the CD19-iCAR library.

We performed a screening campaign in reporter cells modified with the logic gate of CD19-iCAR and ROR1-CAR, but we detected no decrease of NF-κB or NFAT signals. To exclude that reporter cells were not suitable for the analysis of inhibitory CARs, we transferred the same logic gate to primary T cells, which also showed no inhibition of T cell functions and thus confirmed the reporter cell data. It is conceivable that the co-stimulatory domain of the activating CAR, for which we chose 4-1BB, has obliterated the inhibitory capacity of the CD19-iCAR in our logic gate. Indeed, studies observed that CD28 is the primary target of PD-1-mediated inhibition,[171,172] and likewise, the study of Fedorov et al. showed significant inhibition of a CAR with CD28 co-stimulatory domain by iCARs with PD-1 intracellular domain.[83] The selection of the co-stimulatory signal domain could thus presumably affect

the functionality of logic gates with CAR and iCAR. However, in preliminary logic gate experiments with other iCAR signal modules derived from the inhibitory receptors BTLA, CD300a or KIR2DL2, we did not observe inhibition of NF-κB and NFAT signals in reporter cells.

Therefore, we assumed that the iCAR requires spatial proximity to the activating receptor to mediate inhibition, similar to the physiological situation in the immunological synapse formed by the TCR. In the immunological synapse, inhibitory and stimulatory receptors are proximal to the TCR complex, enabling interaction between multiple molecules in central and peripheral clusters.[23] To implement this concept into a logic gate approach, it would be possible to dimerize iCAR and CAR. However, preliminary experiments with constructs that enable dimerization suggest cross-signaling, i.e., the signal generated by the iCAR binding is transferred to the activating domains of the CAR, allowing the CAR to dominate iCAR stimulation. Another possibility to force CAR and iCAR into spatial proximity without dimerization would be by letting them target the same antigen. To this end, we selected CD19 because studies have shown that it forms nanoclusters on the cell surface,[133] increasing the likelihood that iCAR and CAR co-localize within these clusters when binding to CD19. Indeed, we now observed significantly reduced NF-κB and NFAT reporter signals, whereby the iCAR with CD8 spacer and transmembrane domain was most effective. These observations were reproduced in primary T cells showing reduced cytotoxicity and cytokine secretion, which verified the significance of the reporter cells to study inhibitory signal modules in CARs. Thus, the platform could quantify the inhibitory effects of all constructs from the CD19-iCAR library, although this particular logic gate, in which iCAR and CAR recognized the same antigen, has no reasonable application.

In summary, the modification of reporter cells with logic gates and the analysis of reporter signals was straightforward, and it required no extensive expansion steps as in similar approaches with primary T cells. This should significantly reduce the time for screening campaigns of novel CAR applications that aim to modulate specificity or increase selectivity of CAR-T cell therapies, e.g. by CARs with switchable binding modules,[80] chimeric co-stimulatory receptors,[82] or synthetic notch receptors.[173] In order to create functional, reasonable logical gates, future screening campaigns must consider the need for spatial proximity of iCAR and CAR when targeting two different antigens. Another factor that should be considered, but was not addressed in this study, is the expression level of target antigens and CARs, as high expression of the activating CAR and its target antigen may overpower the inhibitory capacity of iCARs on NF-κB and NFAT activation. Furthermore, the kinetics and signal strength of activation, which are determined by the intracellular signal module, could influence the functionality of logic gates. Because activation by CD3ζ and co-stimulatory domains in CARs is likely to occur rapidly, the inhibitory domain in iCARs may not compete with it when its signal transduction tends to be slower or weaker. Here it is conceivable to strengthen signal modules of iCARs by including

additional domains from inhibitory receptors, and to weaken signal modules of CARs by mutations in the stimulatory domains to prevent binding of certain signaling proteins.

## 5.6 Conclusions and perspective: Implementation in translational research

In this study, we reported on the development of a standardized CAR-screening platform for the identification of CAR lead candidates with optimal extracellular and intracellular modules. The platform is based on the detection of the key T cell transcription factors NF-κB and NFAT, which according to our data, serve as indicators for CAR-mediated activation. The integration of inducible reporter genes in the immortalized T cell lymphoma line Jurkat enables rapid and quantitative analysis of NF-κB and NFAT activation by measuring the fluorophores CFP and GFP. Strong activation of immune receptors induces strong activation of transcription factors and thus results in high target gene expression, which is reflected by high reporter gene expression. By using Jurkat cells instead of primary T cells, the platform was designed for convenient handling and sharing between different laboratories.

We demonstrated high-level activation of NF-κB and NFAT reporter genes with CARs specific for the antigens ROR1 and CD19. Using our murine stimulator cell line, which can be modified with multiple human proteins, the platform should also allow the analysis of CARs with specificities other than CD19 or ROR1. Furthermore, we showed that NF-κB/NFAT reporter cells allow screening campaigns to inform the selection of optimal extracellular and intracellular design parameters in CAR modules. The reporter cells rapidly identified CAR lead candidates that provide optimal function in primary T cells, thus validating the accuracy and significance of the CAR-screening platform. Importantly, a screening campaign comprising CAR transduction, enrichment, cell expansion and final analysis of the reporter signal takes less than a week, which compares favorably to the amount of time that is typically required in a screening campaign with primary T cells.

A large-scale screening campaign with a library of CARs with scFv mutations showed that the NF-κB/NFAT reporter cell platform is scalable and allows the analysis of libraries with more than one million different constructs. Further, it offers the possibility to evaluate CAR constructs not only by the affinity of their targeting domains, but by the reporter gene activation triggered by these CARs. In addition, the reporter cell system is attractive as a platform technology for the evaluation of CARs with inhibitory signal modules because the reporter genes allow quantification of the inhibition. This demonstrates that the platform is suitable for the analysis of applications involving CARs with novel functionalities.

The NF-κB/NFAT reporter cells represent an intuitive tool for the analysis of CARs that can be distributed between different laboratories and easily implemented as a standardized screening

platform into the translational research pipeline of CARs. Following the generation of CAR libraries, small- or large-scale screening campaigns can be performed with reporter cells to identify CAR lead candidates with optimal extracellular and intracellular modules. After this pre-selection, appropriate CAR constructs could be further evaluated in primary T cells *in vitro* and *in vivo*. The use of NF-κB/NFAT reporter cells as a CAR-screening platform has the potential to minimize time, effort and costs of screening campaigns compared to the use of primary T cells. Thus, we are confident that our screening platform can facilitate the preclinical development path of novel CAR-T cell products and accelerate the selection of CAR lead candidates with novel design parameters for clinical translation.

# References


1. Rosenberg, S.A., Yang, J.C., and Restifo, N.P. (2004). Cancer immunotherapy: moving beyond current vaccines. Nat. Med. *10*, 909–15.

2. Dudley, M.E., Wunderlich, J.R., Shelton, T.E., Even, J., and Rosenberg, S.A. (2003). Generation of tumor-infiltrating lymphocyte cultures for use in adoptive transfer therapy for melanoma patients. J. Immunother. *26*, 332–42.

3. Sadelain, M., Rivière, I., and Brentjens, R. (2003). Targeting tumours with genetically enhanced T lymphocytes. Nat. Rev. Cancer *3*, 35–45.

4. Curran, K.J., Pegram, H.J., and Brentjens, R.J. (2012). Chimeric antigen receptors for T cell immunotherapy: current understanding and future directions. J. Gene Med. *14*, 405–15.

5. Sadelain, M., Brentjens, R., and Rivière, I. (2013). The basic principles of chimeric antigen receptor design. Cancer Discov. *3*, 388–98.

6. Hartmann, J., Schüßler-Lenz, M., Bondanza, A., and Buchholz, C.J. (2017). Clinical development of CAR T cells-challenges and opportunities in translating innovative treatment concepts. EMBO Mol. Med. *9*, 1183–1197.

7. Maude, S.L., Laetsch, T.W., Buechner, J., Rives, S., Boyer, M., Bittencourt, H., et al. (2018). Tisagenlecleucel in Children and Young Adults with B-Cell Lymphoblastic Leukemia. N. Engl. J. Med. *378*, 439–448.

8. Neelapu, S.S., Locke, F.L., Bartlett, N.L., Lekakis, L.J., Miklos, D.B., Jacobson, C.A., et al. (2017). Axicabtagene Ciloleucel CAR T-Cell Therapy in Refractory Large B-Cell Lymphoma. N. Engl. J. Med. *377*, 2531–2544.

9. Eshhar, Z., Waks, T., Gross, G., and Schindler, D.G. (1993). Specific activation and targeting of cytotoxic lymphocytes through chimeric single chains consisting of antibody-binding domains and the gamma or zeta subunits of the immunoglobulin and T-cell receptors. Proc. Natl. Acad. Sci. U. S. A. *90*, 720–4.

10. Brocker, T., Peter, A., Traunecker, A., and Karjalainen, K. (1993). New simplified molecular design for functional T cell receptor. Eur. J. Immunol. *23*, 1435–9.

11. Kowolik, C.M., Topp, M.S., Gonzalez, S., Pfeiffer, T., Olivares, S., Gonzalez, N., et al. (2006). CD28 costimulation provided through a CD19-specific chimeric antigen receptor enhances in vivo persistence and antitumor efficacy of adoptively transferred T cells. Cancer Res. *66*, 10995–1004.

12. Brentjens, R.J., Latouche, J.-B., Santos, E., Marti, F., Gong, M.C., Lyddane, C., et al. (2003). Eradication of systemic B-cell tumors by genetically targeted human T lymphocytes co-stimulated by CD80 and interleukin-15. Nat. Med. *9*, 279–86.

13. Maude, S.L., Frey, N., Shaw, P.A., Aplenc, R., Barrett, D.M., Bunin, N.J., et al. (2014). Chimeric antigen receptor T cells for sustained remissions in leukemia. N. Engl. J. Med. *371*, 1507–17.

14. Brentjens, R.J., Davila, M.L., Riviere, I., Park, J., Wang, X., Cowell, L.G., et al. (2013). CD19-targeted T cells rapidly induce molecular remissions in adults with chemotherapy-refractory acute lymphoblastic leukemia. Sci. Transl. Med. *5*, 177ra38.

15. Abbas, A.K., Lichtman, A.H., and Pillai, S. (2014). *Cellular and Molecular Immunology*. Elsevier *8ª ed.*, 544pp.

16. Rudolph, M.G., Stanfield, R.L., and Wilson, I.A. (2006). How TCRs bind MHCs, peptides, and coreceptors. Annu. Rev. Immunol. *24*, 419–66.

17. Accardi, L., and Di Bonito, P. (2010). Antibodies in single-chain format against tumour-associated antigens: present and future applications. Curr. Med. Chem. *17*, 1730–55.

18. Aggen, D.H., Chervin, A.S., Schmitt, T.M., Engels, B., Stone, J.D., Richman, S.A., et al. (2012). Single-chain VαVβ T-cell receptors function without mispairing with endogenous TCR chains. Gene Ther. *19*, 365–74.

19. Han, X., Cinay, G.E., Zhao, Y., Guo, Y., Zhang, X., and Wang, P. (2017). Adnectin-Based Design of Chimeric Antigen Receptor for T Cell Engineering. Mol. Ther. *25*, 2466–2476.

20. Siegler, E., Li, S., Kim, Y.J., and Wang, P. (2017). Designed Ankyrin Repeat Proteins as Her2 Targeting Domains in Chimeric Antigen Receptor-Engineered T Cells. Hum. Gene Ther. *28*, 726–736.

21. Birnbaum, M.E., Berry, R., Hsiao, Y.-S., Chen, Z., Shingu-Vazquez, M.A., Yu, X., et al. (2014). Molecular architecture of the αβ T cell receptor-CD3 complex. Proc. Natl. Acad. Sci. U. S. A. *111*, 17576–81.

22. Artyomov, M.N., Lis, M., Devadas, S., Davis, M.M., and Chakraborty, A.K. (2010). CD4 and CD8 binding to MHC molecules primarily acts to enhance Lck delivery. Proc. Natl. Acad. Sci. U. S. A. *107*, 16916–21.

23. Chen, L., and Flies, D.B. (2013). Molecular mechanisms of T cell co-stimulation and co-inhibition. Nat. Rev. Immunol. *13*, 227–42.

24. van der Stegen, S.J.C., Hamieh, M., and Sadelain, M. (2015). The pharmacology of second-generation chimeric antigen receptors. Nat. Rev. Drug Discov. *14*, 499–509.

25. Finney, H.M., Akbar, A.N., and Lawson, A.D.G. (2004). Activation of resting human primary T cells with chimeric receptors: costimulation from CD28, inducible costimulator, CD134, and CD137 in series with signals from the TCR zeta chain. J. Immunol. *172*, 104–13.

26. Pulè, M.A., Straathof, K.C., Dotti, G., Heslop, H.E., Rooney, C.M., and Brenner, M.K. (2005). A chimeric T cell antigen receptor that augments cytokine release and supports clonal expansion of primary human T cells. Mol. Ther. *12*, 933–41.

27. Moritz, D., and Groner, B. (1995). A spacer region between the single chain antibody- and the CD3 zeta-chain domain of chimeric T cell receptor components is required for efficient ligand binding and signaling activity. Gene Ther. *2*, 539–46.

28. Maher, J., Brentjens, R.J., Gunset, G., Rivière, I., and Sadelain, M. (2002). Human T-lymphocyte cytotoxicity and proliferation directed by a single chimeric TCRzeta /CD28 receptor. Nat. Biotechnol. *20*, 70–5.

29. Serrano, L.M., Pfeiffer, T., Olivares, S., Numbenjapon, T., Bennitt, J., Kim, D., et al. (2006). Differentiation of naive cord-blood T cells into CD19-specific cytolytic effectors for posttransplantation adoptive immunotherapy. Blood *107*, 2643–52.

30. Sharma, S., and Juffer, A.H. (2013). An atomistic model for assembly of transmembrane domain of T cell receptor complex. J. Am. Chem. Soc. *135*, 2188–97.

31. Bridgeman, J.S., Hawkins, R.E., Bagley, S., Blaylock, M., Holland, M., and Gilham, D.E. (2010). The optimal antigen response of chimeric antigen receptors harboring the CD3zeta transmembrane domain is dependent upon incorporation of the receptor into the endogenous TCR/CD3 complex. J. Immunol. *184*, 6938–49.

32. Owji, H., Nezafat, N., Negahdaripour, M., Hajiebrahimi, A., and Ghasemi, Y. (2018). A comprehensive review of signal peptides: Structure, roles, and applications. Eur. J. Cell Biol. *97*, 422–441.

33. Kim, J.H., Lee, S.R., Li, L.H., Park, H.J., Park, J.H., Lee, K.Y., et al. (2011). High cleavage efficiency of a 2A peptide derived from porcine teschovirus-1 in human cell lines, zebrafish and mice. PLoS One *6*, 1–8.

34. Wang, X., Chang, W.-C., Wong, C.W., Colcher, D., Sherman, M., Ostberg, J.R., et al. (2011). A transgene-encoded cell surface polypeptide for selection, in vivo tracking, and ablation of engineered cells. Blood *118*, 1255–63.

35. Diaconu, I., Ballard, B., Zhang, M., Chen, Y., West, J., Dotti, G., et al. (2017). Inducible Caspase-9 Selectively Modulates the Toxicities of CD19-Specific Chimeric Antigen Receptor-Modified T Cells. Mol. Ther. *25*, 580–592.

36. Stone, J.D., Chervin, A.S., and Kranz, D.M. (2009). T-cell receptor binding affinities and kinetics: impact on T-cell activity and specificity. Immunology *126*, 165–76.

37. Rudnick, S.I., and Adams, G.P. (2009). Affinity and avidity in antibody-based tumor targeting. Cancer Biother. Radiopharm. *24*, 155–61.

38. Hudecek, M., Lupo-Stanghellini, M.-T., Kosasih, P.L., Sommermeyer, D., Jensen, M.C., Rader, C., et al. (2013). Receptor affinity and extracellular domain modifications affect tumor recognition by ROR1-specific chimeric antigen receptor T cells. Clin. Cancer Res. *19*, 3153–64.

39. Chmielewski, M., Hombach, A., Heuser, C., Adams, G.P., and Abken, H. (2004). T cell activation by antibody-like immunoreceptors: increase in affinity of the single-chain fragment domain above threshold does not increase T cell activation against antigen-positive target cells but decreases selectivity. J. Immunol. *173*, 7647–53.

40. Richman, S.A., Nunez-Cruz, S., Moghimi, B., Li, L.Z., Gershenson, Z.T., Mourelatos, Z., et al. (2018). High-Affinity GD2-Specific CAR T Cells Induce Fatal Encephalitis in a Preclinical Neuroblastoma Model. Cancer Immunol. Res. *6*, 36–46.

41. Maus, M. V., Plotkin, J., Jakka, G., Stewart-Jones, G., Rivière, I., Merghoub, T., et al. (2016). An MHC-restricted antibody-based chimeric antigen receptor requires TCR-like affinity to maintain antigen specificity. Mol. Ther. oncolytics *3*, 1–9.

42. Song, D.-G., Ye, Q., Poussin, M., Chacon, J.A., Figini, M., and Powell, D.J. (2016). Effective adoptive immunotherapy of triple-negative breast cancer by folate receptor-alpha redirected CAR T cells is influenced by surface antigen expression level. J. Hematol. Oncol. *9*, 56.

43. Park, S., Shevlin, E., Vedvyas, Y., Zaman, M., Park, S., Hsu, Y.-M.S., et al. (2017). Micromolar affinity CAR T cells to ICAM-1 achieves rapid tumor elimination while avoiding systemic toxicity. Sci. Rep. *7*, 14366.

44. Caruso, H.G., Hurton, L. V., Najjar, A., Rushworth, D., Ang, S., Olivares, S., et al. (2015). Tuning Sensitivity of CAR to EGFR Density Limits Recognition of Normal Tissue While Maintaining Potent Antitumor Activity. Cancer Res. *75*, 3505–18.

45. Yang, W.P., Green, K., Pinz-Sweeney, S., Briones, A.T., Burton, D.R., and Barbas, C.F. (1995). CDR walking mutagenesis for the affinity maturation of a potent human anti-HIV-1 antibody into the picomolar range. J. Mol. Biol. *254*, 392–403.

46. Fellouse, F.A., Wiesmann, C., and Sidhu, S.S. (2004). Synthetic antibodies from a four-amino-acid code: a dominant role for tyrosine in antigen recognition. Proc. Natl. Acad. Sci. U. S. A. *101*, 12467–72.

47. Alabanza, L., Pegues, M., Geldres, C., Shi, V., Wiltzius, J.J.W., Sievers, S.A., et al. (2017). Function of Novel Anti-CD19 Chimeric Antigen Receptors with Human Variable Regions Is Affected by Hinge and Transmembrane Domains. Mol. Ther. *25*, 2452–2465.

48. Hudecek, M., Sommermeyer, D., Kosasih, P.L., Silva-Benedict, A., Liu, L., Rader, C., et al. (2015). The nonsignaling extracellular spacer domain of chimeric antigen receptors is decisive for in vivo antitumor activity. Cancer Immunol. Res. *3*, 125–35.

49. Jonnalagadda, M., Mardiros, A., Urak, R., Wang, X., Hoffman, L.J., Bernanke, A., et al. (2015). Chimeric antigen receptors with mutated IgG4 Fc spacer avoid fc receptor binding and improve T cell persistence and antitumor efficacy. Mol. Ther. *23*, 757–68.

50. Watanabe, N., Bajgain, P., Sukumaran, S., Ansari, S., Heslop, H.E., Rooney, C.M., et al. (2016). Fine-tuning the CAR spacer improves T-cell potency. Oncoimmunology *5*, e1253656.

51. Qin, L., Lai, Y., Zhao, R., Wei, X., Weng, J., Lai, P., et al. (2017). Incorporation of a hinge domain improves the expansion of chimeric antigen receptor T cells. J. Hematol. Oncol. *10*, 68.

52. Hombach, A.A., Schildgen, V., Heuser, C., Finnern, R., Gilham, D.E., and Abken, H. (2007). T cell activation by antibody-like immunoreceptors: the position of the binding epitope within the target molecule determines the efficiency of activation of redirected T cells. J. Immunol. *178*, 4650–7.

53. Irving, B.A., and Weiss, A. (1991). The cytoplasmic domain of the T cell receptor zeta chain is sufficient to couple to receptor-associated signal transduction pathways. Cell *64*, 891–901.

54. Gong, M.C., Latouche, J.B., Krause, A., Heston, W.D., Bander, N.H., and Sadelain, M. (1999). Cancer patient T cells genetically targeted to prostate-specific membrane antigen specifically lyse prostate cancer cells and release cytokines in response to prostate-specific membrane antigen. Neoplasia *1*, 123–7.

55. Brocker, T., and Karjalainen, K. (1995). Signals through T cell receptor-zeta chain alone are insufficient to prime resting T lymphocytes. J. Exp. Med. *181*, 1653–9.

56. Brocker, T. (2000). Chimeric Fv-zeta or Fv-epsilon receptors are not sufficient to induce activation or cytokine production in peripheral T cells. Blood *96*, 1999–2001.

57. Jenkins, M.K., Chen, C.A., Jung, G., Mueller, D.L., and Schwartz, R.H. (1990). Inhibition of antigen-specific proliferation of type 1 murine T cell clones after stimulation with immobilized anti-CD3 monoclonal antibody. J. Immunol. *144*, 16–22.

58. Stephan, M.T., Ponomarev, V., Brentjens, R.J., Chang, A.H., Dobrenkov, K. V, Heller, G., et al. (2007). T cell-encoded CD80 and 4-1BBL induce auto- and transcostimulation, resulting in potent tumor rejection. Nat. Med. *13*, 1440–9.

59. Brentjens, R.J., Santos, E., Nikhamin, Y., Yeh, R., Matsushita, M., La Perle, K., et al. (2007). Genetically targeted T cells eradicate systemic acute lymphoblastic leukemia xenografts. Clin. Cancer Res. *13*, 5426–35.

60. Savoldo, B., Ramos, C.A., Liu, E., Mims, M.P., Keating, M.J., Carrum, G., et al. (2011). CD28 costimulation improves expansion and persistence of chimeric antigen receptor-modified T cells in lymphoma patients. J. Clin. Invest. *121*, 1822–6.

61. Porter, D.L., Levine, B.L., Kalos, M., Bagg, A., and June, C.H. (2011). Chimeric antigen receptor-modified T cells in chronic lymphoid leukemia. N. Engl. J. Med. *365*, 725–33.

62. Zhao, Z., Condomines, M., van der Stegen, S.J.C., Perna, F., Kloss, C.C., Gunset, G., et al. (2015). Structural Design of Engineered Costimulation Determines Tumor Rejection Kinetics and Persistence of CAR T Cells. Cancer Cell *28*, 415–428.

63. Carpenito, C., Milone, M.C., Hassan, R., Simonet, J.C., Lakhal, M., Suhoski, M.M., et al. (2009). Control of large, established tumor xenografts with genetically retargeted human T cells containing CD28 and CD137 domains. Proc. Natl. Acad. Sci. U. S. A. *106*, 3360–5.

64. Künkele, A., Johnson, A.J., Rolczynski, L.S., Chang, C. a., Hoglund, V., Kelly-Spratt, K.S., et al. (2015). Functional Tuning of CARs Reveals Signaling Threshold above Which CD8+ CTL Antitumor Potency Is Attenuated due to Cell Fas-FasL-Dependent AICD. Cancer Immunol. Res. *3*, 368–79.

65. Zhong, X.-S., Matsushita, M., Plotkin, J., Riviere, I., and Sadelain, M. (2010). Chimeric antigen receptors combining 4-1BB and CD28 signaling domains augment PI3kinase/AKT/Bcl-XL activation and CD8+ T cell-mediated tumor eradication. Mol. Ther. *18*, 413–20.

66. Guedan, S., Posey, A.D., Shaw, C., Wing, A., Da, T., Patel, P.R., et al. (2018). Enhancing CAR T cell persistence through ICOS and 4-1BB costimulation. JCI insight *3*.

67. Weng, J., Lai, P., Qin, L., Lai, Y., Jiang, Z., Luo, C., et al. (2018). A novel generation 1928zT2 CAR T cells induce remission in extramedullary relapse of acute lymphoblastic leukemia. J. Hematol. Oncol. *11*, 25.

68. Milone, M.C., Fish, J.D., Carpenito, C., Carroll, R.G., Binder, G.K., Teachey, D., et al. (2009). Chimeric receptors containing CD137 signal transduction domains mediate enhanced survival of T cells and increased antileukemic efficacy in vivo. Mol. Ther. *17*, 1453–64.

69. Priceman, S.J., Gerdts, E.A., Tilakawardane, D., Kennewick, K.T., Murad, J.P., Park, A.K., et al. (2018). Co-stimulatory signaling determines tumor antigen sensitivity and persistence of CAR T cells targeting PSCA+ metastatic prostate cancer. Oncoimmunology *7*, e1380764.

70. Kawalekar, O.U., O'Connor, R.S., Fraietta, J.A., Guo, L., McGettigan, S.E., Posey, A.D., et al. (2016). Distinct Signaling of Coreceptors Regulates Specific Metabolism Pathways and Impacts Memory Development in CAR T Cells. Immunity *44*, 380–90.

71. Long, A.H., Haso, W.M., Shern, J.F., Wanhainen, K.M., Murgai, M., Ingaramo, M., et al. (2015). 4-1BB costimulation ameliorates T cell exhaustion induced by tonic signaling of chimeric antigen receptors. Nat. Med. *21*, 581–90.

72. Gomes-Silva, D., Mukherjee, M., Srinivasan, M., Krenciute, G., Dakhova, O., Zheng, Y., et al. (2017). Tonic 4-1BB Costimulation in Chimeric Antigen Receptors Impedes T Cell Survival and Is Vector-Dependent. Cell Rep. *21*, 17–26.

73. Gross, G., and Eshhar, Z. (2016). Therapeutic Potential of T Cell Chimeric Antigen Receptors (CARs) in Cancer Treatment: Counteracting Off-Tumor Toxicities for Safe CAR T Cell Therapy. Annu. Rev. Pharmacol. Toxicol. *56*, 59–83.

74. Davila, M.L., Kloss, C.C., Gunset, G., and Sadelain, M. (2013). CD19 CAR-targeted T cells induce long-term remission and B Cell Aplasia in an immunocompetent mouse model of B cell acute lymphoblastic leukemia. PLoS One *8*, e61338.

75. Kochenderfer, J.N., Wilson, W.H., Janik, J.E., Dudley, M.E., Stetler-Stevenson, M., Feldman, S. a, et al. (2010). Eradication of B-lineage cells and regression of lymphoma in a patient treated with autologous T cells genetically engineered to recognize CD19. Blood *116*, 4099–102.

76. Morgan, R.A., Yang, J.C., Kitano, M., Dudley, M.E., Laurencot, C.M., and Rosenberg, S.A. (2010). Case report of a serious adverse event following the administration of T cells transduced with a chimeric antigen receptor recognizing ERBB2. Mol. Ther. *18*, 843–51.

77. Lamers, C.H.J., Sleijfer, S., Vulto, A.G., Kruit, W.H.J., Kliffen, M., Debets, R., et al. (2006). Treatment of metastatic renal cell carcinoma with autologous T-lymphocytes genetically retargeted against carbonic anhydrase IX: first clinical experience. J. Clin. Oncol. *24*, e20-2.

78. Paszkiewicz, P.J., Fräßle, S.P., Srivastava, S., Sommermeyer, D., Hudecek, M., Drexler, I., et al. (2016). Targeted antibody-mediated depletion of murine CD19 CAR T cells permanently reverses B cell aplasia. J. Clin. Invest. *126*, 4262–4272.

79. Juillerat, A., Marechal, A., Filhol, J.-M., Valton, J., Duclert, A., Poirot, L., et al. (2016). Design of chimeric antigen receptors with integrated controllable transient functions. Sci. Rep. *6*, 18950.

80. Albert, S., Arndt, C., Feldmann, A., Bergmann, R., Bachmann, D., Koristka, S., et al. (2017). A novel nanobody-based target module for retargeting of T lymphocytes to EGFR-expressing cancer cells via the modular UniCAR platform. Oncoimmunology *6*, e1287246.

81. Lanitis, E., Poussin, M., Klattenhoff, A.W., Song, D., Sandaltzopoulos, R., June, C.H., et al. (2013). Chimeric antigen receptor T Cells with dissociated signaling domains exhibit focused antitumor activity with reduced potential for toxicity in vivo. Cancer Immunol. Res. *1*, 43–53.

82. Kloss, C.C., Condomines, M., Cartellieri, M., Bachmann, M., and Sadelain, M. (2013). Combinatorial antigen recognition with balanced signaling promotes selective tumor eradication by engineered T cells. Nat. Biotechnol. *31*, 71–5.

83. Fedorov, V.D., Themeli, M., and Sadelain, M. (2013). PD-1- and CTLA-4-based inhibitory chimeric antigen receptors (iCARs) divert off-target immunotherapy responses. Sci. Transl. Med. *5*, 215ra172.

84. Chan, A.C., Iwashima, M., Turck, C.W., and Weiss, A. (1992). ZAP-70: a 70 kd protein-tyrosine kinase that associates with the TCR zeta chain. Cell *71*, 649–62.

85. Balagopalan, L., Coussens, N.P., Sherman, E., Samelson, L.E., and Sommers, C.L. (2010). The LAT story: a tale of cooperativity, coordination, and choreography. Cold Spring Harb. Perspect. Biol. *2*, a005512.

86. Smith-Garvin, J.E., Koretzky, G.A., and Jordan, M.S. (2009). T cell activation. Annu. Rev. Immunol. *27*, 591–619.

87. Li, Q., and Verma, I.M. (2002). NF-kappaB regulation in the immune system. Nat. Rev. Immunol. *2*, 725–34.

88. Tergaonkar, V. (2006). NFkappaB pathway: a good signaling paradigm and therapeutic target. Int. J. Biochem. Cell Biol. *38*, 1647–53.

89. Macian, F. (2005). NFAT proteins: key regulators of T-cell development and function. Nat. Rev. Immunol. *5*, 472–84.

90. Macián, F., García-Cózar, F., Im, S.-H., Horton, H.F., Byrne, M.C., and Rao, A. (2002). Transcriptional mechanisms underlying lymphocyte tolerance. Cell *109*, 719–31.

91. Diehn, M., Alizadeh, A.A., Rando, O.J., Liu, C.L., Stankunas, K., Botstein, D., et al. (2002). Genomic expression programs and the integration of the CD28 costimulatory signal in T cell activation. Proc. Natl. Acad. Sci. U. S. A. *99*, 11796–801.

92. Boomer, J.S., and Green, J.M. (2010). An enigmatic tail of CD28 signaling. Cold Spring Harb. Perspect. Biol. *2*, a002436.

93. Acuto, O., and Michel, F. (2003). CD28-mediated co-stimulation: a quantitative support for TCR signalling. Nat. Rev. Immunol. *3*, 939–51.

94. Cannons, J.L., Lau, P., Ghumman, B., DeBenedette, M.A., Yagita, H., Okumura, K., et al. (2001). 4-1BB ligand induces cell division, sustains survival, and enhances effector function of CD4 and CD8 T cells with similar efficacy. J. Immunol. *167*, 1313–24.

95. McPherson, A.J., Snell, L.M., Mak, T.W., and Watts, T.H. (2012). Opposing roles for TRAF1 in the alternative versus classical NF-κB pathway in T cells. J. Biol. Chem. *287*, 23010–9.

96. Cannons, J.L., Choi, Y., and Watts, T.H. (2000). Role of TNF receptor-associated factor 2 and p38 mitogen-activated protein kinase activation during 4-1BB-dependent immune response. J. Immunol. *165*, 6193–204.

97. Lee, H.-W., Nam, K.-O., Park, S.-J., and Kwon, B.S. (2003). 4-1BB enhances CD8+ T cell expansion by regulating cell cycle progression through changes in expression of cyclins D and E and cyclin-dependent kinase inhibitor p27kip1. Eur. J. Immunol. *33*, 2133–41.

98. Marangoni, F., Murooka, T.T., Manzo, T., Kim, E.Y., Carrizosa, E., Elpek, N.M., et al. (2013). The transcription factor NFAT exhibits signal memory during serial T cell interactions with antigen-presenting cells. Immunity *38*, 237–49.

99. Maguire, O., Tornatore, K.M., O'Loughlin, K.L., Venuto, R.C., and Minderman, H. (2013). Nuclear translocation of nuclear factor of activated T cells (NFAT) as a quantitative pharmacodynamic parameter for tacrolimus. Cytometry. A *83*, 1096–104.

100. Brogdon, J.L., Leitenberg, D., and Bottomly, K. (2002). The potency of TCR signaling differentially regulates NFATc/p activity and early IL-4 transcription in naive CD4+ T cells. J. Immunol. *168*, 3825–32.

101. Thaker, Y.R., Schneider, H., and Rudd, C.E. (2015). TCR and CD28 activate the transcription factor NF-κB in T-cells via distinct adaptor signaling complexes. Immunol. Lett. *163*, 113–9.

102. Song, J., So, T., and Croft, M. (2008). Activation of NF-kappaB1 by OX40 contributes to antigen-driven T cell expansion and survival. J. Immunol. *180*, 7240–8.

103. Kingeter, L.M., Paul, S., Maynard, S.K., Cartwright, N.G., and Schaefer, B.C. (2010). Cutting edge: TCR ligation triggers digital activation of NF-kappaB. J. Immunol. *185*, 4520–4.

104. King, F.J., Selinger, D.W., Mapa, F.A., Janes, J., Wu, H., Smith, T.R., et al. (2009). Pathway Reporter Assays Reveal Small Molecule Mechanisms of Action. J. Assoc. Lab. Autom. *14*, 374–382.

105. Karlsson, H., Svensson, E., Gigg, C., Jarvius, M., Olsson-Strömberg, U., Savoldo, B., et al. (2015). Evaluation of Intracellular Signaling Downstream Chimeric Antigen Receptors. PLoS One *10*, e0144787.

106. Terakura, S., Yamamoto, T.N., Gardner, R. a, Turtle, C.J., Jensen, M.C., and Riddell, S.R. (2012). Generation of CD19-chimeric antigen receptor modified CD8+ T cells derived from virus-specific central memory T cells. Blood *119*, 72–82.

107. Zheng, W., O'Hear, C.E., Alli, R., Basham, J.H., Abdelsamed, H.A., Palmer, L.E., et al. (2018). PI3K orchestration of the in vivo persistence of chimeric antigen receptor-modified T cells. Leukemia *32*, 1157–1167.

108. Davenport, A.J., Cross, R.S., Watson, K.A., Liao, Y., Shi, W., Prince, H.M., et al. (2018). Chimeric antigen receptor T cells form nonclassical and potent immune synapses driving rapid cytotoxicity. Proc. Natl. Acad. Sci. U. S. A. *115*, E2068–E2076.

109. Davenport, A.J., Jenkins, M.R., Cross, R.S., Yong, C.S., Prince, H.M., Ritchie, D.S., et al. (2015). CAR-T Cells Inflict Sequential Killing of Multiple Tumor Target Cells. Cancer Immunol. Res. *3*, 483–94.

110. Schaft, N., Lankiewicz, B., Gratama, J.W., Bolhuis, R.L.H., and Debets, R. (2003). Flexible and sensitive method to functionally validate tumor-specific receptors via activation of NFAT. J. Immunol. Methods *280*, 13–24.

111. Schroten, C., Kraaij, R., Veldhoven, J.L.M., Berrevoets, C.A., den Bakker, M.A., Ma, Q., et al. (2010). T cell activation upon exposure to patient-derived tumor tissue: a functional assay to select patients for adoptive T cell therapy. J. Immunol. Methods *359*, 11–20.

112. Frigault, M.J., Lee, J., Basil, M.C., Carpenito, C., Motohashi, S., Scholler, J., et al. (2015). Identification of chimeric antigen receptors that mediate constitutive or inducible proliferation of T cells. Cancer Immunol. Res. *3*, 356–67.

113. Chmielewski, M., Kopecky, C., Hombach, A.A., and Abken, H. (2011). IL-12 release by engineered T cells expressing chimeric antigen receptors can effectively Muster an antigen-independent macrophage response on tumor cells that have shut down tumor antigen expression. Cancer Res. *71*, 5697–706.

114. Li, G., Boucher, J.C., Kotani, H., Park, K., Zhang, Y., Shrestha, B., et al. (2018). 4-1BB enhancement of CAR T function requires NF-κB and TRAFs. JCI insight *3*.

115. Ghosh, A., Smith, M., James, S.E., Davila, M.L., Velardi, E., Argyropoulos, K. V, et al. (2017). Donor CD19 CAR T cells exert potent graft-versus-lymphoma activity with diminished graft-versus-host activity. Nat. Med. *23*, 242–249.

116. Karimi, M.A., Lee, E., Bachmann, M.H., Salicioni, A.M., Behrens, E.M., Kambayashi, T., et al. (2014). Measuring cytotoxicity by bioluminescence imaging outperforms the standard chromium-51 release assay. PLoS One *9*, e89357.

117. Kueberuwa, G., Kalaitsidou, M., Cheadle, E., Hawkins, R.E., and Gilham, D.E. (2018). CD19 CAR T Cells Expressing IL-12 Eradicate Lymphoma in Fully Lymphoreplete Mice through Induction of Host Immunity. Mol. Ther. oncolytics *8*, 41–51.

118. Shipkova, M., and Wieland, E. (2012). Surface markers of lymphocyte activation and markers of cell proliferation. Clin. Chim. Acta. *413*, 1338–49.

119. Golubovskaya, V., and Wu, L. (2016). Different Subsets of T Cells, Memory, Effector Functions, and CAR-T Immunotherapy. Cancers (Basel). *8*, 36.

120. Sommermeyer, D., Hudecek, M., Kosasih, P.L., Gogishvili, T., Maloney, D.G., Turtle, C.J., et al. (2016). Chimeric antigen receptor-modified T cells derived from defined CD8+ and CD4+ subsets confer superior antitumor reactivity in vivo. Leukemia *30*, 492–500.

121. Minter, R.R., Sandercock, A.M., and Rust, S.J. (2017). Phenotypic screening-the fast track to novel antibody discovery. Drug Discov. Today. Technol. *23*, 83–90.

122. Janzen, W.P. (2014). Screening technologies for small molecule discovery: the state of the art. Chem. Biol. *21*, 1162–70.

123. Riddell, S.R., and Greenberg, P.D. (1990). The use of anti-CD3 and anti-CD28 monoclonal antibodies to clone and expand human antigen-specific T cells. J. Immunol. Methods *128*, 189–201.

124. Monjezi, R., Miskey, C., Gogishvili, T., Schleef, M., Schmeer, M., Einsele, H., et al. (2017). Enhanced CAR T-cell engineering using non-viral Sleeping Beauty transposition from minicircle vectors. Leukemia *31*, 186–194.

125. Nicholson, I.C., Lenton, K.A., Little, D.J., Decorso, T., Lee, F.T., Scott, A.M., et al. (1997). Construction and characterisation of a functional CD19 specific single chain Fv fragment for immunotherapy of B lineage leukaemia and lymphoma. Mol. Immunol. *34*, 1157–65.

126. Yang, J., Baskar, S., Kwong, K.Y., Kennedy, M.G., Wiestner, A., and Rader, C. (2011). Therapeutic potential and challenges of targeting receptor tyrosine kinase ROR1 with monoclonal antibodies in B-cell malignancies. PLoS One *6*, e21018.

127. Guest, R.D., Hawkins, R.E., Kirillova, N., Cheadle, E.J., Arnold, J., O'Neill, A., et al. (2005). The role of extracellular spacer regions in the optimal design of chimeric immune receptors: evaluation of four different scFvs and antigens. J. Immunother. *28*, 203–11.

128. Jutz, S., Leitner, J., Schmetterer, K., Doel-Perez, I., Majdic, O., Grabmeier-Pfistershammer, K., et al. (2016). Assessment of costimulation and coinhibition in a triple parameter T cell reporter line: Simultaneous measurement of NF-κB, NFAT and AP-1. J. Immunol. Methods *430*, 10–20.

129. Qi, J., Li, X., Peng, H., Cook, E.M., Dadashian, E.L., Wiestner, A., et al. (2018). Potent and selective antitumor activity of a T cell-engaging bispecific antibody targeting a membrane-proximal epitope of ROR1. Proc. Natl. Acad. Sci. U. S. A. *115*, E5467–E5476.

130. Suzuki, K., Bose, P., Leong-Quong, R.Y.Y., Fujita, D.J., and Riabowol, K. (2010). REAP: A two minute cell fractionation method. BMC Res. Notes *3*, 294.

131. Jutz, S., Hennig, A., Paster, W., Asrak, Ö., Dijanovic, D., Kellner, F., et al. (2017). A cellular platform for the evaluation of immune checkpoint molecules. Oncotarget *8*, 64892–64906.

132. Carter, L., Fouser, L.A., Jussif, J., Fitz, L., Deng, B., Wood, C.R., et al. (2002). PD-1:PD-L inhibitory pathway affects both CD4(+) and CD8(+) T cells and is overcome by IL-2. Eur. J. Immunol. *32*, 634–43.

133. Mattila, P.K., Feest, C., Depoil, D., Treanor, B., Montaner, B., Otipoby, K.L., et al. (2013). The actin and tetraspanin networks organize receptor nanoclusters to regulate B cell receptor-mediated signaling. Immunity *38*, 461–74.

134. Stewart, B.W., and Wild, C.P. (2014). *World cancer report 2014*. Int. Agency Res. Cancer, 632pp.

135. Farkona, S., Diamandis, E.P., and Blasutig, I.M. (2016). Cancer immunotherapy: the beginning of the end of cancer? BMC Med. *14*, 73.

136. Khalaf, H., Jass, J., and Olsson, P.-E. (2010). Differential cytokine regulation by NF-kappaB and AP-1 in Jurkat T-cells. BMC Immunol. *11*, 26.

137. Ferreira, V., Sidénius, N., Tarantino, N., Hubert, P., Chatenoud, L., Blasi, F., et al. (1999). In vivo inhibition of NF-kappa B in T-lineage cells leads to a dramatic decrease in cell proliferation and cytokine production and to increased cell apoptosis in response to mitogenic stimuli, but not to abnormal thymopoiesis. J. Immunol. *162*, 6442–50.

138. Klein-Hessling, S., Muhammad, K., Klein, M., Pusch, T., Rudolf, R., Flöter, J., et al. (2017). NFATc1 controls the cytotoxicity of CD8+ T cells. Nat. Commun. *8*, 511.

139. Kiani, A., Viola, J.P., Lichtman, A.H., and Rao, A. (1997). Down-regulation of IL-4 gene transcription and control of Th2 cell differentiation by a mechanism involving NFAT1. Immunity *7*, 849–60.

140. Porter, C.M., and Clipstone, N.A. (2002). Sustained NFAT signaling promotes a Th1-like pattern of gene expression in primary murine CD4+ T cells. J. Immunol. *168*, 4936–45.

141. Mittal, A., Papa, S., Franzoso, G., and Sen, R. (2006). NF-kappaB-dependent regulation of the timing of activation-induced cell death of T lymphocytes. J. Immunol. *176*, 2183–9.

142. Gioia, L., Siddique, A., Head, S.R., Salomon, D.R., and Su, A.I. (2018). A genome-wide survey of mutations in the Jurkat cell line. BMC Genomics *19*, 334.

143. Abraham, R.T., and Weiss, A. (2004). Jurkat T cells and development of the T-cell receptor signalling paradigm. Nat. Rev. Immunol. *4*, 301–8.

144. Bartelt, R.R., Cruz-Orcutt, N., Collins, M., and Houtman, J.C.D. (2009). Comparison of T cell receptor-induced proximal signaling and downstream functions in immortalized and primary T cells. PLoS One *4*, e5430.

145. Imboden, J.B., Weiss, A., and Stobo, J.D. (1985). The antigen receptor on a human T cell line initiates activation by increasing cytoplasmic free calcium. J. Immunol. *134*, 663–5.

146. Shatrova, A.N., Mityushova, E. V., Aksenov, N.A., and Marakhova, I.I. (2015). CD25 expression on the surface of Jurkat cells. Cell tissue biol. *9*, 364–370.

147. Khlusov, I.A., Litvinova, L.S., Shupletsova, V. V., Dunets, N.A., Khaziakhmatova, O.G., Yurova, K.A., et al. (2017). Morphofunctional changes of Jurkat T lymphoblasts upon short-term contact with a relief calcium phosphate surface. Cell tissue biol. *11*, 59–64.

148. Anmole, G., Kuang, X.T., Toyoda, M., Martin, E., Shahid, A., Le, A.Q., et al. (2015). A robust and scalable TCR-based reporter cell assay to measure HIV-1 Nef-mediated T cell immune evasion. J. Immunol. Methods *426*, 104–13.

149. Cheng, Z.J., Garvin, D., Paguio, A., Moravec, R., Engel, L., Fan, F., et al. (2014). Development of a robust reporter-based ADCC assay with frozen, thaw-and-use cells to measure Fc effector function of therapeutic antibodies. J. Immunol. Methods *414*, 69–81.

150. Rosskopf, S., Leitner, J., Paster, W., Morton, L.T., Hagedoorn, R.S., Steinberger, P., et al. (2018). A Jurkat 76 based triple parameter reporter system to evaluate TCR functions and adoptive T cell strategies. Oncotarget *9*, 17608–17619.

151. Gonzales, A.M., and Orlando, R.A. (2009). A Jurkat transcriptional reporter cell line for high-throughput analysis of the nuclear factor-kappaB signaling pathway. N. Biotechnol. *26*, 244–50.

152. Leitner, J., Kuschei, W., Grabmeier-Pfistershammer, K., Woitek, R., Kriehuber, E., Majdic, O., et al. (2010). T cell stimulator cells, an efficient and versatile cellular system to assess the role of costimulatory ligands in the activation of human T cells. J. Immunol. Methods *362*, 131–41.

153. Mestas, J., and Hughes, C.C.W. (2004). Of mice and not men: differences between mouse and human immunology. J. Immunol. *172*, 2731–8.

154. Zhang, S., Chen, L., Wang-Rodriguez, J., Zhang, L., Cui, B., Frankel, W., et al. (2012). The onco-embryonic antigen ROR1 is expressed by a variety of human cancers. Am. J. Pathol. *181*, 1903–10.

155. Kochenderfer, J.N., and Rosenberg, S.A. (2013). Treating B-cell cancer with T cells expressing anti-CD19 chimeric antigen receptors. Nat. Rev. Clin. Oncol. *10*, 267–76.

156. Lanitis, E., Poussin, M., Hagemann, I.S., Coukos, G., Sandaltzopoulos, R., Scholler, N., et al. (2012). Redirected antitumor activity of primary human lymphocytes transduced with a fully human anti-mesothelin chimeric receptor. Mol. Ther. *20*, 633–43.

157. Gogishvili, T., Danhof, S., Prommersberger, S., Rydzek, J., Schreder, M., Brede, C., et al. (2017). SLAMF7-CAR T cells eliminate myeloma and confer selective fratricide of SLAMF7+ normal lymphocytes. Blood *130*, 2838–2847.

158. Jetani, H., Garcia-Cadenas, I., Nerreter, T., Thomas, S., Rydzek, J., Meijide, J.B., et al. (2018). CAR T-cells targeting FLT3 have potent activity against FLT3-ITD+ AML and act synergistically with the FLT3-inhibitor crenolanib. Leukemia *32*, 1168–1179.

159. Liu, L., Sommermeyer, D., Cabanov, A., Kosasih, P., Hill, T., and Riddell, S.R. (2016). Inclusion of Strep-tag II in design of antigen receptors for T-cell immunotherapy. Nat. Biotechnol. *34*, 430–4.

160. Brown, R.T., Ades, I.Z., and Nordan, R.P. (1995). An acute phase response factor/NF-kappa B site downstream of the junB gene that mediates responsiveness to interleukin-6 in a murine plasmacytoma. J. Biol. Chem. *270*, 31129–35.

161. Tone, Y., Kojima, Y., Furuuchi, K., Brady, M., Yashiro-Ohtani, Y., Tykocinski, M.L., et al. (2007). OX40 gene expression is up-regulated by chromatin remodeling in its promoter region containing Sp1/Sp3, YY1, and NF-kappa B binding sites. J. Immunol. *179*, 1760–7.

162. Kane, L.P., and Weiss, A. (2003). The PI-3 kinase/Akt pathway and T cell activation: pleiotropic pathways downstream of PIP3. Immunol. Rev. *192*, 7–20.

163. Ho, I.-C., Tai, T.-S., and Pai, S.-Y. (2009). GATA3 and the T-cell lineage: essential functions before and after T-helper-2-cell differentiation. Nat. Rev. Immunol. *9*, 125–35.

164. Man, K., Gabriel, S.S., Liao, Y., Gloury, R., Preston, S., Henstridge, D.C., et al. (2017). Transcription Factor IRF4 Promotes CD8+ T Cell Exhaustion and Limits the Development of Memory-like T Cells during Chronic Infection. Immunity *47*, 1129–1141.e5.

165. Peng, H., Nerreter, T., Chang, J., Qi, J., Li, X., Karunadharma, P., et al. (2017). Mining Naïve Rabbit Antibody Repertoires by Phage Display for Monoclonal Antibodies of Therapeutic Utility. J. Mol. Biol. *429*, 2954–2973.

166. Rajpal, A., Beyaz, N., Haber, L., Cappuccilli, G., Yee, H., Bhatt, R.R., et al. (2005). A general method for greatly improving the affinity of antibodies by using combinatorial libraries. Proc. Natl. Acad. Sci. U. S. A. *102*, 8466–71.

167. Shirasu, N., Shibaguci, H., Kuroki, M., Yamada, H., and Kuroki, M. (2010). Construction and molecular characterization of human chimeric T-cell antigen receptors specific for carcinoembryonic antigen. Anticancer Res. *30*, 2731–8.

168. Eyquem, J., Mansilla-Soto, J., Giavridis, T., van der Stegen, S.J.C., Hamieh, M., Cunanan, K.M., et al. (2017). Targeting a CAR to the TRAC locus with CRISPR/Cas9 enhances tumour rejection. Nature *543*, 113–117.

169. Voigt, K., Gogol-Döring, A., Miskey, C., Chen, W., Cathomen, T., Izsvák, Z., et al. (2012). Retargeting sleeping beauty transposon insertions by engineered zinc finger DNA-binding domains. Mol. Ther. *20*, 1852–62.

170. Hudecek, M., Schmitt, T.M., Baskar, S., Lupo-Stanghellini, M.T., Nishida, T., Yamamoto, T.N., et al. (2010). The B-cell tumor-associated antigen ROR1 can be targeted with T cells modified to express a ROR1-specific chimeric antigen receptor. Blood *116*, 4532–41.

171. Kamphorst, A.O., Wieland, A., Nasti, T., Yang, S., Zhang, R., Barber, D.L., et al. (2017). Rescue of exhausted CD8 T cells by PD-1-targeted therapies is CD28-dependent. Science *355*, 1423–1427.

172. Hui, E., Cheung, J., Zhu, J., Su, X., Taylor, M.J., Wallweber, H.A., et al. (2017). T cell costimulatory receptor CD28 is a primary target for PD-1-mediated inhibition. Science *355*, 1428–1433.

173. Roybal, K.T., Williams, J.Z., Morsut, L., Rupp, L.J., Kolinko, I., Choe, J.H., et al. (2016). Engineering T Cells with Customized Therapeutic Response Programs Using Synthetic Notch Receptors. Cell *167*, 419–432.e16.

# List of figures

# List of tables

# List of abbreviations

The specification of physical quantities is based on the guidelines of the international system of units. Special abbreviations for technical terms that are not included in the list are explained in the text.

| Abbreviation | Prefix | Factor |
|---|---|---|
| p | pico- | $10^{-12}$ |
| n | nano- | $10^{-9}$ |
| µ | micro- | $10^{-6}$ |
| m | milli- | $10^{-3}$ |
| c | centi- | $10^{-2}$ |
| k | kilo- | $10^{3}$ |

| | |
|---|---|
| °C | Degrees Celsius |
| 7-AAD | 7-Aminoactinomycin D |
| AA | Amino acid |
| AF647 | Alexa Fluor 647 |
| AICD | Activation-induced cell death |
| ANOVA | Analysis of variance |
| APC | Allophycocyanin |
| ATCC | American Type Culture Collection |
| B-ALL | B cell acute lymphoblastic leukemia |
| BTLA | B and T lymphocyte attenuator |
| $Ca^{2+}$ | Calcium ion |
| CAIX | Carbonic anhydrase 9 |
| CAR | Chimeric antigen receptor |
| CD | Cluster of differentiation |
| CDK4 | Cyclin-dependent kinase 4 |
| CDR | Complementarity determining region |
| CEA | Carcinoembryonic antigen |
| CFP | Cyan fluorescent protein |
| CFSE | Carboxyfluorescein succinimidyl ester |
| CMV | Cytomegalovirus |
| $CO_2$ | Carbon dioxide |
| CREB | cAMP response element-binding protein |

| | |
|---|---|
| CRISPR | Clustered Regularly Interspaced Short Palindromic Repeats |
| CTLA-4 | Cytotoxic T lymphocyte-associated protein 4 |
| DAG | Diacylglycerol |
| DARPin | Designed ankyrin repeat protein |
| $dH_2O$ | Distilled water |
| DNA | Deoxyribonucleic acid |
| e.g. | *Exempli gratia* (Latin “for example”) |
| ECL | Enhanced chemiluminescence |
| EF1 | Elongation factor 1 |
| EGFR | Epidermal growth factor receptor |
| EGFRt | Truncated epidermal growth factor receptor |
| ELISA | Enzyme-linked immunosorbent assay |
| f.c. | Final concentration |
| FACS | Fluorescence-activated cell sorting |
| Fc | Fragment crystallizable |
| FDA | Food and Drug Administration |
| ffluc | Firefly luciferase |
| FITC | Fluorescein isothiocyanate |
| FoxO3 | Forkhead box O3 |
| g | Gram |
| GD2 | Disialoganglioside 2 |
| GFP | Green fluorescent protein |
| GM-CSF | Granulocyte-macrophage colony-stimulating factor |
| GRB2 | Growth factor receptor-bound protein 2 |
| Gy | Gray (unit) |
| HER2 | Human epidermal growth factor receptor 2 |
| HER2t | Truncated human epidermal growth factor receptor 2 |
| HLA | Human leukocyte antigen |
| HVEM | Herpesvirus entry mediator |
| i.e. | *Id est* (Latin “that is”) |
| ICAM-1 | Intercellular adhesion molecule 1 |
| iCAR | Inhibitory chimeric antigen receptor |
| IFNγ | Interferon gamma |
| IgG | Immunoglobulin G |
| IL | Interleukin |
| $IP_3$ | Inositol trisphosphate |

| | |
|---|---|
| ITAM | Immunoreceptor tyrosine-based activation motif |
| $K_d$ | Dissociation constant |
| KIR2DL2 | Killer cell immunoglobulin-like receptor 2DL2 |
| L | Liter |
| LAT | Linker for activation of T cells |
| Lck | Lymphocyte-specific protein tyrosine kinase |
| LNGFR | Low-affinity nerve growth factor receptor |
| M | Molarity |
| m | Meter |
| mAb | Monoclonal antibody |
| MAPK/ERK | Mitogen-activated protein kinase/extracellular signal-regulated kinase |
| mbOKT3 | Membrane-bound OKT3 |
| MFI | Mean fluorescence intensity |
| MHC | Major histocompatibility complex |
| mTOR | Mammalian target of rapamycin |
| NF-κB | Nuclear factor-κB |
| NFAT | Nuclear factor of activated T cells |
| NHL | Non-Hodgkin lymphoma |
| NK cell | Natural killer cell |
| NKT cell | Natural killer T cell |
| NT | Nucleotide |
| NY-ESO-1 | New York esophageal squamous cell carcinoma 1 |
| PBMCs | Peripheral blood mononuclear cells |
| PCR | Polymerase chain reaction |
| PD-1 | Programmed cell death 1 |
| PD-L1 | Programmed cell death ligand 1 |
| PE | Phycoerythrin |
| PI3K | Phosphatidylinositol-3-kinase |
| PKCδ | Protein kinase C delta |
| PKCθ | Protein kinase C theta |
| PLCγ1 | Phospholipase C gamma 1 |
| PSCA | Prostate stem cell antigen |
| PSMA | Prostate-specific membrane antigen |
| PVDF | Polyvinylidene fluoride |
| RNA | Ribonucleic acid |
| ROR1 | Receptor tyrosine kinase-like orphan receptor 1 |

| | |
|---|---|
| scFv | Single-chain fragment variable |
| SD | Standard deviation |
| SLAMF7 | Signaling lymphocyte activation molecule |
| SLP-76 | SH2 domain containing leukocyte protein of 76kDa |
| STAT | Signal transducer and activator of transcription |
| TCR | T cell receptor |
| TNFα | Tumor necrosis factor alpha |
| U | Unit |
| UV | Ultraviolet |
| v/v | Volume/volume % |
| $V_H$ | Variable heavy |
| $V_L$ | Variable light |
| w/v | Weight/volume % |
| x g | fold gravitational acceleration (g = 9.81 m/s$^2$) |
| ZAP-70 | Zeta-chain-associated protein kinase 70 |

## Affidavit

I hereby confirm that my thesis entitled ‘‘NF-κB/NFAT Reporter Cell Platform for Chimeric Antigen Receptor (CAR)-Library Screening’’ is the result of my own work. I did not receive any help or support from commercial consultants. All sources and/or materials applied are listed and specified in the thesis.

Furthermore, I confirm that this thesis has not been submitted as part of another examination process neither in identical nor in similar form.

Place, date

Signature

## Eidesstattliche Erklärung

Hiermit erkläre ich an Eides statt, die Dissertation „NF-κB/NFAT-Reporterzellplattform für das Screening von Chimären Antigenrezeptor (CAR)-Bibliotheken“ eigenständig, d.h. insbesondere selbständig und ohne Hilfe eines kommerziellen Promotionsberaters, angefertigt und keine anderen als die von mir angegebenen Quellen und Hilfsmittel verwendet zu haben.

Ich erkläre außerdem, dass die Dissertation weder in gleicher noch in ähnlicher Form bereits in einem anderen Prüfungsverfahren vorgelegen hat.

Ort, Datum

Unterschrift

# Statement on copyright and self-plagiarism

The data presented in this thesis have been partially published in the journal Molecular Therapy as an original article entitled “Chimeric antigen receptor library screening using a novel NF-κB/NFAT reporter cell platform”. In accordance with the regulations of the parent publisher Elsevier, data, text passages and illustrations from the manuscript were used in identical or modified form in this thesis.

### Individual author contributions and legal second publication rights

Rydzek, J., Nerreter, T., Peng, H., Jutz, S., Leitner, J., Steinberger, P., Einsele, H., Rader, C., and Hudecek, M. (2018) Chimeric antigen receptor library screening using a novel NF-κB/NFAT reporter cell platform. Molecular Therapy (*In Press*).

| **Participated in** | **Authors** (Responsibility decreasing from left to right) | | | | | |
|---|---|---|---|---|---|---|
| Conceptualization | Rydzek, J. | Hudecek, M. | Steinberger, P. | | | |
| Methodology | Rydzek, J. | Nerreter, T. | Hudecek, M. | | | |
| Investigation | Rydzek, J. | Nerreter, T. | Peng, H. | | | |
| Resources | Jutz, S. | Peng, H. | Leitner, J. | Steinberger, P. | Rader, C. | |
| Manuscript Writing | | | | | | |
| Original Draft | Rydzek, J. | Hudecek, M. | | | | |
| Review & Editing | Rydzek, J. | Hudecek, M. | Steinberger, P. | Rader, C. | Leitner, J. | Peng, H. |
| Visualization | Rydzek, J. | Hudecek, M. | | | | |
| Supervision | Hudecek, M. | Steinberger, P. | Einsele H. | | | |

**Explanations**

Rydzek, J. designed the study, carried out the experiments, evaluated and interpreted the data, and wrote the manuscript. Steinberger, P and Einsele, H. supervised the study. Nerreter, T. helped with methodology and CAR library preparation. Peng, H. performed the mutagenesis to create the scFv library. Jutz, S. and Leitner, J. provided the NF-κB/NFAT reporter cells and the BW5147 stimulator cells. Steinberger, P., Rader, C., Leitner, J. and Peng, H. reviewed and edited the manuscript. Hudecek, M. is the principal investigator, supervised the project and contributed to study design, writing and final proofreading for the manuscript. Huppa, J. was acknowledged to provide fluorophore-labeled soluble ROR1 protein.